RM No. SL7H20

RESEARCH MEMORANDUM

for the

Bureau of Aeronautics, Navy Department

WIND-TUNNEL TESTS OF THE 1/25-SCALE POWERED MODEL OF THE MARTIN JRM-1 AIRPLANE

IV - TESTS WITH GROUND BOARD AND WITH MODIFIED WING AND HULL - TED NO. NACA 232

By

Vernard E. Lockwood and Bernard J. Smith

Langley Memorial Aeronautical Laboratory
Langley Field, Va.

NATIONAL ADVISORY COMMITTEE FOR AERONAUTICS

WASHINGTON

SEP 4 1947

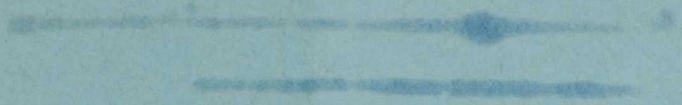

NATIONAL ADVISORY COMMITTEE FOR AERONAUTICS

RESEARCH MEMORANDUM

for the

Bureau of Aeronautics, Navy Department

WIND-TUNNEL TESTS OF THE 1/25-SCALE POWERED MODEL OF THE MARTIN JRM-1 AIRPLANE

IV - TESTS WITH GROUND BOARD AND WITH MODIFIED WING AND HULL - TED NO. NACA 232

By Vernard E. Lockwood and Bernard J. Smith

SUMMARY

Wind-tunnel tests were made of a 1/25-scale model of the Martin JRM-1 airplane to determine:

(1) The longitudinal stability and control characteristics of the JRM-1 model near the water and lateral and directional stability characteristics with power while moving on the surface of the water, the latter being useful for the design of tip floats

(2) The stability and stalling characteristics of the wing with a modified airfoil contour

(3) Stability characteristics of a hull of larger design gross weight

The test results indicated that the elevator was powerful enough to trim the original model in a landing configuration at any lift coefficient within the specified range of centers of gravity.

The ground-board tests for evaluating the aerodynamic forces and moments on an airplane in a simulated cross wind indicate a high dihedral effect in the presence of the ground board and, consequently, during low-speed taxying and take-off, large overturning moments would result which would have to be overcome by the tip floats.

Tests of the modified wing indicated that changing the airfoil contour of the outer wing panel (from an NACA 230 series to an NACA 44 series at the tip) did not materially change the longitudinal-stability characteristics from that of the original wing. The stalling characteristics, however, were improved by the modification by giving a gradual stall over the wing which resulted in a flat-top lift curve.

Langley tank model 180 hull in combination with the modified outer wing panels gave approximately the same longitudinal stability as the original JRM-1 hull with the same wing and tail combination; however, slightly more effective dihedral and directional stability were evident for the large hull.

INTRODUCTION

At the request of the Bureau of Aeronautics, Navy Department, wind-tunnel tests were made to investigate the aerodynamic characteristics of a 1/25-scale powered model of the Martin JRM-1 airplane. Results of a preliminary investigation of the original model have been presented in reference 1, while the results of investigations of the model equipped with a 1/25-scale XPB2M-1R tail assembly and with various modifications of the JRM-1 tail assembly have been given in references 2 and 3, respectively.

The present paper includes the results of an investigation of the original model with a ground board in place and an investigation of the model with modified outer wing panels. The latter investigation consists of a series of tests with the JRM-1 hull which was designed for 145,000 pounds and a second series of tests with a hull designed by the Hydrodynamics Division of the Langley Laboratory for a contemplated 165,000-pound version of the JRM-1 (Langley tank model 180).

The ground-board investigation included conventional landing tests with the model mounted above the ground board with just enough clearance to reach the angle of attack for stall and tests with the model mounted in the ground board to simulate water taxying conditions. The latter tests were designed to provide general information necessary for evaluating the aerodynamic forces and moments with a cross wind at low speeds during the take-off, and the righting moments required of tip floats during low-speed taxying.

The investigation of the modified outer wing panel, which was designed to improve the stalling characteristics of the wing, con-

sisted of tuft studies and force tests to determine stalling characteristics. The effect of the wing modification on the longitudinal and lateral stability of the model was also determined.

Tests with the model 180 hull were a duplication of the power-off part of the longitudinal- and lateral-stability tests with the JRM-1 hull mentioned above, and were made to find the effect of the change in hull contour on the aerodynamic characteristics of the model. No power-on tests were made with the model 180 hull.

COEFFICIENTS AND SYMBOLS

The results of the tests are presented as standard NACA coefficients of forces and moments. Rolling-, yawing-, and pitching-moment coefficients are given about the center-of-gravity location shown in figure 1. The data are referred to the stability axes, which are a system of axes having their origin at the center of gravity and in which the Z-axis is in the plane of symmetry and perpendicular to the relative wind, the X-axis is in the plane of symmetry and perpendicular to the Z-axis, and the Y-axis is perpendicular to the plane of symmetry. The positive directions of the stability axes, of angular displacements of the airplane and control surfaces, and of hinge moments are shown in figure 2.

The coefficients and symbols are defined as follows:

C_L lift coefficient (Lift/qS)

C_X longitudinal-force coefficient (X/qS)

C_Y lateral-force coefficient (Y/qS)

C_l rolling-moment coefficient (L/qSb)

C_m pitching-moment coefficient (M/qSc')

C_n yawing-moment coefficient (N/qSb)

C_h hinge-moment coefficient ($H/qb'\bar{c}^2$)

T_c' effective thrust coefficient based on wing area (Thrust/qS)

nD/V propeller diameter-advance ratio

Lift = -Z

X, Y, Z	forces along axes, pounds
L, M, N	moments about axes, pound-feet
H	hinge moment of control surface, pound-feet
T_e	propeller effective thrust, (total for four engines), pounds
q	free-stream dynamic pressure, pounds per square foot ($\rho V^2/2$)
q_t	effective dynamic pressure at tail, pounds per square foot
S	wing area of model (5.90 sq ft)
S_t	horizontal-tail area of model (1.315 sq ft)
c	airfoil section chord, feet
c'	wing mean aerodynamic chord (M.A.C.), (0.830 ft)
$\bar{c}$	root-mean-square chord of a control surface back of hinge line, feet
b	wing span of model (8.00 ft)
b'	control-surface span along hinge line, feet
V	air velocity, feet per second
D	propeller diameter (0.667 ft)
n	propeller speed, revolutions per second

and

ρ	mass density of air, slugs per cubic foot
α	angle of attack of hull base line, degrees
ϕ	angle of roll, degrees
ψ	angle of yaw, degrees
ϵ	average downwash angle at the tail, degrees

i_t angle of stabilizer with respect to hull base line, degrees, positive when trailing edge is down

δ control-surface deflection, degrees

β propeller blade angle at 0.75 radius, degrees

F_W wheel force, pounds

n_p neutral-point location, percent wing mean aerodynamic chord (center-of-gravity location for neutral stability in trimmed flight)

c.g. center of gravity

R.N. Reynolds number

Subscripts:

e elevator

f flap

t horizontal tail

ψ denotes partial derivatives of a coefficient with respect to yaw $\left(\text{example: } C_{l_\psi} = \partial C_l / \partial \psi\right)$

MODEL AND APPARATUS

The Martin JRM-1 airplane is a four-engine personnel and cargo-transport flying boat of 145,000-pound-design gross weight having a maximum of 9000 brake horsepower available for take-off. Specifications of this airplane are given in tables I and II. The permissible limits for the center-of-gravity travel (fig. 3) were obtained from reference 4. The airplane loading within these limits is not specified.

A three-view drawing of the model as originally received from the Glenn L. Martin Company is presented in figure 1. A drawing of the model mounted above the ground board for the conventional landing tests and a photograph of the model set in the ground board for simulated on-the-water tests are presented in figures 4 and 5, respectively. The ground board, which was specially constructed for this investigation, had a built-in turntable designed to rotate with

the model. A rectangular section, large enough to accommodate the hull, was cut out of the turntable to permit the ground board to be raised around the model to simulate various drafts of the hull corresponding to specified loading conditions. The center of the turntable was located directly below the normal center of gravity of the model and the two were rotated as a unit when the model was yawed through the desired range. The hull contour at the water line (top surface of ground board) was approximated by attaching cardboard to the turntable. (See fig. 5.) The draft was measured from the point of the step up to the water line (top surface of ground board).

For the investigation with the modified outer wing panels, the original wing which had an airfoil section which varied from an NACA 23020 at the root to an NACA 23012 at the theoretical tip (48-inch station) was cut off at a point 21 inches from the center line of the model (fig. 6), and the outer panel replaced by one which varied from the NACA 23018.65 section at the 21-inch station to an NACA 4413.35 section at the 45.61-inch station. The intermediate sections were determined by connecting corresponding chordwise stations of the cut section (21-inch station) and the 45.61-inch station by straight lines. The tips were made to conform to the plan form of the original tips. The new outer panels were given geometric twist of 2.7° so that the wing would have no aerodynamic twist.

Langley tank model 180 designed by the Hydrodynamic Division of the Langley Laboratory represents a hull for a large long-range transport seaplane having a design gross weight of 165,000 pounds. A comparison of the JRM-1 hull and model 180 showing their relative disposition about the normal center of gravity is given in figure 7. Model 180 shows close adherence to the form of a streamline body and at the time was designed to incorporate the latest improvements in hydrodynamic characteristics. Although the over-all length is greater, the length-beam ratio of hull 180 is 5.9 as compared with 6.68 for the JRM-1. Model 180 has a 30° vee step instead of the transverse step. The tail pylon of the model 180 is considerably thinner than previously designed hulls such as the JRM-1 and the aerodynamic efficiency of the vertical tail is thereby increased. The details of the design of model 180 are given in reference 5.

Although the propellers on the airplane are three bladed, the model was equipped with 8-inch-diameter (approximate scale diameter) four-blade propellers consisting of two identical two-blade wooden propellers mounted in tandem and rotated 90° with respect to each other. (See fig. 5.) The propellers used in the ground-board investigation had blade angles of 30.2° and 32.5° at 0.75 radius

and were powered by a 20-horsepower electric motor. The propellers used in the modified wing investigation had blade angles of 17.6° and 23.0° at 0.75 radius and were powered by four individual 5-horsepower motors, one motor being mounted in each nacelle. The speed of the motors was determined by an electric tachometer whose error is within ±0.2 percent.

TESTS AND RESULTS

Test Conditions

The test conditions for the various model configurations are given in the following table:

Model configuration	q (lb/sq ft)	V (mph approx.)	Test R.N.	Effective R.N.
Landing tests original model	16.37	80	6.20×10^5	1.00×10^6
On-the-water tests original model	1.03 2.30 16.37	20 30 80	1.55 2.33 6.20	.25 .37 1.00
Modified wing JRM-1 hull	4.09 16.37	40 80	3.10 6.20	.50 1.00
Modified wing hull 180	4.09 16.37	40 80	3.10 6.20	.50 1.00

The test Reynolds number is based on the wing mean aerodynamic chord of 0.830 foot. The effective Reynolds number (for maximum lift coefficients) is based on the turbulence factor of 1.6 for this tunnel.

Corrections

The data obtained with the ground board in place were not corrected for tares caused by the model support strut because of the impracticability of obtaining tares. Jet-boundary corrections were not applied because they have been shown to be negligible for the ground-board test installation. All other data have been

corrected for tares caused by the model support strut, and jet-boundary corrections have been applied to the angles of attack, the longitudinal-force coefficients, and the tail-on pitching-moment coefficient. The corrections were computed as follows by the use of reference 6:

$$\Delta\alpha = 0.626C_L$$

$$\Delta C_X = -0.0098C_L{}^2$$

$$\Delta C_m = -4.86C_L\left(\frac{0.191}{\sqrt{q_t/q}} - 0.115\right)\left(\frac{\partial C_m}{\partial i_t}\right)$$

where $\Delta\alpha$ is in degrees. All jet-boundary corrections were added to the test data.

For the on-the-water ground-board tests (model set in the ground board) where the model was rolled as well as yawed and pitched, no corrections were applied to the data for the increased angle of roll due to deflection of the support strut under load. It is believed that this would not exceed $1/3^\circ$ for the largest rolling moment encountered in the tests. The angle of roll given in the data is the angle at zero yaw.

Test Procedure

Propeller calibrations were made by measuring the longitudinal force of the model with flaps retracted and tail off at an angle of attack of -5.5° (angle at which thrust line is level) for a range of propeller speeds. Thrust coefficients were determined from the relation

$$T_c' = C_{X(\text{propellers operating})} - C_{X(\text{propellers removed})}$$

The results of the model propeller calibrations are presented in figure 8.

The variation of thrust coefficient with lift coefficient for two power conditions, A and B, is shown in figure 9. Power A

and power B represent the full-scale thrust conditions for an airplane weight of 145,000 and 90,000 pounds, respectively, at a take-off brake horsepower of 9000. The thrust coefficients of the airplane were reproduced during power-on tests by using figures 8 and 9 to match the propeller speed and lift coefficient of the model.

Static longitudinal stability and control of the model near the ground were determined from the conventional landing tests made throughout the angle-of-attack range at various stabilizer and elevator settings with flaps deflected 40° and the propellers operating at zero thrust. To determine the aerodynamic forces and moments associated with an airplane in a cross wind on the water, yaw tests were made with the model pitched and rolled to various attitudes which the airplane might assume while taxying or taking off. The tests were made at various thrust coefficients to correspond to certain desired velocities and thrust on the full-scale airplanes. These thrust coefficients, corresponding to the full-scale conditions, are given in the following table:

Thrust condition	V (fps)	T_c'
Maximum	40	4.500
Maximum	60	1.765
Maximum	90	.753
1/4 maximum	110	.119
Maximum	120	.397

At each angle of attack for the power-on yaw tests the propeller speeds were held constant throughout the yaw range approximating a constant power output.

Propellers of large pitch were used in the model tests to secure the high thrust conditions that were requested which necessitated deviation from the airplane torque conditions. It is estimated that the torque coefficients developed by the model propellers were about twice the values for the airplane propellers.

Static longitudinal-stability characteristics of the model with the modified outer wing panels were determined from pitch tests for various power conditions and flap configurations. Lateral-stability derivatives were obtained from pitch tests at angles of yaw of ±5° by assuming linear characteristics over this small yaw range.

Presentation of Data

The results of the tests are presented in figures 10 to 38 which are grouped as indicated in the following outline:

Data	Figure
I. Ground-board tests (original model)	
A. Longitudinal stability and control in landing	
1. Stabilizer and elevator data	10 to 11
2. Neutral points, downwash, q ratios, and elevator trim positions	12 to 14
B. Cross-wind characteristics during landing, taxying, and take-off maneuvers	
1. Landing, negative draft ($\psi = \pm 30^\circ$, draft = -0.96 in.)	15 to 16
2. Taxying and take-offs ($\psi = \pm 30^\circ$, draft = -0.96 in.)	17 to 18
3. Taxying and take-offs ($\psi = 0^\circ$ to 90°, draft = 1.80 in.)	19 to 20
II. Modified outer-wing panels (original hull)	
A. Longitudinal stability	
1. Stabilizer effectiveness (various power conditions)	21 to 22
2. Neutral points, downwash, q ratios	23
B. Stalling characteristics	
1. Tuft studies (sketches and photographs showing effect of windmilling propellers and power on stall progression)	24 to 27
2. Force tests	28 to 29
C. Lateral stability	
1. Stability derivatives	30 to 31
2. Effect of tail ($\psi = \pm 30^\circ$)	32
III. Hull model 180 with modified outer wing panels	
A. Longitudinal stability	
1. Stabilizer effectiveness	33 to 34
2. Neutral points	35
B. Lateral and directional stability	
1. Stability derivatives	36 to 37
2. Effect of tail ($\psi = \pm 30^\circ$)	38

DISCUSSION

Original Model (Ground-Board Tests)

Longitudinal stability and control in landing.- The data of figures 10 and 11, respectively, have been used to make an evaluation of the longitudinal stability and control characteristics of the JRM-1 airplane in a landing configuration clear of the water ($\delta_f = 40^\circ$, $T_c' = 0$ with the ground board in place simulating the presence of water).

The stick-fixed neutral points are presented in figure 12 and are compared with those obtained without the ground board (fig. 18, reference 1). The neutral points were calculated by the graphical method given in reference 7.

The neutral points show greater stability with the ground board in place than without it as would be expected. This shift of neutral point varies from 2-percent mean aerodynamic chord at low lift coefficients to 7-percent at high lift coefficients. The downwash and dynamic-pressure ratios for the test condition are given in figure 13 along with data without the ground board, taken from reference 1. As would be expected, the rate of change of downwash with angle of attack $d\epsilon/d\alpha$ is less with the ground board in place than without the ground board, which explains to a large degree the greater stability of the model with the ground board in place.

The elevator-control characteristics are presented in figures 12 and 14. The elevator appears to be powerful enough to trim the model throughout the range of lift coefficients and specified range of centers of gravity shown in figure 12. Figure 14 shows the estimated elevator deflection required for trim and the corresponding wheel forces for the normal center of gravity. The elevator wheel forces were calculated assuming zero tab deflection, an elevator linkage factor of 0.433, and an elevator boost ratio of 0.825.

Lateral stability during taxying, take-off, and landing.- Figures 15 and 16 show the characteristics of the model in a landing or take-off attitude clear of the water as is noted by the negative draft. Figures 17 to 20 show the characteristics of the model during taxying and take-offs on the water at various attitudes of pitch, roll, yaw, and draft.

The effective dihedral of the model in the presence of the ground board is considerably larger than when the model is not in the presence of the ground board. For example, without the ground board $C_{l_\psi} = 0.0004$ (fig. 27, reference 1) whereas with the ground board in place (fig. 15) $C_{l_\psi} = 0.0016$ at $C_L = 0.92$. The dihedral effect becomes even greater with the model rolled and the hull set within the ground board resulting in large overturning moments which will have to be equalized by the floats. (See figs. 19 and 20.) The maximum values of these rolling or overturning moments ($C_l \approx 0.23$) were obtained with the highest thrust coefficient between angles of yaw of 50° and 70°. (See fig. 19(a).) The maximum values of the rolling-moment coefficients are probably slightly smaller than would have been obtained had the airplane torque coefficient been simulated. An indication of the model torque coefficient is given by the value of C_l at $\psi = 0°$ (figs. 17 to 20) which is about half the torque of the propeller, the remainder being accounted for by the nullifying effect of wing interference.

The yawing-moment-coefficient curves indicate that the model generally possesses directional stability to about 20° yaw and restoring moments to 90° yaw. The decline of the yawing moments at angles of yaw greater than 20° is probably due to stall over the vertical tail. The thrust, however, introduces considerable variation in the magnitude of the yawing moments, especially at the larger thrust coefficients.

Original Hull with Modified Outer Wing Panels

Longitudinal stability.- The neutral points (computed from the data presented in figs. 21 and 22) for the model with the modified outer wing panels are compared with those of the original model (reference 1) in figure 23. The comparison indicates that the longitudinal stability of the model with the modified outer wing panels is approximately the same as the original model for most power and flap conditions. Both models show a considerable margin of instability for the rearmost center of gravity. For one condition, power B, $\delta_f = 0°$, the original model shows a smaller margin of stability at high lift coefficients than the modified wing model, but the difference may be the result of fairing of the curves and small inaccuracies that occurred in the original model data.

Stalling characteristics.- The stalling characteristics of the model were determined by photographs of the tufted wing.

Sketches were made from tuft photographs for the propeller-off condition, and a comparison with the original wing (reference 1) is shown in figures 24 and 25. The results of the stall studies of the modified wing with windmilling propellers are also shown in figures 24 and 25. Photographs of the tufted model with the application of power A are given in figures 26 and 27.

A comparison of the tuft studies (propellers off, flaps up, fig. 24) of the new wing with those of the original wing show that the flow is essentially the same up to an angle of attack of about 11°. In both cases, separation starts near the trailing edge of the wing between the engine nacelles at an angle of attack of about 4° and gradually spreads outward and forward. Increasing the angle of attack beyond 11° causes the tips on the original wing to stall suddenly, while, with the modified outer panels, the stall continues to spread gradually outward until the outermost tips finally stall at an angle of attack of about 17°. With the flaps deflected 40° (fig. 25), the stall progression appears to be quite similar to the case with undeflected flap. The original wing stalls completely at an angle of attack of about 11°, while the modified wing maintains lift at the tips, even at 13°.

A comparison of the tuft studies with power on (figs. 26 and 27) with those of figures 45 and 46 (reference 1) shows stalling characteristics similar to those noted above for the power-off condition. Separation is delayed by the new outer panels, and the stalling angle is consequently increased with the tips maintaining lift up to the highest angle of attack tested which results in a flat-top lift curve. This results in a higher maximum value of C_L (figs. 28 and 29) and probably an improvement in aileron effectiveness.

It is interesting to note how the propeller rotation influences the stall behind the nacelles. At a large angle of attack (α = 12.4°, fig. 27) the stall has progressed to a point on the trailing edge inside of the left outboard nacelle while on the right side of the wing the stalled area along the trailing edge has only reached the point where the new panel is attached.

Lateral stability.- The effect of power, lift coefficient, and flaps on the lateral-stability parameters is shown in figures 30 and 31.

With the modified wing panels the model generally possesses less positive dihedral effect than the original model (reference 1). However, one condition (power A, δ_f = 0°) indicates the opposite: more dihedral effect with the modified wing than with the original

wing. The difference in effective dihedral is as much as 2° with flaps up, and 5° with flaps extended.

Hull Model 180 with Modified Outer Wing Panels

Longitudinal stability.– A comparison of the neutral points of hull 180 with those of the JRM–1 hull (fig. 35), indicates that the longitudinal stability of the hulls is approximately the same throughout most of the lift range. The difference in neutral-point position near maximum lift is within the accuracy of the method employed in determining the neutral points.

Lateral and directional stability.– The lateral-stability parameters for hull 180 and the JRM–1 hull are compared in figures 36 and 37 for the windmilling condition. Hull 180 shows slightly more directional stability and greater effective dihedral throughout the lift range than the JRM–1 model for both flap configurations. The greater directional stability is probably the result of model 180 having a thinner tail pylon which would increase the aerodynamic efficiency of the whole surface.

The tail–on and tail–off characteristics of hull 180 at large angles of yaw are shown in figure 38 for the flaps–up configuration.

CONCLUSIONS

Results of wind–tunnel tests of the 1/25–scale model of the Martin JRM–1 airplane with the ground board in place, with the modified outer wing panels, and with a hull of different design (Langley tank model 180) indicated the following conclusions:

1. With the ground board in place, simulating a landing attitude, the elevator of the original model appeared to be powerful enough to trim the model at any lift coefficient within the specified range of center of gravity.

2. The ground–board tests for evaluating aerodynamic forces and moments on an airplane involved in a cross wind during taxying at low speed during the take–off showed that the model had high dihedral effect and possessed large overturning moments which would have to be corrected by the tip floats. Considerable variations in the magnitude of the yawing moments also existed as a result of the high thrust coefficient.

3. Changing the airfoil contour of the outer wing panel (from an NACA 230 series to an NACA 44 series at the tip) did not materially change the longitudinal-stability characteristics. The stalling characteristics were improved by obtaining a gradual stall over the wing which resulted in a flat-top lift curve. For most power and flap conditions tested, the modified outer wing panels generally gave less dihedral effect than the original wing.

4. Langley tank model 180 hull in combination with the modified outer wing panels gave approximately the same longitudinal stability as the JRM-1 hull, with the same wing and tail combination; however, slightly more effective dihedral and directional stability were evident for hull 180.

Langley Memorial Aeronautical Laboratory
National Advisory Committee for Aeronautics
Langley Field, Va.

Vernard E. Lockwood
Vernard E. Lockwood
Aeronautical Engineer

Bernard J. Smith
Aeronautical Engineer

Approved: Thomas A. Harris.

Thomas A. Harris
Chief of Stability Research Division

DBC

REFERENCES

1. Lockwood, Vernard E., and Smith, Bernard J.: Wind-Tunnel Tests of the 1/25-Scale Powered Model of the Martin JRM-1 Airplane. I - Preliminary Investigation - TED No. NACA 232. NACA MR No. L5E28, Bur. Aero., 1945.

2. Lockwood, Vernard E., and Smith, Bernard J.: Wind-Tunnel Tests of the 1/25-Scale Powered Model of the Martin JRM-1 Airplane. II - Aerodynamic Characteristics with XPB2M-1R Tail - TED No. NACA 232. NACA MR No. L6D04, Bur. Aero., 1946.

3. Smith, Bernard J., and Lockwood, Vernard E.: Wind-Tunnel Tests of the 1/25-Scale Powered Model of the Martin JRM-1 Airplane. III - Effect of Tail Configuration on Longitudinal Stability - TED No. NACA 232. NACA MR No. L6G18, Bur. Aero., 1946.

4. Anon.: Detail Specification for Model JRM-1 Airplane Class VJR Personnel and Cargo Transport Airplane (Four Engine). NAVAER SD-322-1, Bur. Aero., Aug. 2, 1943.

5. Parkinson, John B., Olson, Roland E., and Haar, Marvin I.: Tank Investigation of a Powered Dynamic Model of a Large Long-Range Flying Boat - Langley Tank Model 180. NACA TN No. 1237, 1947.

6. Swanson, Robert S., and Schuldenfrei, Marvin J.: Jet-Boundary Corrections to the Downwash Behind Powered Models in Rectangular Wind Tunnels with Numerical Values for 7- by 10-Foot Closed Wind Tunnels. NACA ARR, Aug. 1942.

7. Schuldenfrei, Marvin: Some Notes on the Determination of the Stick-Fixed Neutral Point from Wind-Tunnel Data. NACA RB No. 3120, 1943.

TABLE I

PHYSICAL CHARACTERISTICS OF THE MARTIN JRM-1 AIRPLANE

Type . . . . . Personnel and cargo transport (flying boat)

Engines (four):

Manufacturer's designation	R-3350-8
Ratings:	
Normal power	2000 bhp at 2400 rpm at sea level 1800 bhp at 2400 rpm at 13,600 ft
Take-off power	2250 bhp at 2600 rpm at sea level
Propeller gear ratio	16:7

Propeller:

Type	Curtiss 1016
Diameter, ft	16.5
Blade design	1016-104-18
Number of blades	3
Activity factor	91.0
Side-force factor	76.5

NATIONAL ADVISORY
COMMITTEE FOR AERONAUTICS

TABLE II

AIRPLANE WING AND TAIL-SURFACE DATA

	Wing	Horizontal tail	Vertical tail
Area, sq ft	3686.0	822.4	373.6
Span, ft	200.00	61.67	23.33
Aspect ratio	10.85	4.58	1.46
Taper ratio	0.254	0.643	0.530
Dihedral, deg	[a]0	[b]8.0	-----
Sweepback, leading edge, deg	3.68	8.05	11.65
Root section	NACA 23020	NACA 0015-63	NACA 0009-63
Tip section	NACA 23012	NACA 0008-63	NACA 0009-63
Angle of incidence at root, deg	5.5	3.0	-----
Angle of incidence at tip, deg	5.5	3.0	-----
Mean aerodynamic chord, ft	20.74	14.04	17.22
Root chord, ft	29.50	16.72	21.60
Theoretical tip chord, ft	7.50	10.76	11.46

[a]Dihedral measured on upper surface.
[b]Dihedral measured on chord line.

NATIONAL ADVISORY
COMMITTEE FOR AERONAUTICS

FIGURE LEGENDS

Figure 1.- $\frac{1}{25}$-scale model of the Martin JRM-1 airplane.

Figure 2.- System of axes and control-surface hinge moments and deflections. Positive values of forces, moments, and angles are indicated by arrows. Positive values of tab hinge moments and deflections are in the same directions as the positive values for the control surfaces to which the tabs are attached.

Figure 3.- JRM-1 center-of-gravity location on mean aerodynamic chord.

Figure 4.- Position of the $\frac{1}{25}$-scale model of Martin JRM-1 airplane and the ground board in the wind tunnel, $\alpha = 0^\circ$.

Figure 5.- The $\frac{1}{25}$-scale model of Martin JRM-1 airplane set in the ground board for on-the-water tests. Draft = 1.8 inches, $\phi = 3^\circ$, $\delta_f = 20^\circ$, $\alpha = 5.9^\circ$.

Figure 6.- Geometry of modified outer wing panels for $\frac{1}{25}$-scale model of Martin JRM-1 airplane. (Spanwise stations refer to distance from model centerline. All dimensions in inches.)

Figure 7.- Comparison of hull lines of original JRM-1 model (145,000 lb) and Langley Tank model 180 (165,000 lb). $\frac{1}{25}$-scale, (Dimensions in inches)

Figure 8.- Variation of thrust coefficient with propeller diameter-advance ratio of 8-inch-diameter four-blade propellers on $\frac{1}{25}$-scale model of Martin JRM-1 airplane. $\alpha = -5.5^\circ$.

Figure 9.- Thrust coefficient available at any lift coefficient for the Martin JRM-1 airplane. Total take-off power 9000 BHP.

Figure 10.- The effect of the stabilizer on the aerodynamic characteristics in pitch of the $\frac{1}{25}$-scale model of Martin JRM-1 airplane. Ground board in place. $\phi = 0^\circ$, $T_c' = 0$, $q \cong 16.37$ lb per sq ft, $\beta = 30.2^\circ$, δ_f 40°, $(\text{Draft})_{\alpha=0^\circ} = 2.1$ in.

FIGURE LEGENDS.- Continued

Figure 11.- The effect of elevator deflection on the aerodynamic characteristics of the $\frac{1}{25}$-scale model of Martin JRM-1 airplane. Ground board in place, $\phi = 0^\circ$, $T_c' = 0$, $q = 16.37$ lb per sq ft, $\beta = 30.2^\circ$, $\delta_f = 40^\circ$, $i_t = 3^\circ$, $(\text{Draft})_{\alpha=0^\circ} \cong -2.1$ in.

Figure 11.- Continued.

Figure 11.- Concluded.

Figure 12.- Elevator-fixed neutral points and trim ranges for $\frac{1}{25}$-scale model of Martin JRM-1 airplane. Ground board in place. $i_t = 3.0^\circ$, $\delta_f = 40^\circ$, $T_c' = 0$. Vertical location of c.g. at 29.8-percent M.A.C.

Figure 13.- The effect of the ground board on the dynamic pressure ratios and downwash at the tail of $\frac{1}{25}$-scale model of the Martin JRM-1 airplane, $\delta_f = 40^\circ$.

Figure 14.- Estimated elevator angle and wheel force required for trim for the Martin JRM-1 airplane. Estimate made from model tests with ground board in place (fig. 11).

Figure 15.- Effect of angle of attack on the aerodynamic characteristics in yaw of $\frac{1}{25}$-scale model of Martin JRM-1 airplane. Draft = -0.96 in., $\phi = 0^\circ$, $T_c' = 0.119$, $q = 16.37$ lb per sq ft. $\beta = 30.2^\circ$, $\delta_f = 0^\circ$.

Figure 15.- Concluded.

Figure 16.- Effect of angle of attack on the aerodynamic characteristics in yaw of $\frac{1}{25}$-scale model of Martin JRM-1 airplane. Draft = -0.96 in., $\phi = 0^\circ$, $T_c' = 0.119$, $q = 16.37$ lb per sq ft, $\beta = 30.2^\circ$, $\delta_f = 55^\circ$.

Figure 16.- Concluded.

Figure 17.- Effect of thrust on the aerodynamic characteristics in yaw of $\frac{1}{25}$-scale model of Martin JRM-1 airplane. Draft = 0.96 in, $\phi = 5.0^\circ$, $q = 2.30$ lb per sq ft, $\beta = 32.5$, $\delta_f = 0^\circ$.

(a) $\alpha = 1.9^\circ$

FIGURE LEGENDS.- Continued

Figure 17.- Continued.

(a) Concluded.

Figure 17.- Continued.

(b) $\alpha = 5.9^\circ$.

Figure 17.- Continued.

(b) Concluded.

Figure 17.- Continued.

(c) $\alpha = 7.9^\circ$.

Figure 17.- Concluded.

(c) Concluded.

Figure 18.- Effect of thrust on the aerodynamic characteristics in yaw of $\frac{1}{25}$-scale model of Martin JRM-1 airplane. Draft = 0.96 in, $\phi = 5.0^\circ$, $q = 2.30$ lb per sq ft, $\beta = 32.5^\circ$, $\delta_f = 20^\circ$.

(a) $\alpha = 1.9^\circ$.

Figure 18.- Continued.

(a) Concluded.

Figure 18.- Continued.

(b) $\alpha = 5.9^\circ$.

Figure 18.- Continued.

(b) Concluded.

Figure 18.- Continued.

(c) $\alpha = 7.9^\circ$.

FIGURE LEGENDS.- Continued

Figure 18.- Concluded.

(c) Concluded.

Figure 19.- Effect of thrust on the aerodynamic characteristics in yaw of $\frac{1}{25}$-scale model of Martin JRM-1 airplane. Draft = 1.8 in, $\phi = 3.0^\circ$, $\beta = 32.5^\circ$, $\delta_f = 0^\circ$.

(a) $\alpha = 1.9^\circ$

Figure 19.- Continued.

(a) Concluded.

Figure 19.- Continued.

(b) $\alpha = 5.9^\circ$

Figure 19.- Concluded.

(b) Concluded.

Figure 20.- Effect of thrust on the aerodynamic characteristics in yaw of $\frac{1}{25}$-scale model of Martin JRM-1 airplane. Draft = 1.8 in., $\phi = 3.0^\circ$, $\beta = 32.5^\circ$, $\delta_f = 20^\circ$.

(a) $\alpha = 1.9^\circ$.

Figure 20.- Continued.

(a) Concluded.

Figure 20.- Continued.

(b) $\alpha = 5.9^\circ$.

Figure 20.- Concluded.

(b) Concluded.

FIGURE LEGENDS.- Continued

Figure 21.- The effect of the stabilizer on the aerodynamic characteristics in pitch of the $\frac{1}{25}$-scale model of the Martin JRM-1 airplane. Modified outer wing panels. q = 4.09 lb/sq ft, $\delta_f = 0^\circ$.

(a) Power A.

Figure 21.- Continued.

(b) Power B.

Figure 21.- Concluded.

(c) Windmilling.

Figure 22.- The effect of the stabilizer on the aerodynamic characteristics in pitch of the $\frac{1}{25}$-scale model of the Martin JRM-1 airplane. Modified outer wing panels, q = 4.09 lb/sq ft, $\delta_f = 40^\circ$.

(a) Power A.

Figure 22.- Continued.

(b) Power B.

Figure 22.- Concluded.

(c) Windmilling.

Figure 23.- Neutral-point variation with lift coefficient for $\frac{1}{25}$-scale model of Martin JRM-1 airplane.

(a) $\delta_f = 0^\circ$.

Figure 23.- Concluded.

(b) $\delta_f = 40^\circ$.

Figure 24.- Interpretation of air flow over wing of $\frac{1}{25}$-scale model of Martin JRM-1 airplane from tuft photographs of the original wing (ref. 1) and modified outer wing panel. q = 16.37 lb per sq ft, $\delta_f = 0^\circ$.

FIGURE LEGENDS.- Continued

Figure 24.- Continued.

Figure 24.- Concluded.

Figure 25.- Interpretation of air flow over wing of $\frac{1}{25}$-scale model of Martin JRM-1 airplane from tuft photographs of the original wing (ref. 1) and modified outer wing panel. q = 16.37 lb per sq ft, $\delta_f = 40^\circ$.

Figure 25.- Concluded.

Figure 26.- Tuft studies of $\frac{1}{25}$-scale model of the Martin JRM-1 airplane with modified outer wing panels. Power A, $\delta_f = 0^\circ$.

Figure 26.- Continued.

Figure 26.- Continued.

Figure 26.- Concluded.

Figure 27.- Tuft studies of $\frac{1}{25}$-scale model of the Martin JRM-1 airplane with modified outer wing panels. Power A, $\delta_f = 40^\circ$.

Figure 27.- Continued.

Figure 27.- Continued.

Figure 27.- Continued.

Figure 27.- Concluded.

Figure 28.- Effect of the tail and the propellers on the aerodynamic characteristics in pitch of $\frac{1}{25}$-scale model of the Martin JRM-1 airplane. Modified outer wing panels. q = 16.37 lb per sq ft, $\delta_f = 0^\circ$.

Figure 29.- Effect of the tail and the propellers on the aerodynamic characteristics in pitch of $\frac{1}{25}$-scale model of the Martin JRM-1 airplane. Modified outer wing panels. q = 16.37 lb per sq ft, $\delta_f = 40^\circ$.

FIGURE LEGENDS.- Continued

Figure 30.- Lateral stability derivatives of the $\frac{1}{25}$-scale model of the Martin JRM-1 airplane. Modified outer wing panels. q = 4.09 lb/sq ft, $\delta_f = 0^\circ$.

Figure 31.- Lateral-stability derivatives of the $\frac{1}{25}$-scale model of the Martin JRM-1 airplane. Modified outer wing panels, q = 4.09 lb/sq ft, $\delta_f = 40^\circ$.

Figure 32.- Effect of the tail on the aerodynamic characteristics in yaw of $\frac{1}{25}$-scale model of the Martin JRM-1 airplane. $\alpha = 2.5^\circ$, $\delta_f = 0^\circ$, windmilling propellers, modified outer wing panels. q = 16.37 lb per sq ft.

Figure 32.- Concluded.

Figure 33.- The effect of the stabilizer on the aerodynamic characteristics in pitch of the $\frac{1}{25}$-scale model of a long-range flying boat; JRM-1 tail and modified outer wing panels. Hull model 180. q = 4.09 lb/sq ft, windmilling propellers. $\delta_f = 0^\circ$.

Figure 34.- The effect of the stabilizer on the aerodynamic characteristics in pitch of the $\frac{1}{25}$-scale model of a long-range flying boat; JRM-1 tail and modified outer wing panels. Hull model 180. q = 4.09 lb/sq ft, windmilling propellers. $\delta_f = 40^\circ$.

Figure 35.- Neutral point variation with lift coefficient for $\frac{1}{25}$-scale model of a long-range flying boat; JRM-1 tail and modified outer wing panels. Hull model 180. Windmilling propellers.

Figure 36.- Lateral stability derivatives of the $\frac{1}{25}$-scale model of a long-range flying boat; JRM-1 tail and modified outer wing panels. Hull model 180. q = 4.09 lb/sq ft, propellers windmilling. $\delta_f = 0^\circ$.

Figure 37.- Lateral stability derivatives of the $\frac{1}{25}$-scale model of a long-range flying boat; JRM-1 tail and modified outer wing panels. Hull model 180. q = 4.09 lb/sq ft, windmilling propellers, $\delta_f = 40^\circ$.

FIGURE LEGENDS.- Concluded

Figure 38.- Effect of the tail on the aerodynamic characteristics in yaw of the $\frac{1}{25}$-scale model of a long-range flying boat; JRM-1 tail and modified outer wing panels. Hull model 180. q = 4.09 lb/sq ft, windmilling propellers, $\alpha = 2.5^{\circ}$, $\delta_f = 0^{\circ}$.

Figure 38.- Concluded.

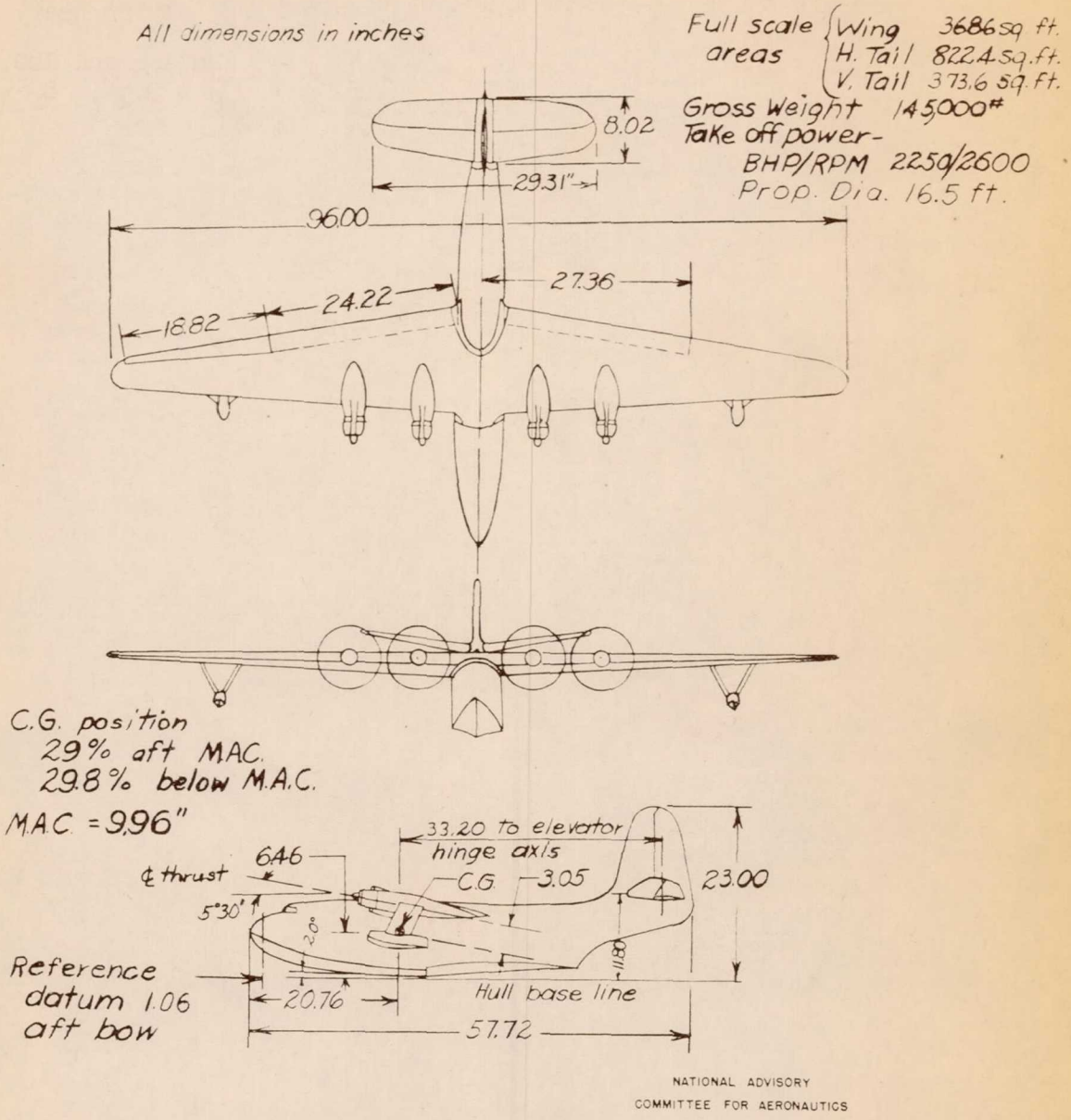

Figure 1.- 1/25-scale model of the Martin JRM-1 airplane.

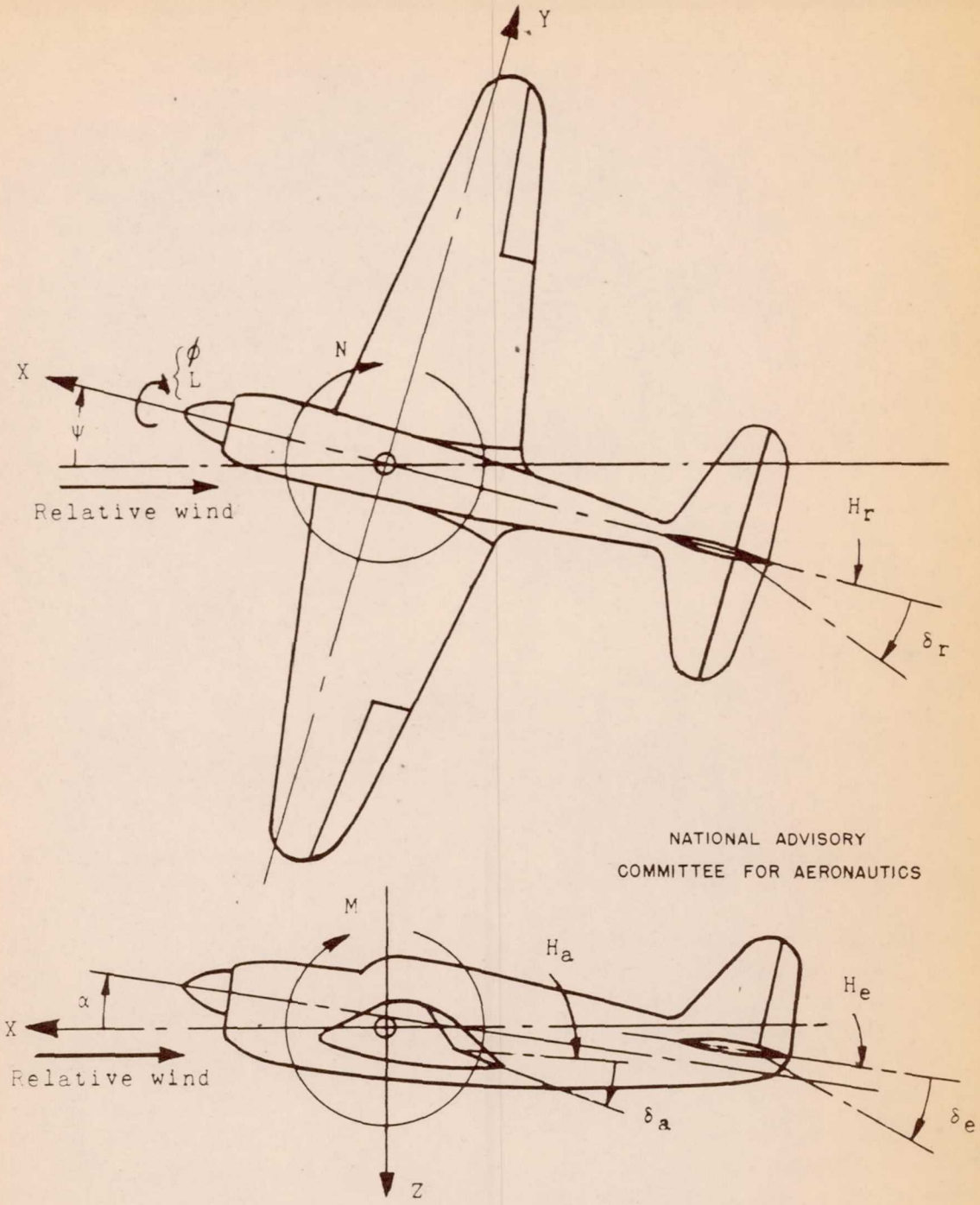

Figure 2.- System of axes and control-surface hinge moments and deflections. Positive values of forces, moments, and angles are indicated by arrows. Positive values of tab hinge moments and deflections are in the same directions as the positive values for the control surfaces to which the tabs are attached.

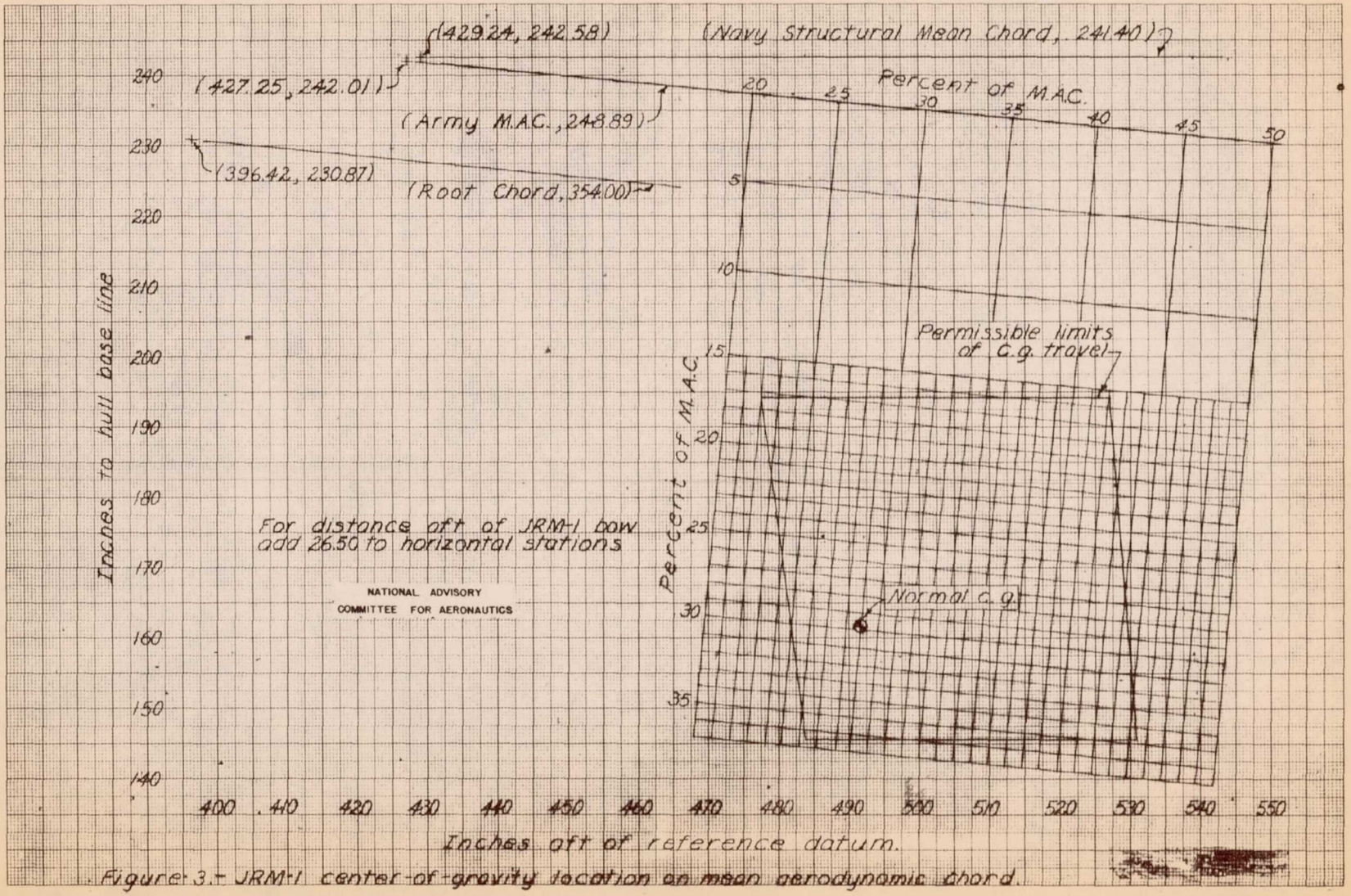

Figure 3.- JRM-1 center-of-gravity location on mean aerodynamic chord.

Fig. 3

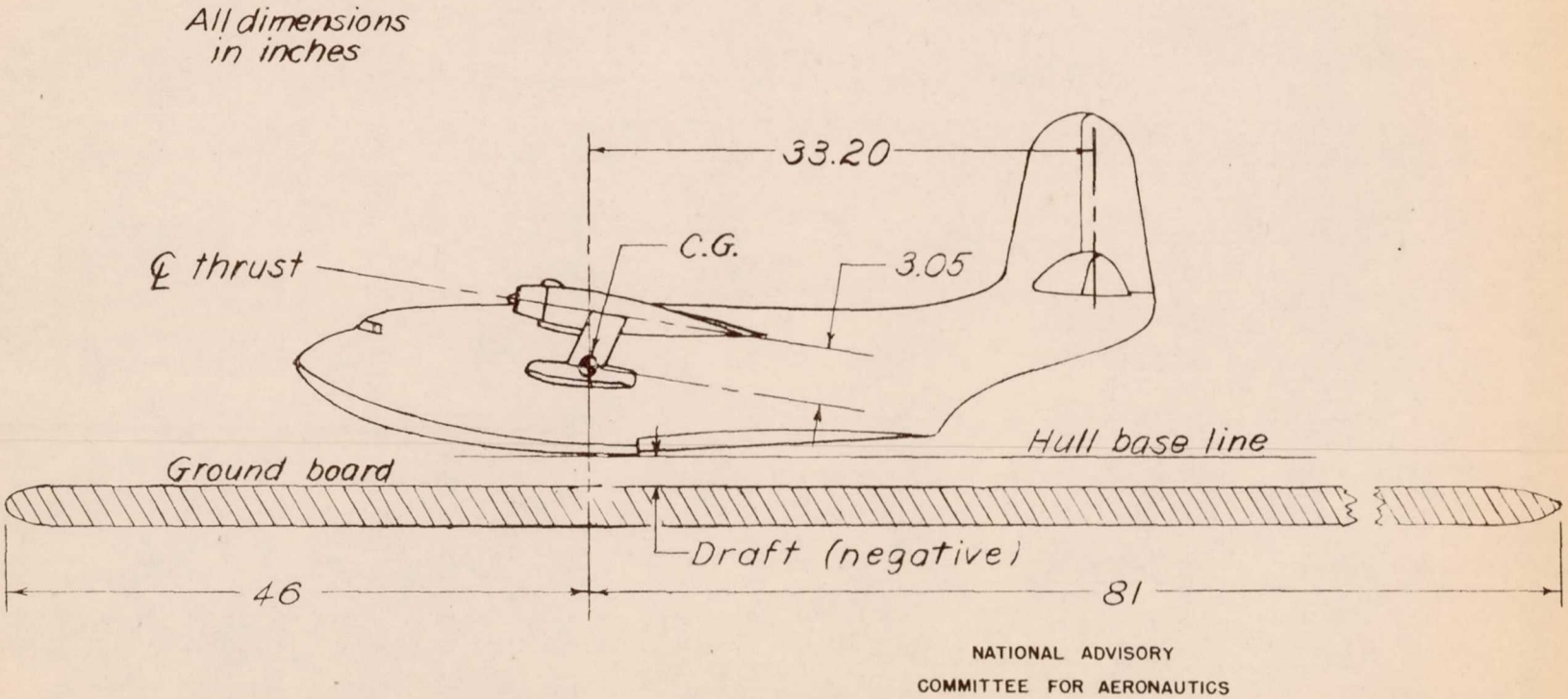

Figure 4.- Position of the 1/25-scale model of Martin JRM-1 airplane and the ground board in the wind tunnel, $\alpha = 0°$.

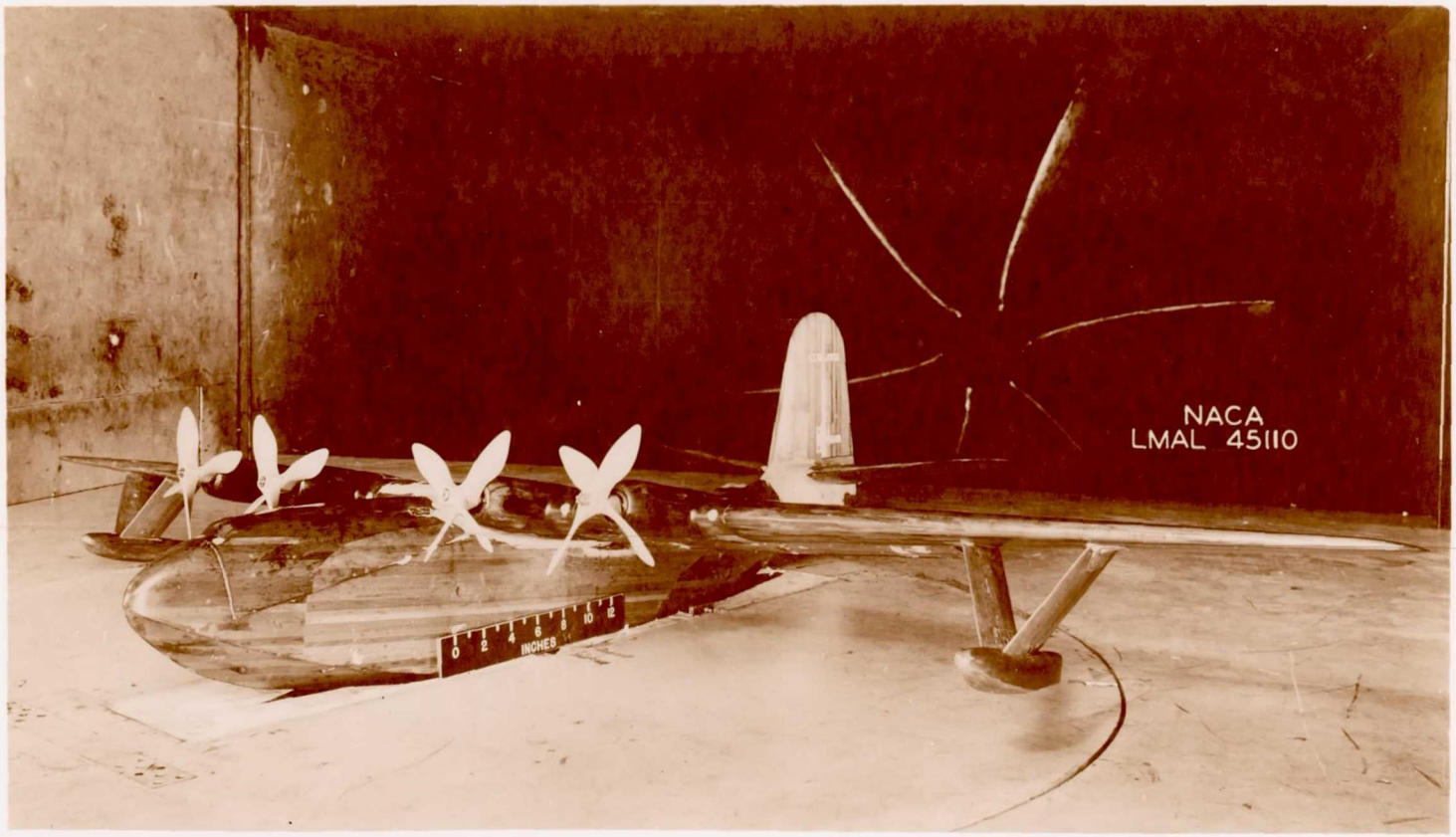

Figure 5.- The $\frac{1}{25}$-scale model of Martin JRM-1 airplane set in the ground board for on-the-water tests. Draft = 1.8 inches, $\emptyset = 3^{\circ}$, $\delta_f = 20^{\circ}$, $\alpha = 5.9^{\circ}$.

NATIONAL ADVISORY COMMITTEE FOR AERONAUTICS
LANGLEY MEMORIAL AERONAUTICAL LABORATORY - LANGLEY FIELD, VA.

Sta. 21.00 ORDINATES		
Station	Upper	Lower
0.0	0.0	0.0
.119	.407	.180
.239	.522	.267
.478	.682	.378
.716	.788	.459
.955	.868	.521
1.432	.969	.618
1.910	1.019	.685
2.388	1.039	.725
2.865	1.039	.744
3.820	.988	.734
4.775	.892	.678
5.730	.764	.591
6.685	.609	.479
7.640	.434	.346
8.595	.236	.193
9.072	.131	.109
9.550	.019	.019
L.E. Rad = 0.363		
Slope of rad = 0.305		
NACA 23018.65 airfoil		

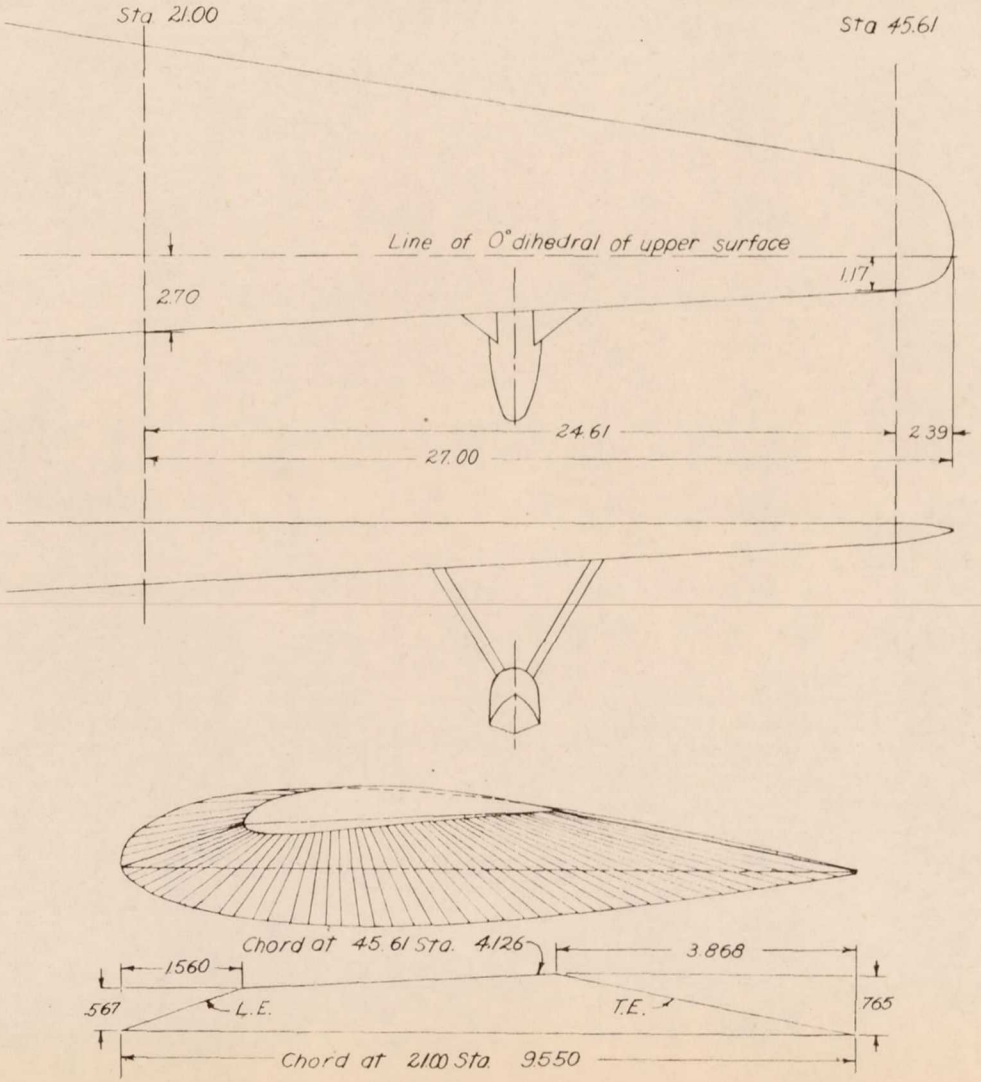

Sta. 45.61 ORDINATES		
Station	Upper	Lower
0.0	0.0	0.0
.052	.112	.066
.103	.154	.090
.206	.214	.117
.309	.259	.131
.413	.295	.139
.619	.351	.143
.825	.390	.139
1.032	.416	.131
1.238	.430	.121
1.650	.431	.101
2.063	.404	.082
2.476	.357	.062
2.888	.293	.044
3.301	.214	.028
3.713	.119	.016
3.920	.064	.010
4.126	.006	.006
L.E. Rad = 0.081		
Slope of Rad = .200		
NACA 4413.35 airfoil		

NATIONAL ADVISORY
COMMITTEE FOR AERONAUTICS

Figure 6.- Geometry of modified outer wing panels for 1/25-scale model of Martin JRM-1 airplane. (Spanwise stations refer to distance from model centerline. All dimensions in inches.)

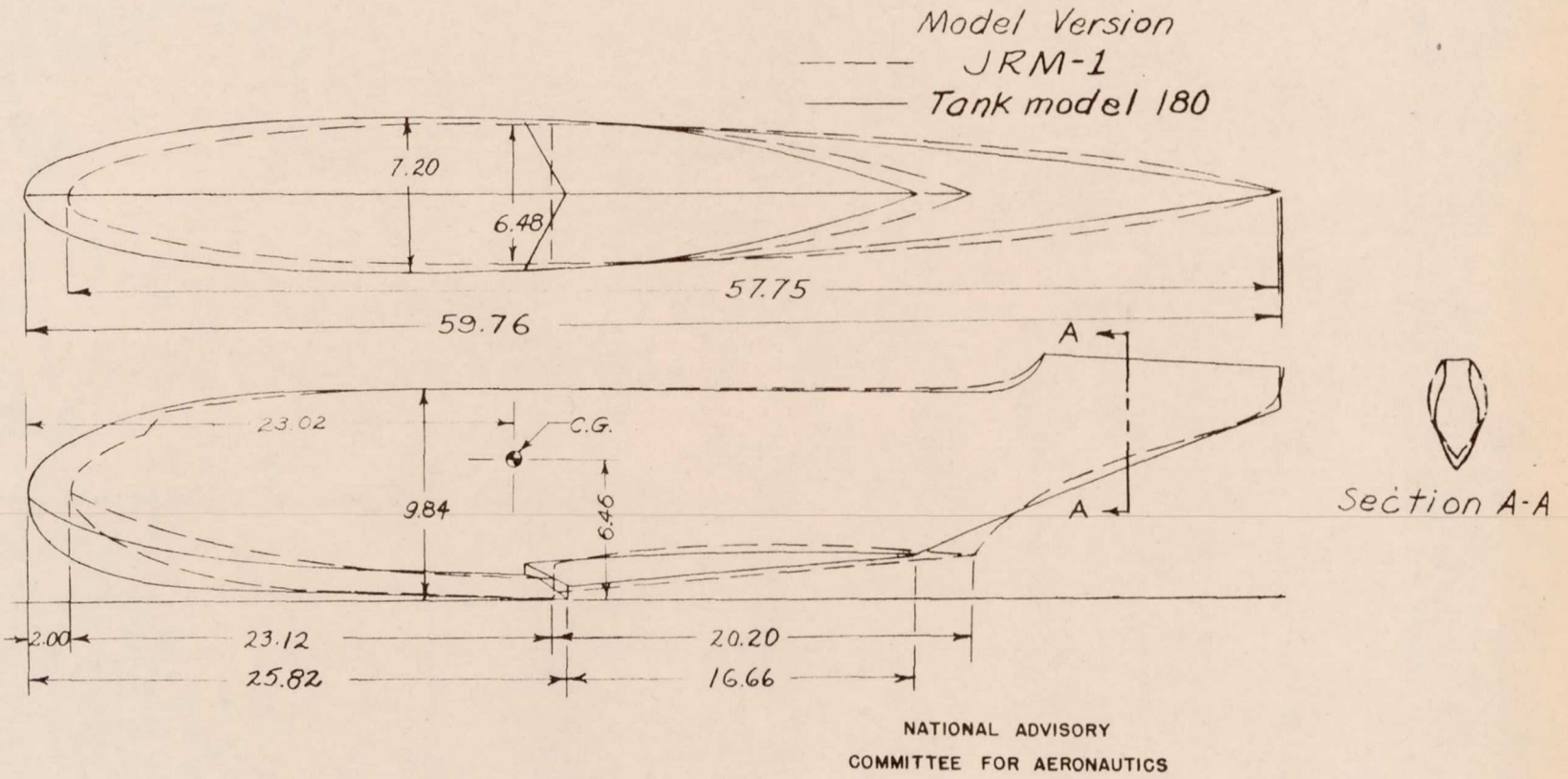

Figure 7 .-Comparison of hull lines of original JRM-1 model (145,000 lb) and Langley Tank model 180 (165,000 lb). 1/25-scale, (Dimensions in inches)

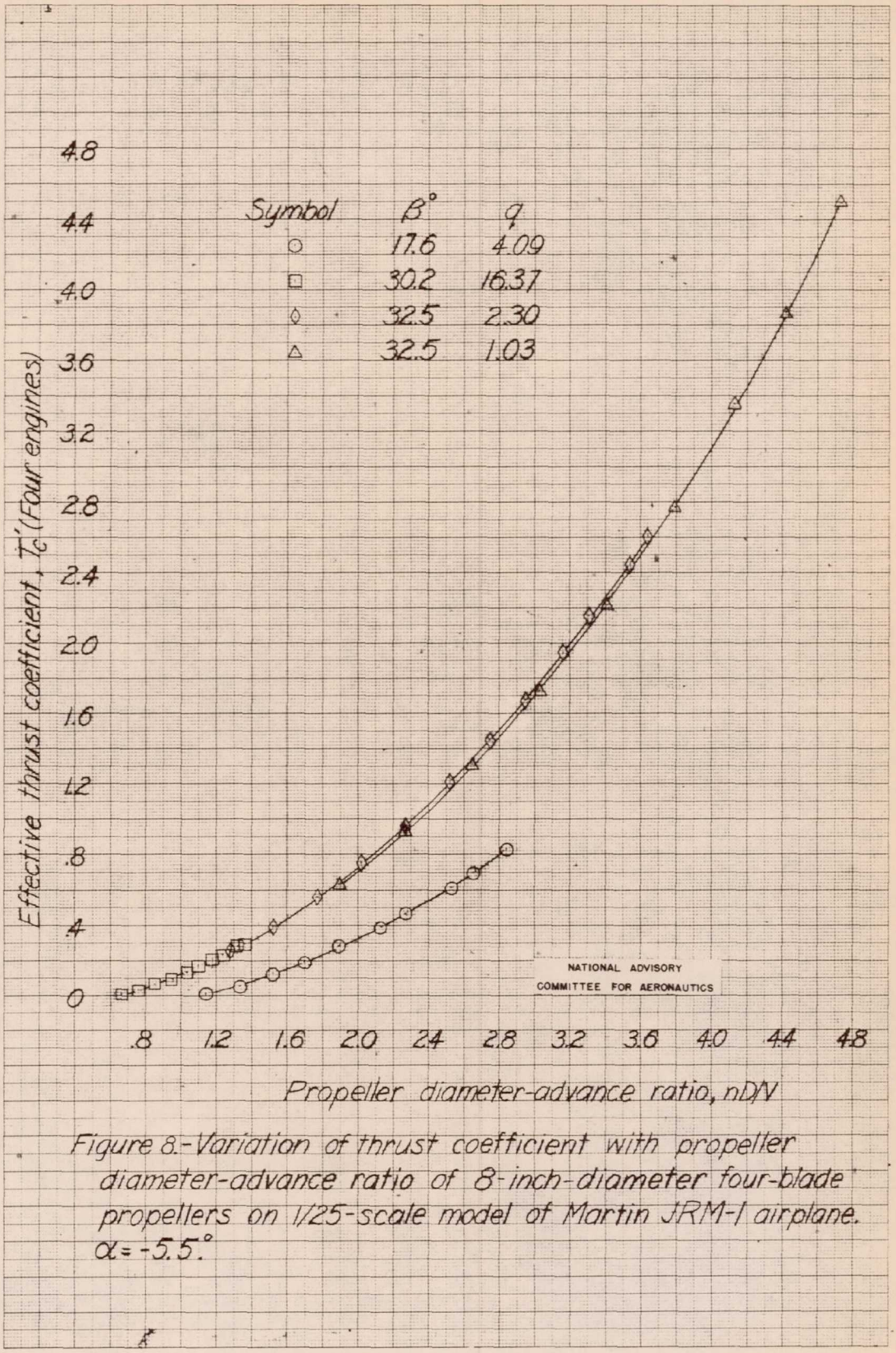

Figure 8.- Variation of thrust coefficient with propeller diameter-advance ratio of 8-inch-diameter four-blade propellers on 1/25-scale model of Martin JRM-1 airplane. $\alpha = -5.5°$.

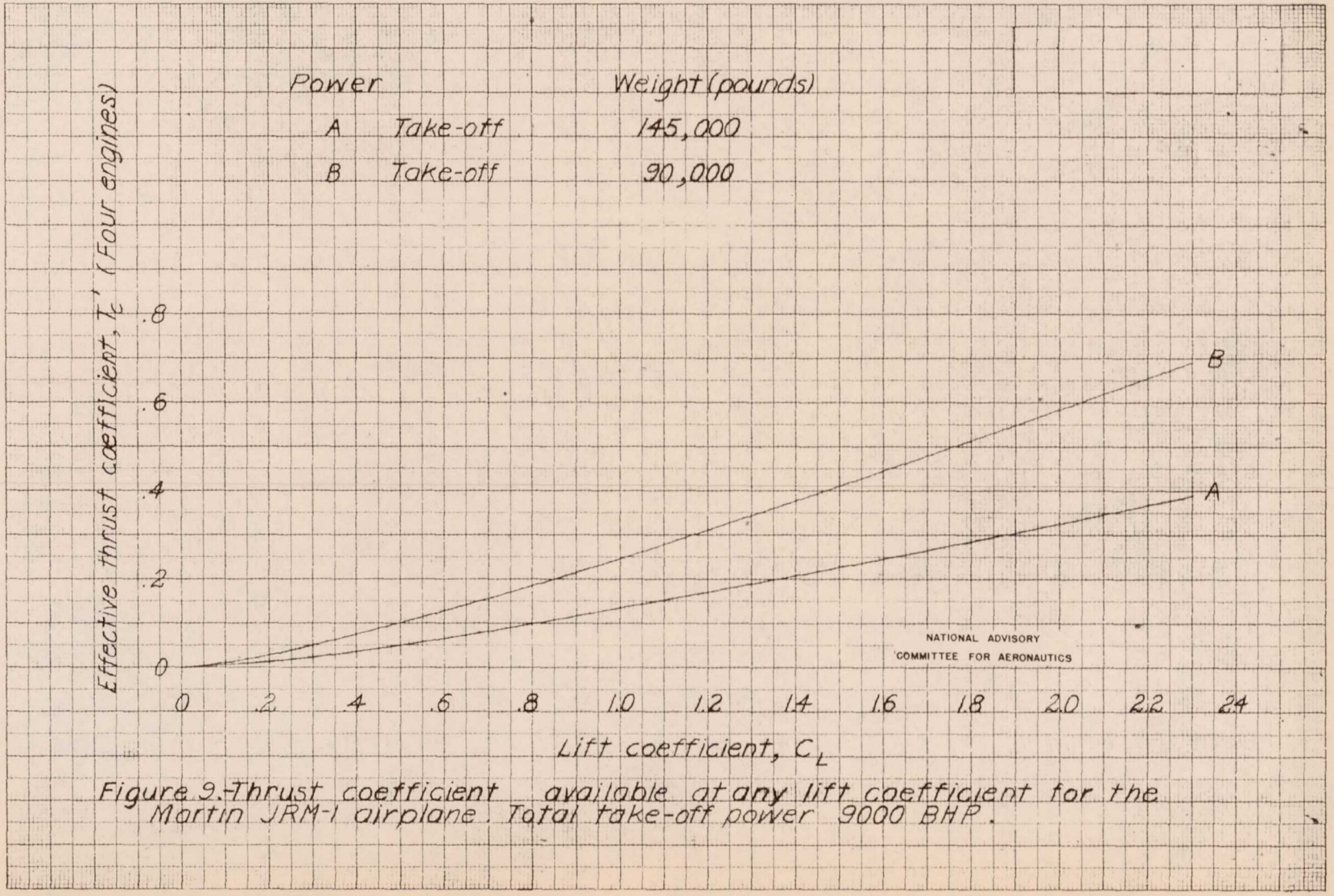

Figure 9.-Thrust coefficient available at any lift coefficient for the Martin JRM-1 airplane. Total take-off power 9000 BHP.

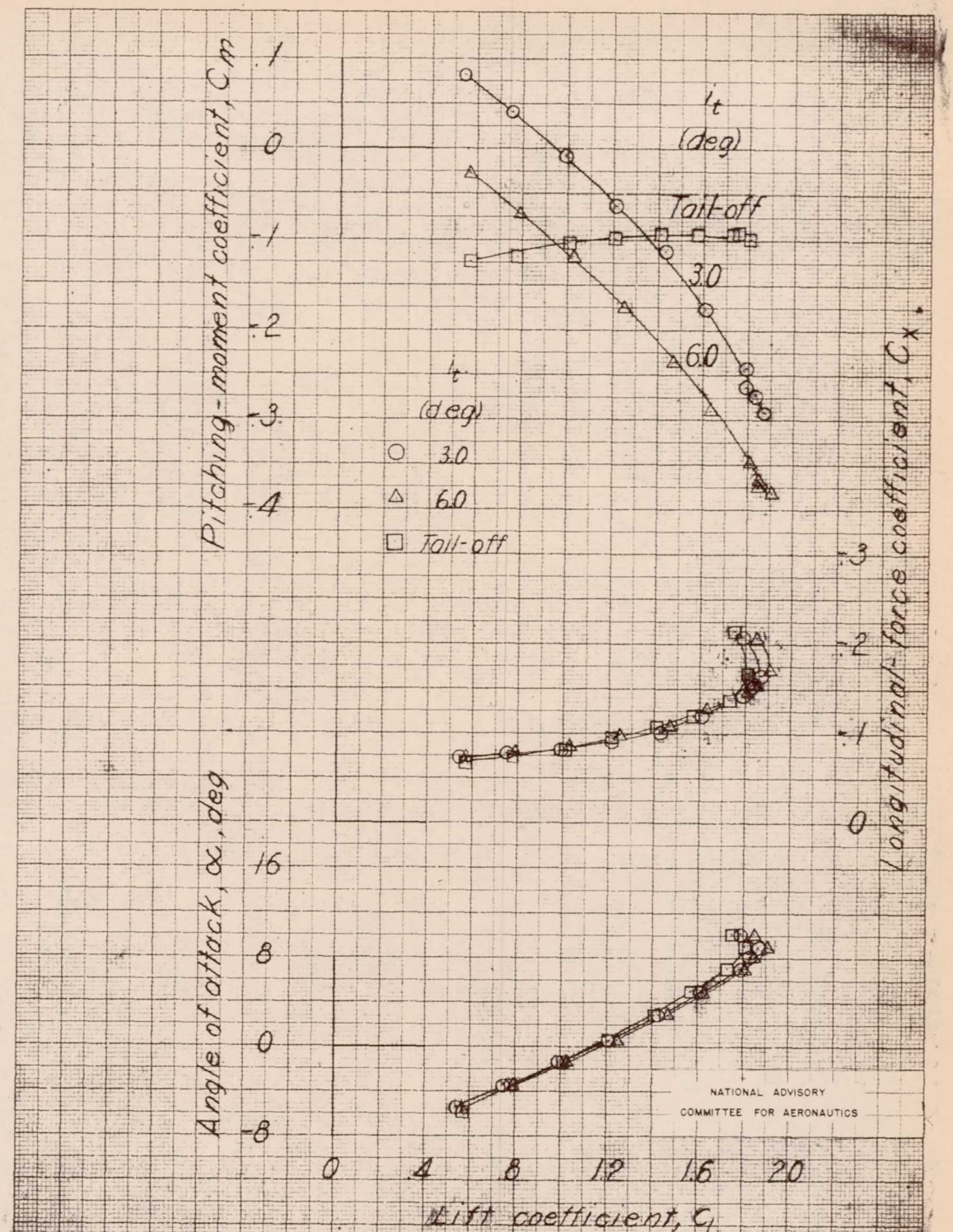

Figure 10-The effect of the stabilizer on the aerodynamic characteristics in pitch of the 1/25-scale model of Martin JRM-1 airplane. Ground board in place. $\phi = 0°$, $I_c' = 0$, $q = 16.37$ lb. per sq ft, $\beta = 30.2°$, $\delta_f = 40°$, $(D_r/ft)_{\alpha=0°} = -2.1$ in.

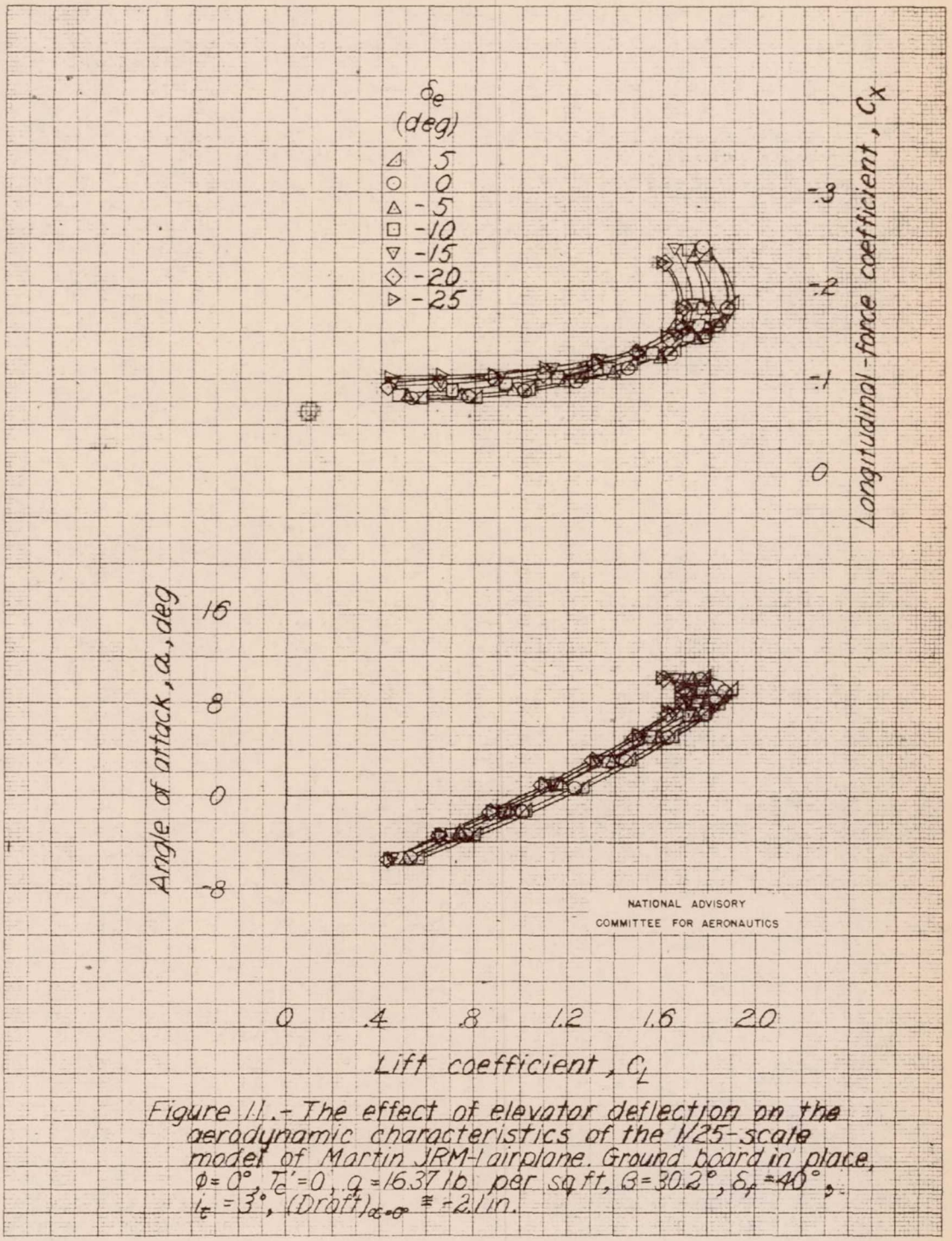

Figure 11.- The effect of elevator deflection on the aerodynamic characteristics of the 1/25-scale model of Martin JRM-1 airplane. Ground board in place, $\phi = 0°$, $T_c' = 0$, $q = 16.37$ lb per sq ft, $\beta = 30.2°$, $\delta_f = 40°$, $i_t = 3°$, $(Draft)_{\alpha=0} \cong -2.1$ in.

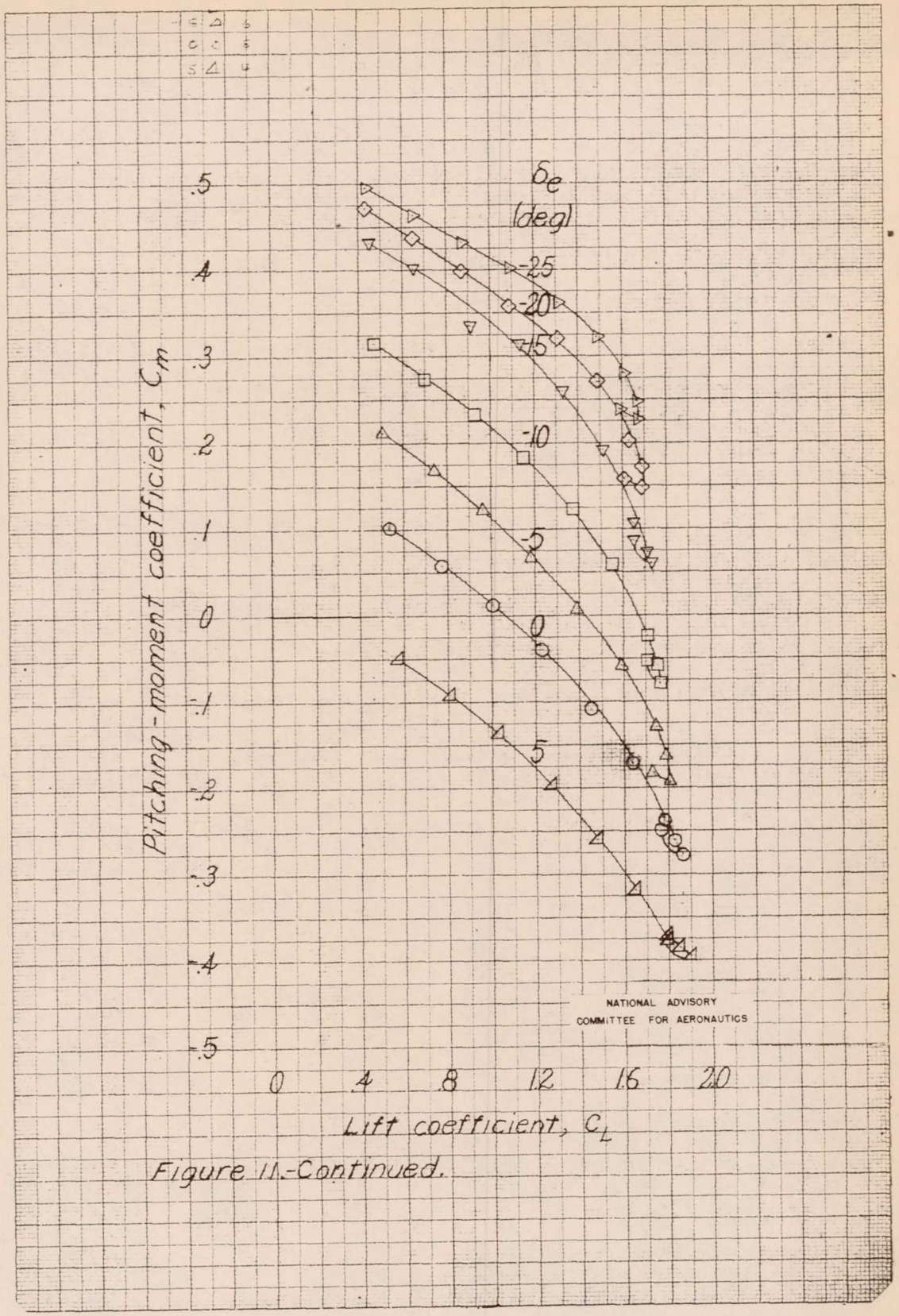

Figure 11.-Continued.

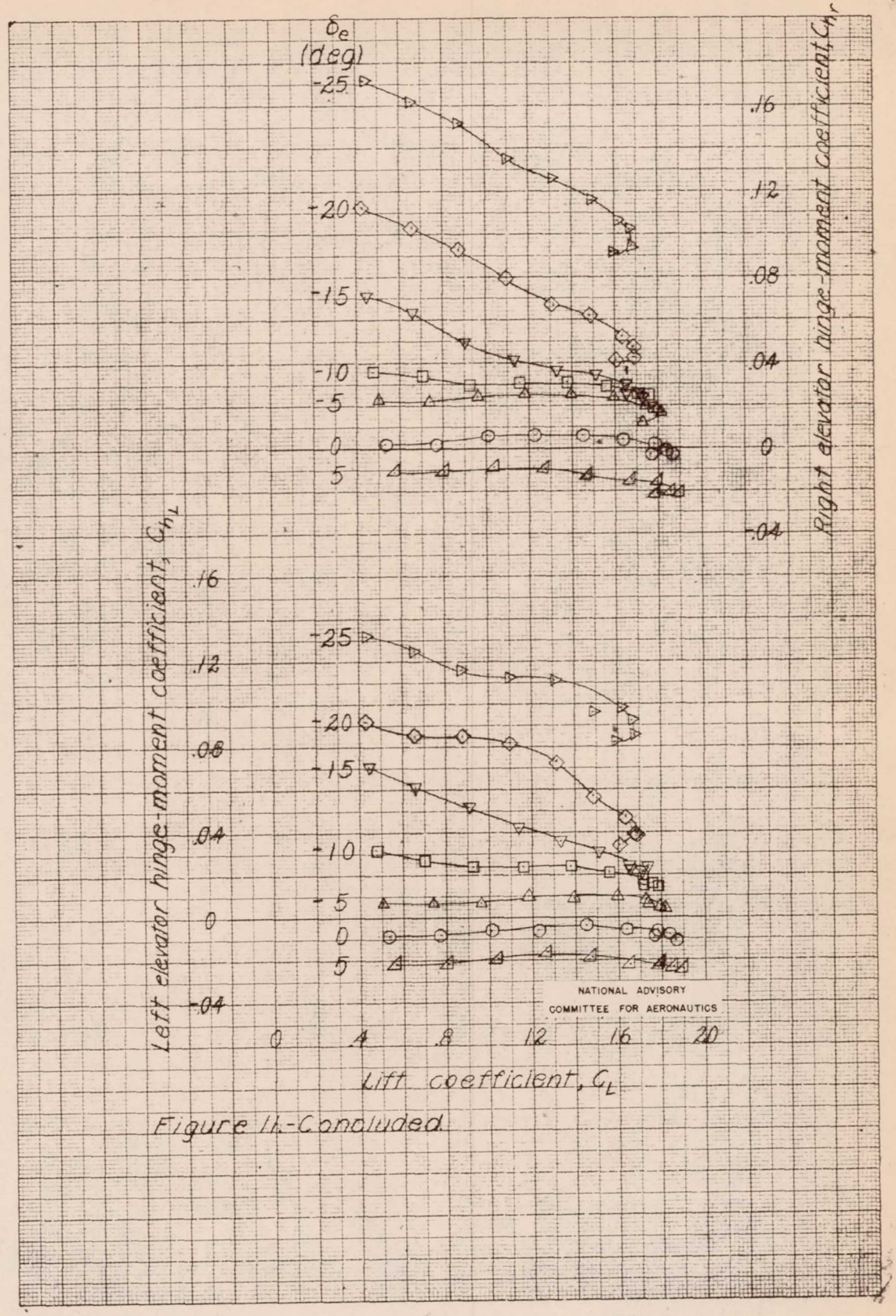

Figure 11.-Concluded.

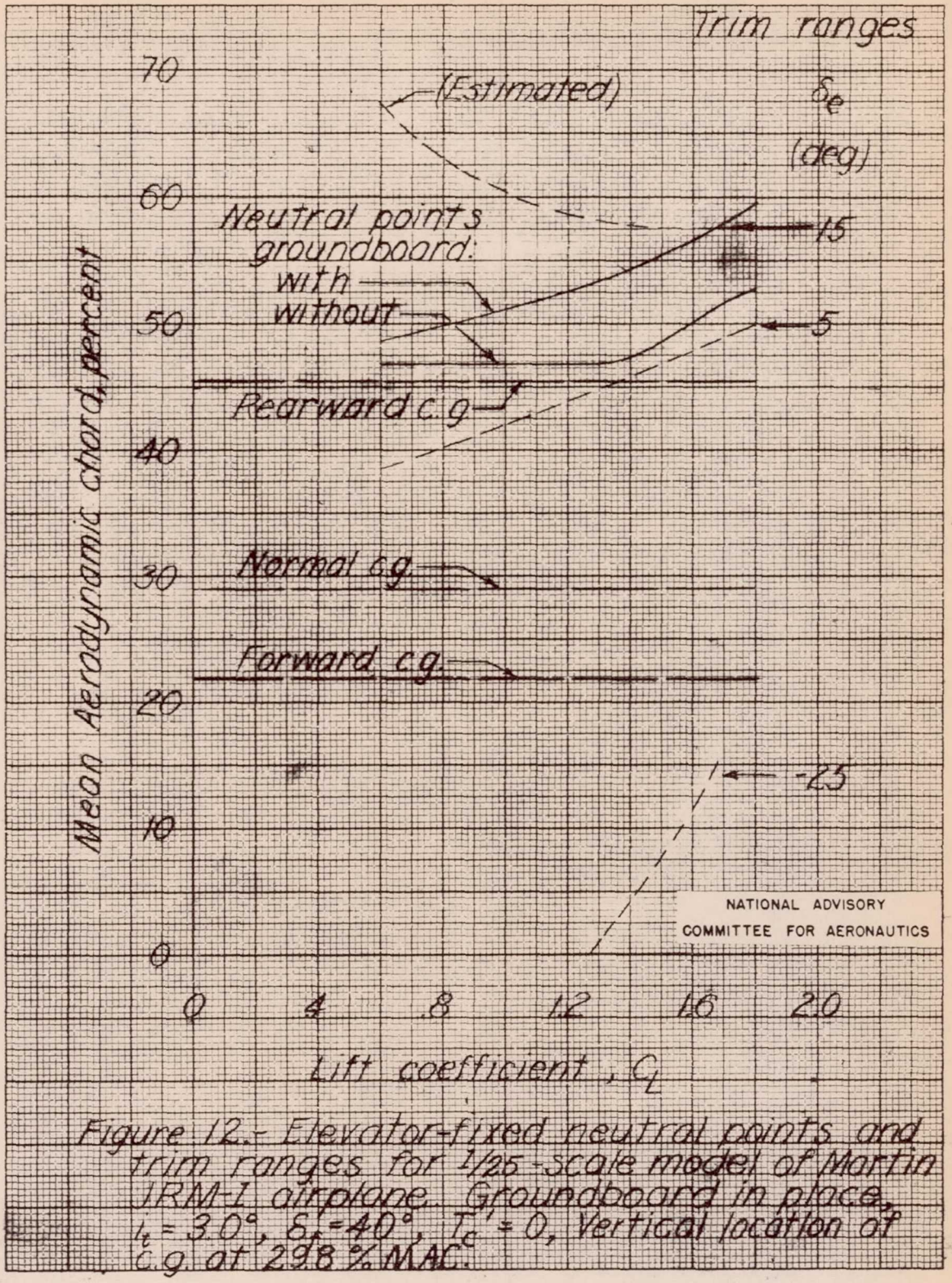

Figure 12.- Elevator-fixed neutral points and trim ranges for 1/25-scale model of Martin JRM-1 airplane. Groundboard in place, $i_t = 3.0°$, $\delta_f = 40°$, $T_c' = 0$, Vertical location of c.g. at 29.8 % MAC.

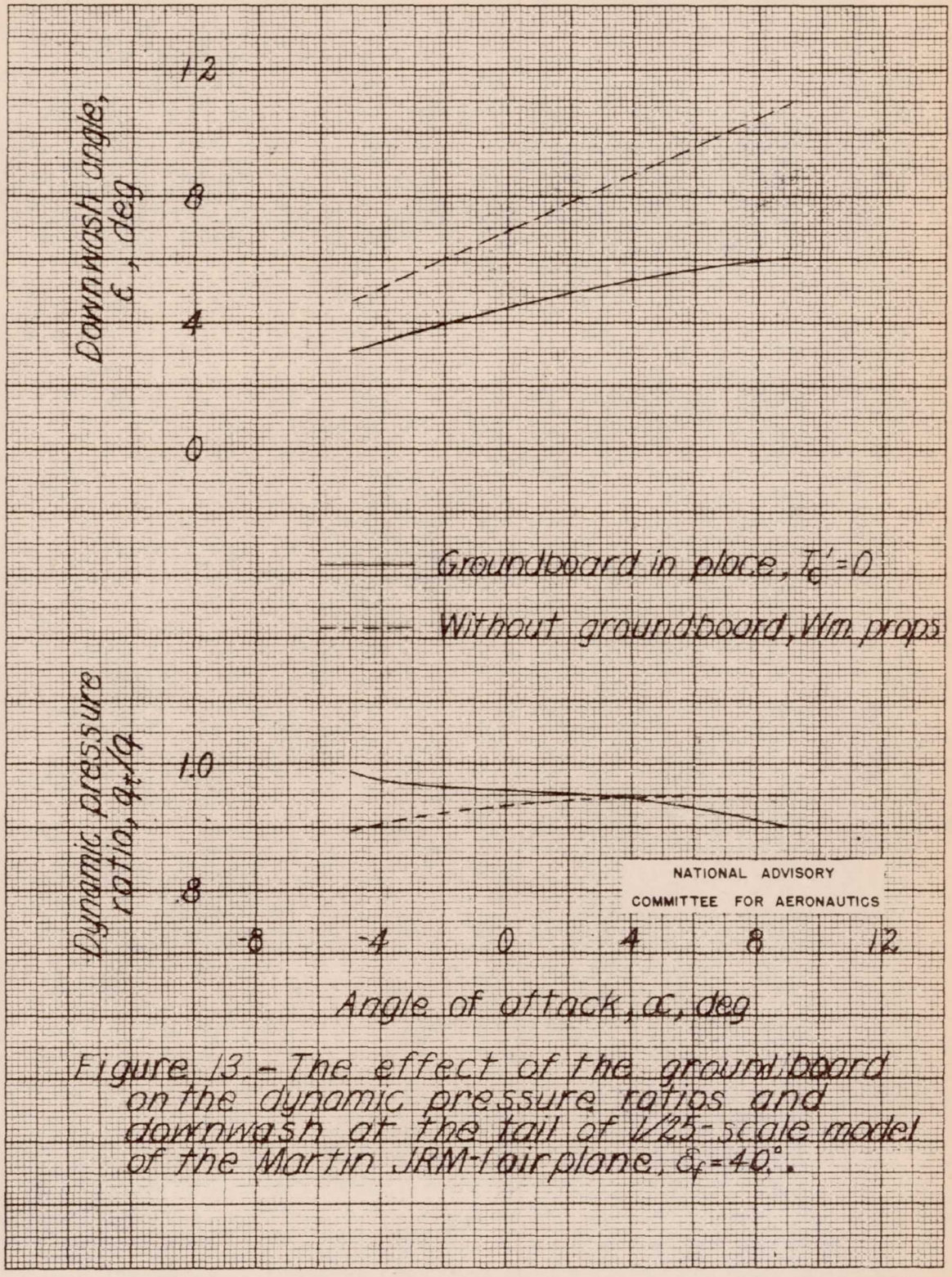

Figure 13.- The effect of the groundboard on the dynamic pressure ratios and downwash at the tail of 1/25-scale model of the Martin JRM-1 airplane. $\delta_f = 40°$.

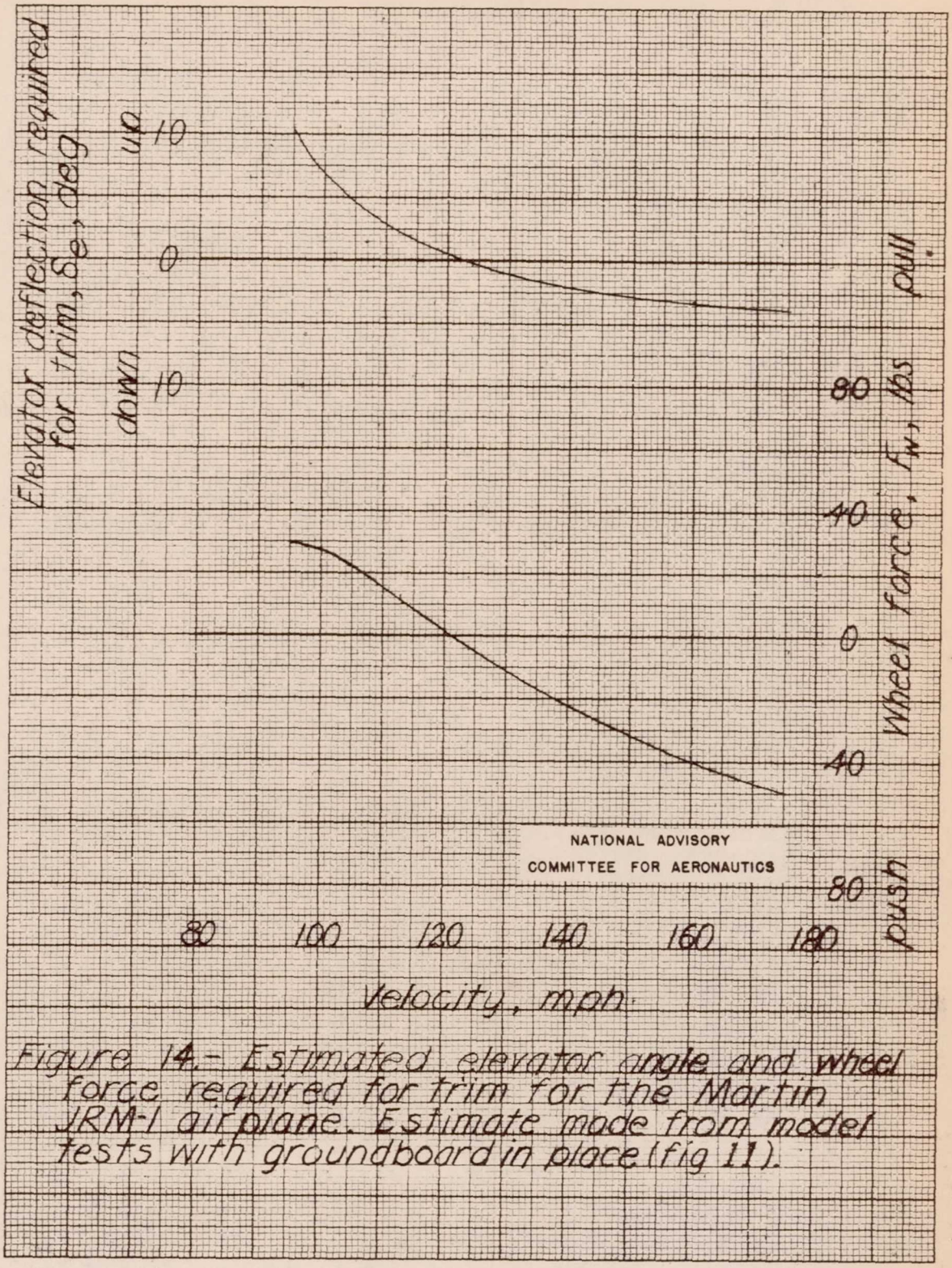

Figure 14.- Estimated elevator angle and wheel force required for trim for the Martin JRM-1 airplane. Estimate made from model tests with groundboard in place (fig 11).

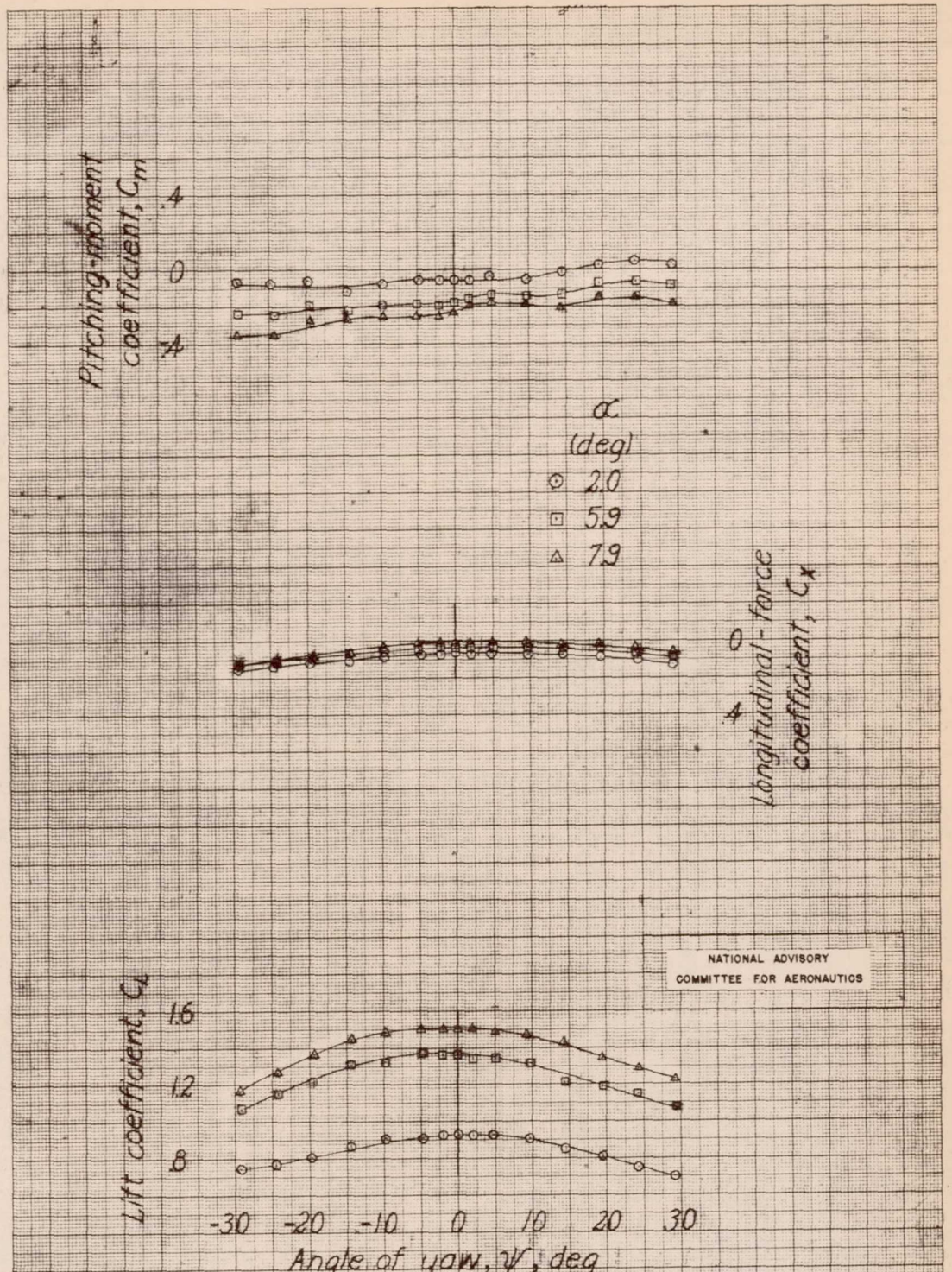

Figure 15.- Effect of angle of attack on the aerodynamic characteristics in yaw of 1/25-scale model of Martin JRM-1 airplane. Draft = -0.96 in.; $\theta = 0°$, $T_c' = 0.119$, $q = 16.37$ lb./per sq ft, $\beta = 30.2°$, $\delta_f = 0°$.

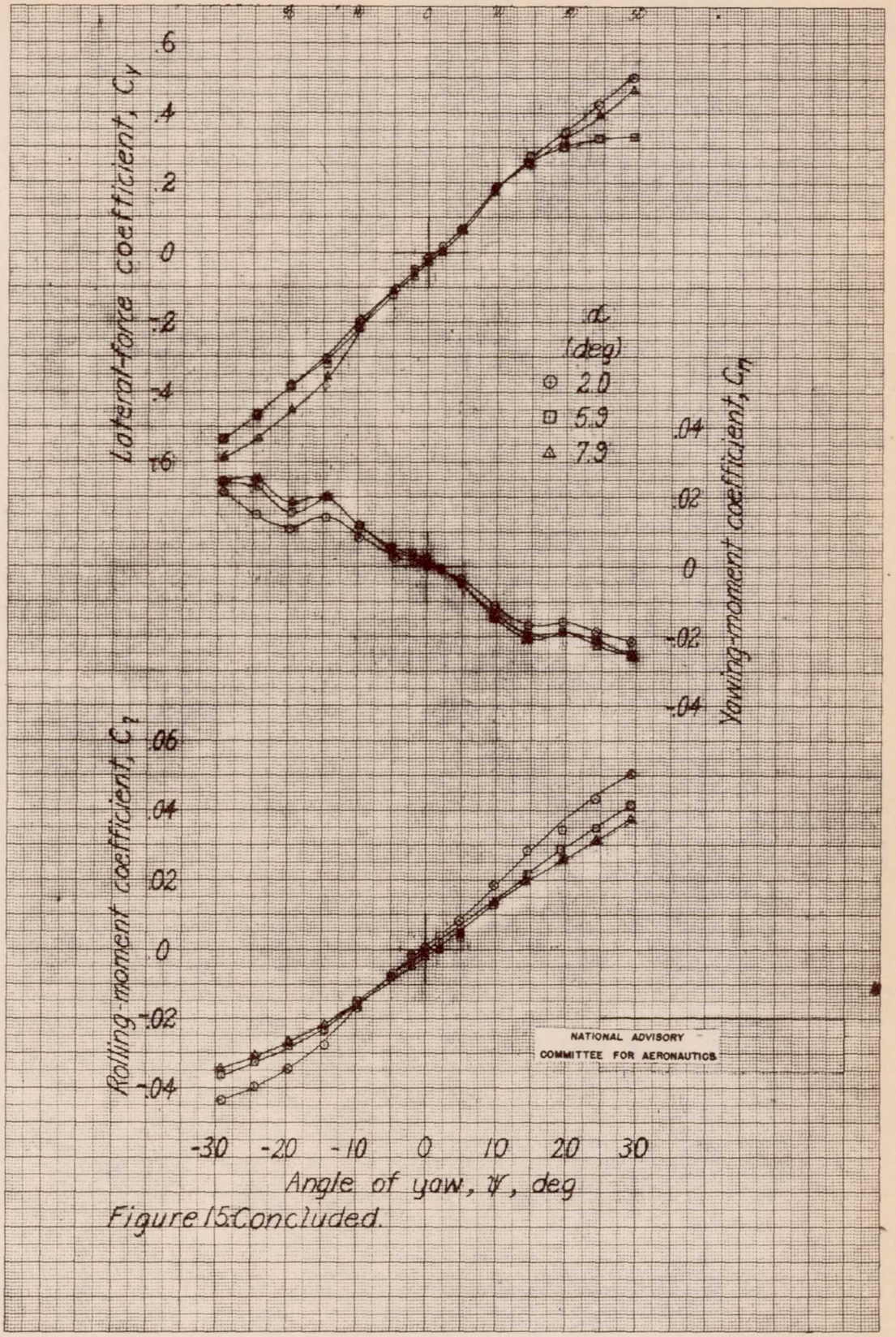

Figure 15.Concluded.

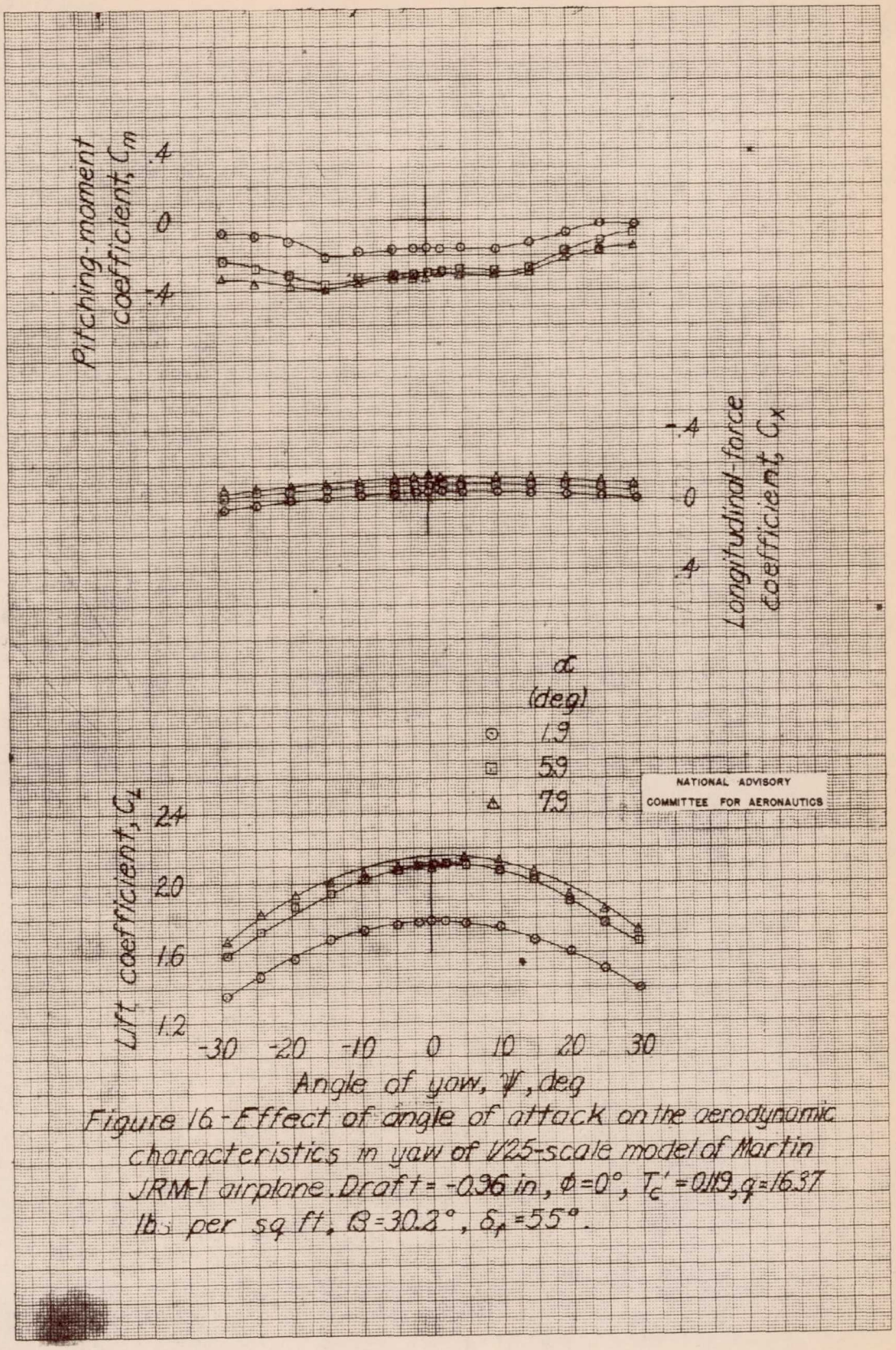

Figure 16.- Effect of angle of attack on the aerodynamic characteristics in yaw of 1/25-scale model of Martin JRM-1 airplane. Draft = -0.36 in., $\phi = 0°$, $T_c' = 0.119$, $q = 16.37$ lbs per sq ft, $\beta = 30.2°$, $\delta_f = 55°$.

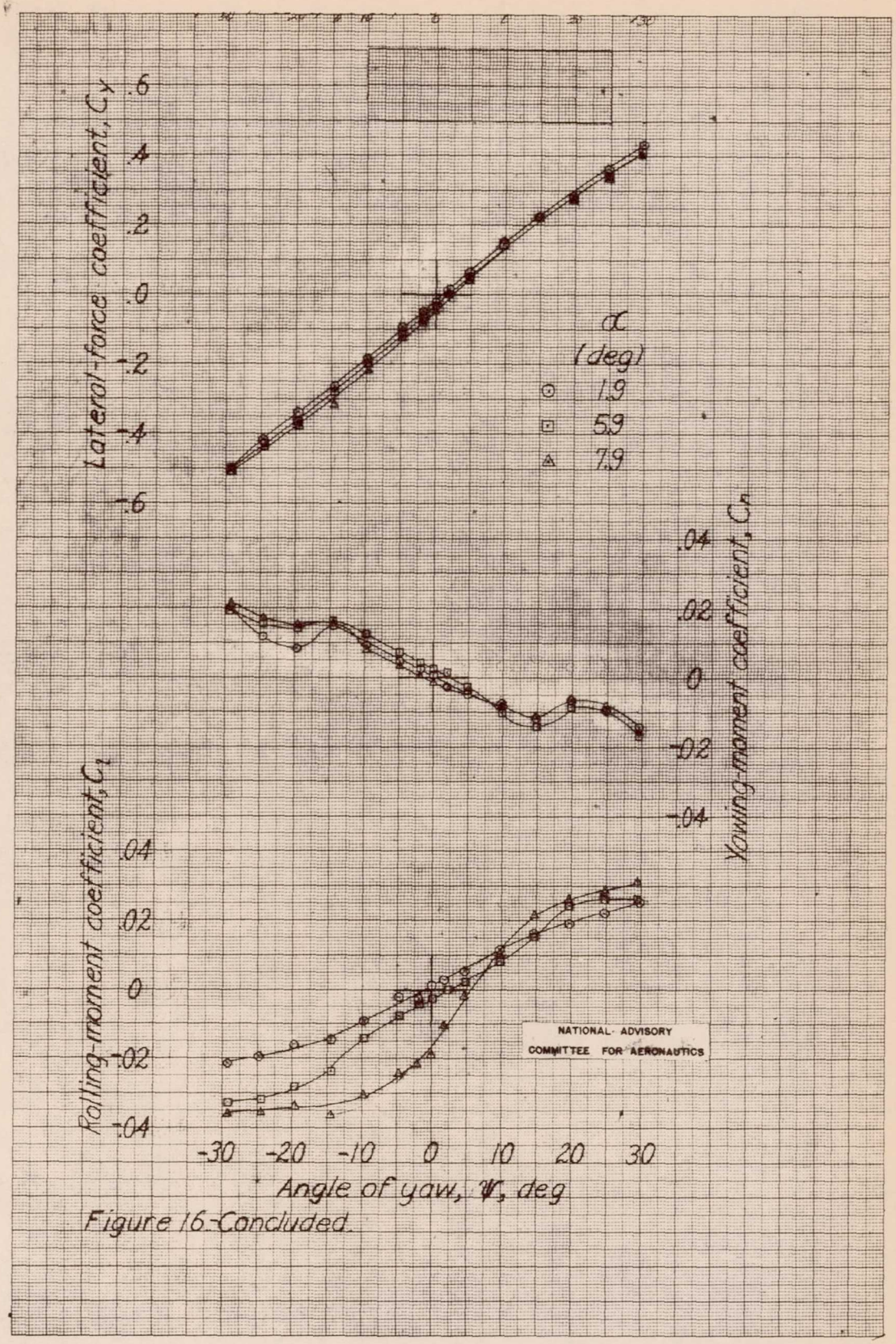

Figure 16.-Concluded.

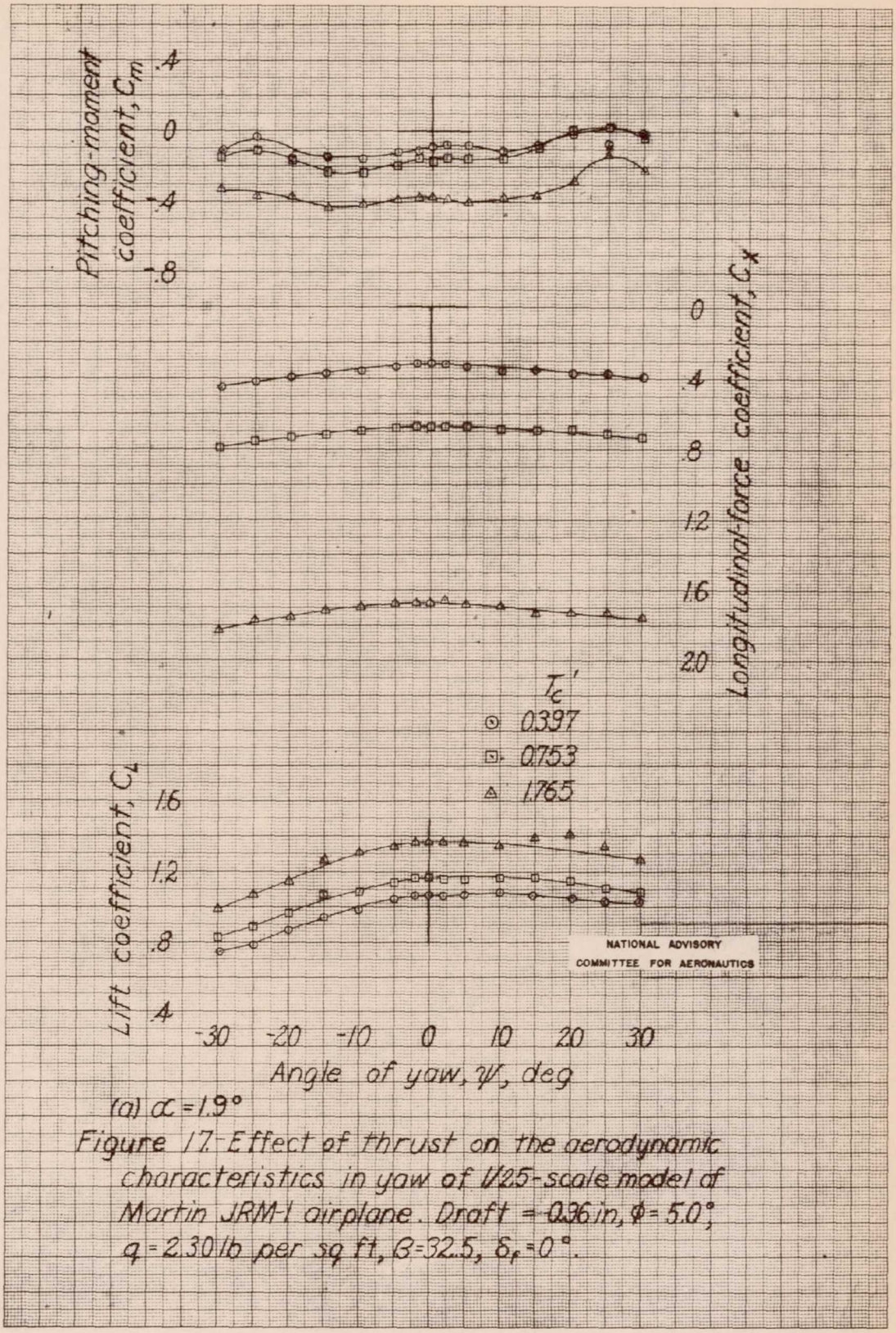

(a) $\alpha = 1.9°$

Figure 17.- Effect of thrust on the aerodynamic characteristics in yaw of 1/25-scale model of Martin JRM-1 airplane. Draft = 0.36 in., $\phi = 5.0°$; $q = 2.30$ lb per sq ft, $\beta = 32.5$, $\delta_f = 0°$.

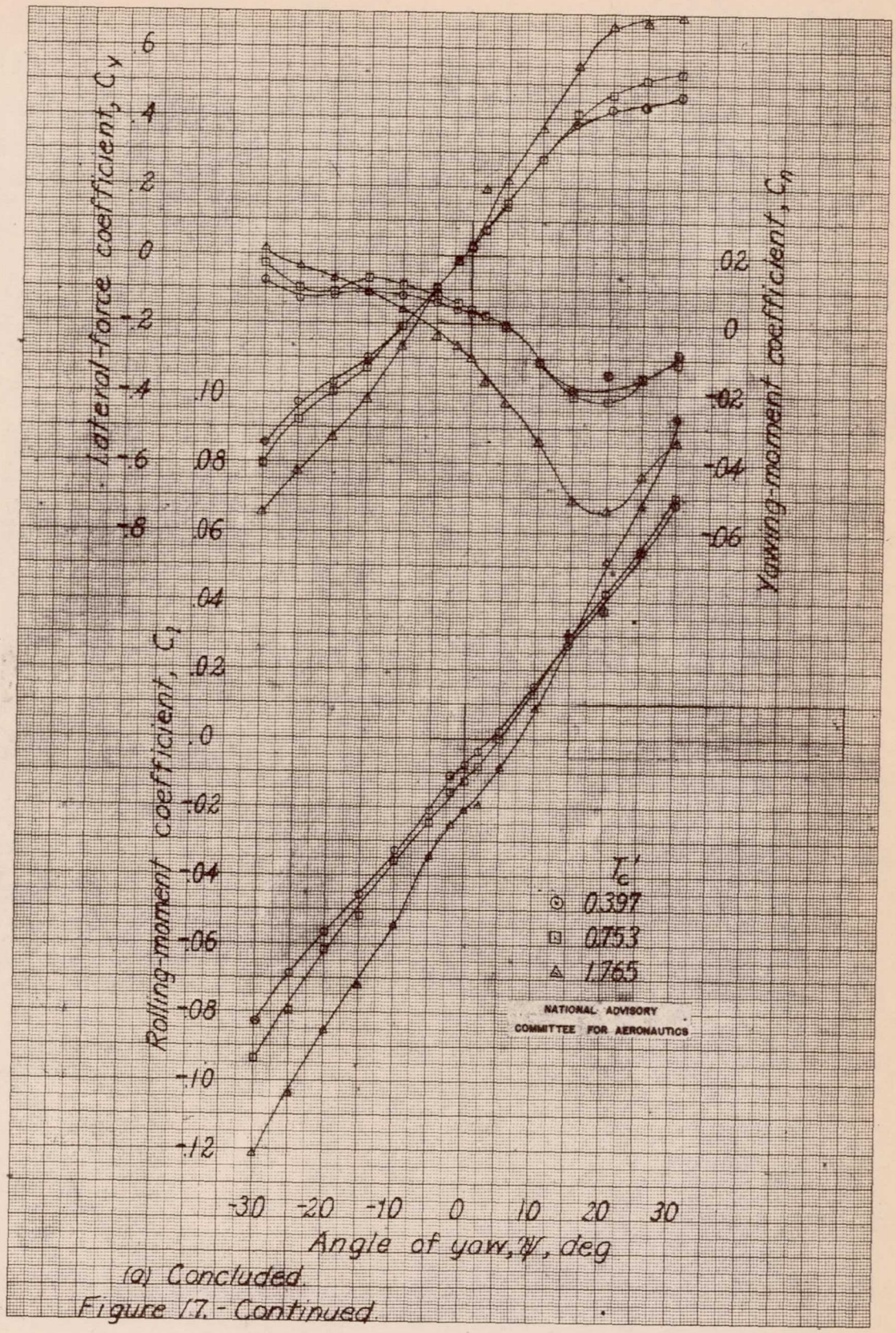

(a) Concluded.

Figure 17.- Continued.

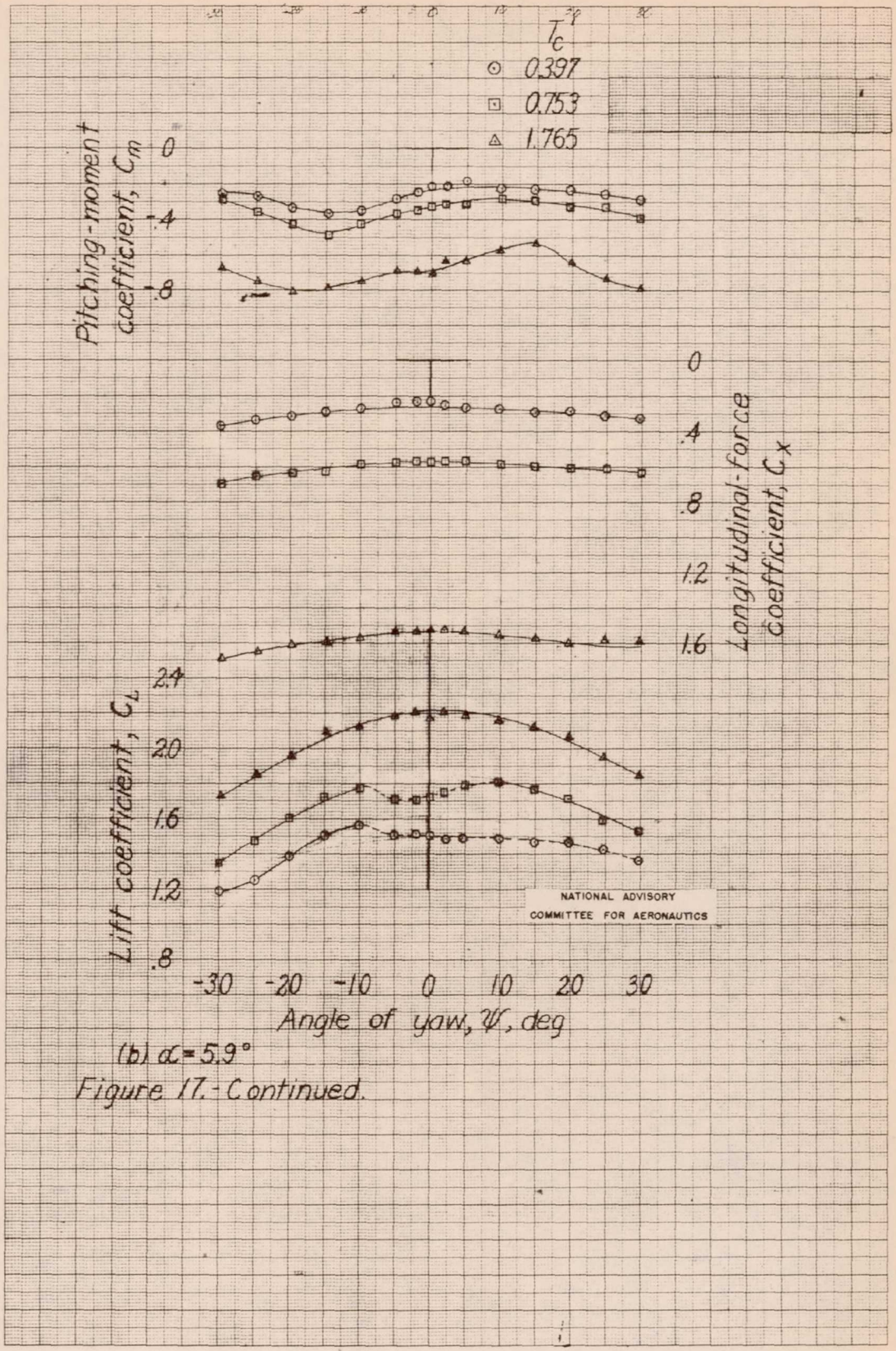

(b) $\alpha = 5.9°$

Figure 17.- Continued.

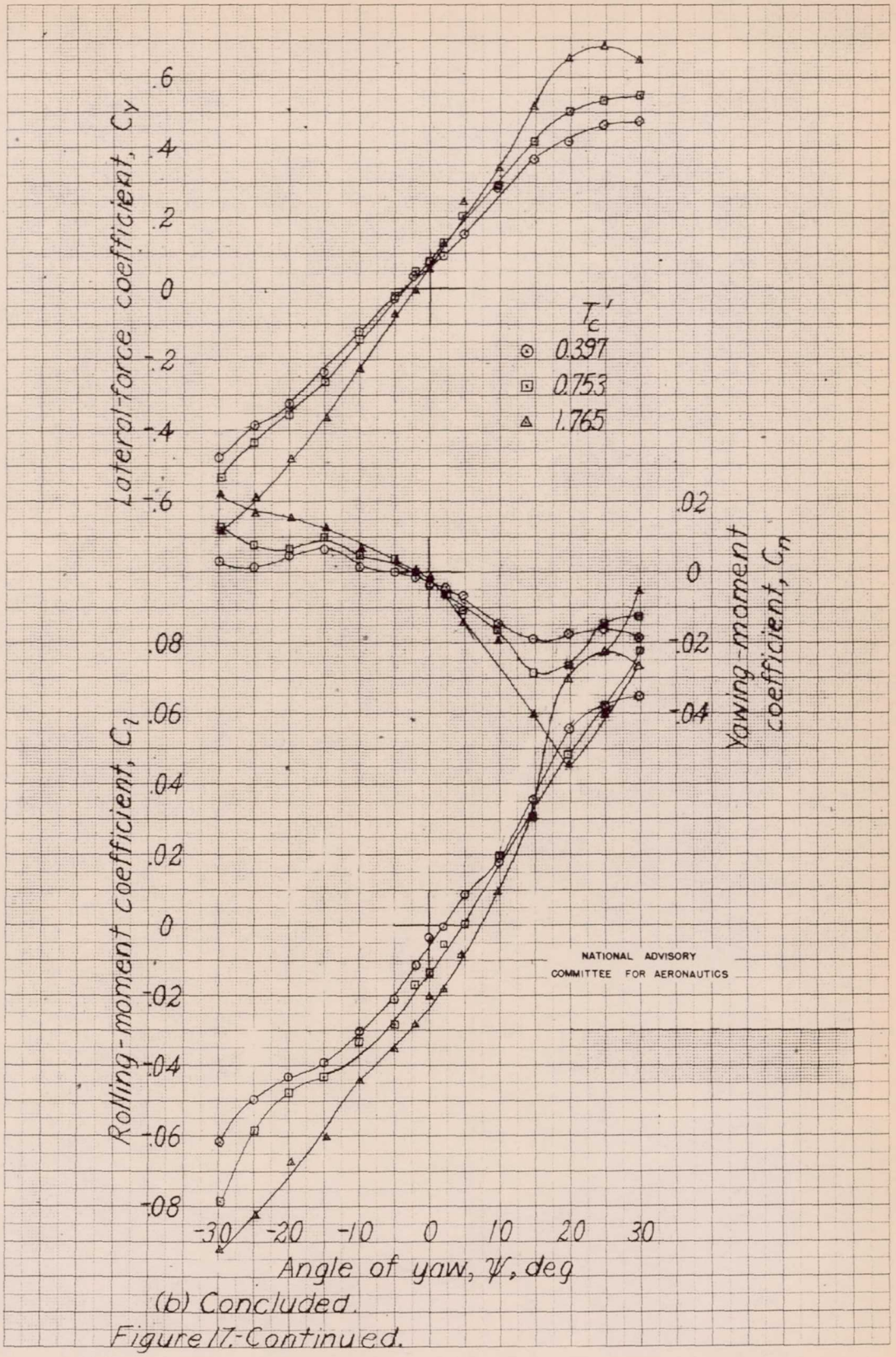

(b) Concluded.

Figure 17.-Continued.

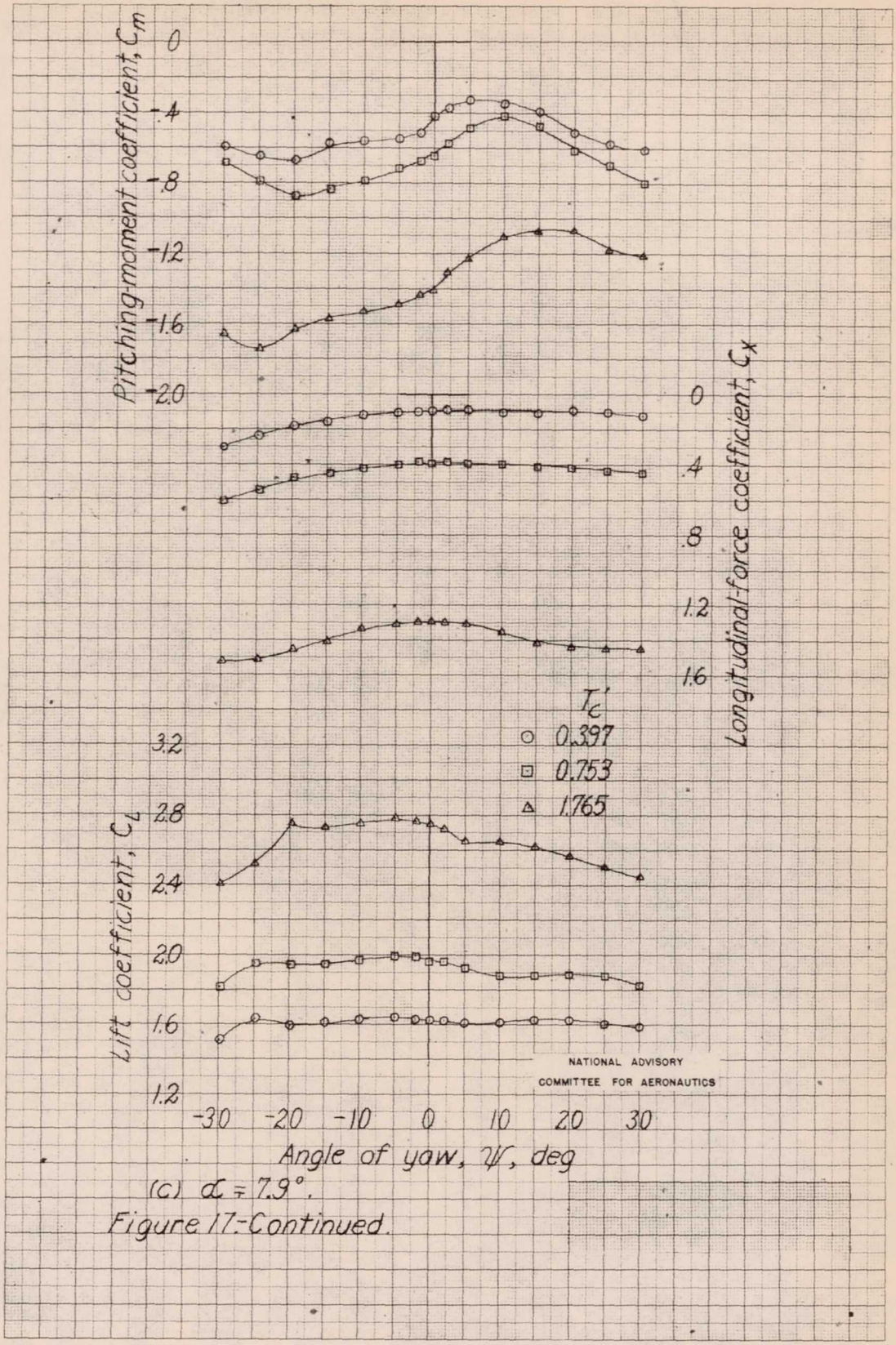

(c) $\alpha = 7.9°$.

Figure 17.-Continued.

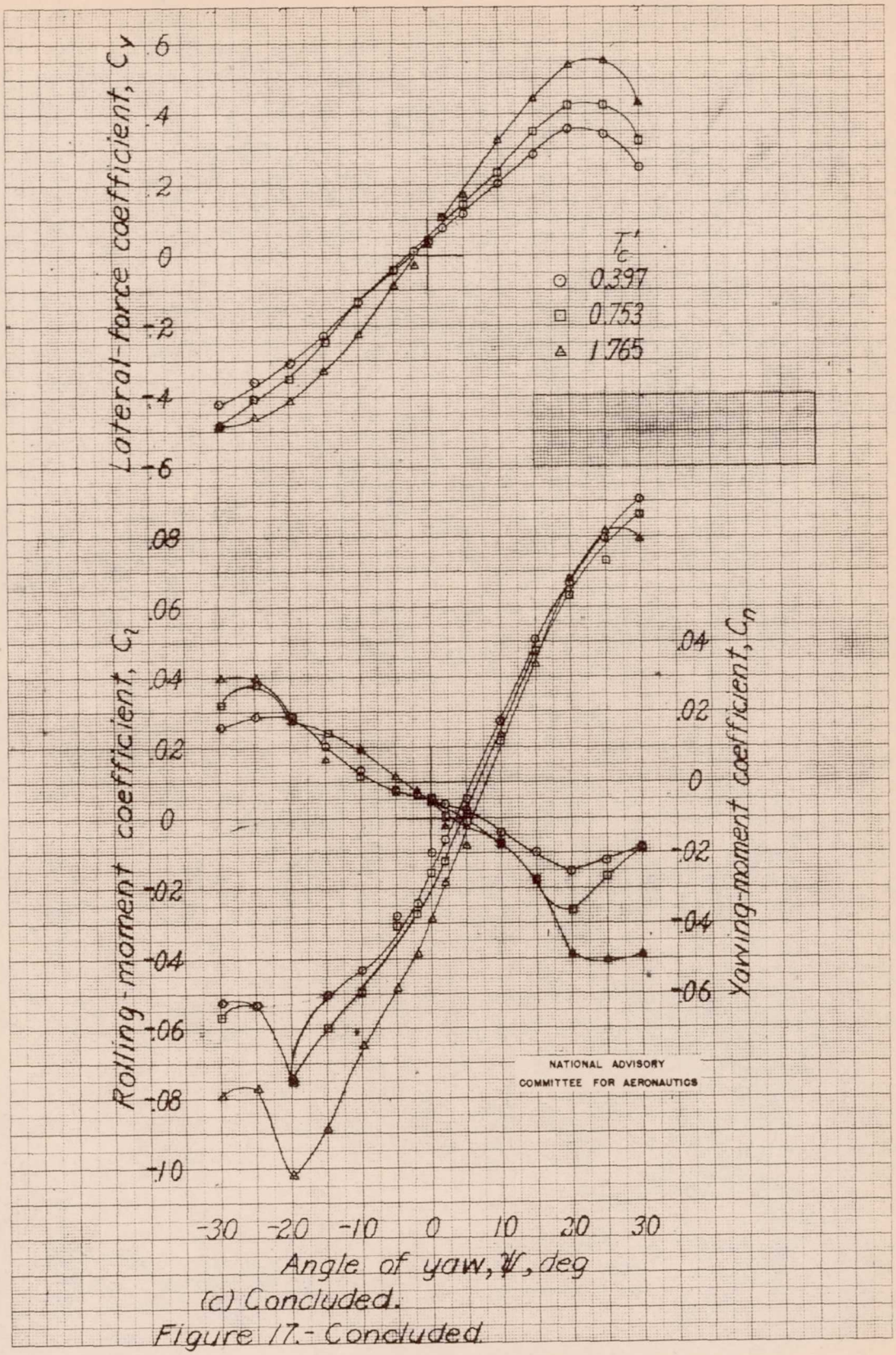

(c) Concluded.

Figure 17.- Concluded.

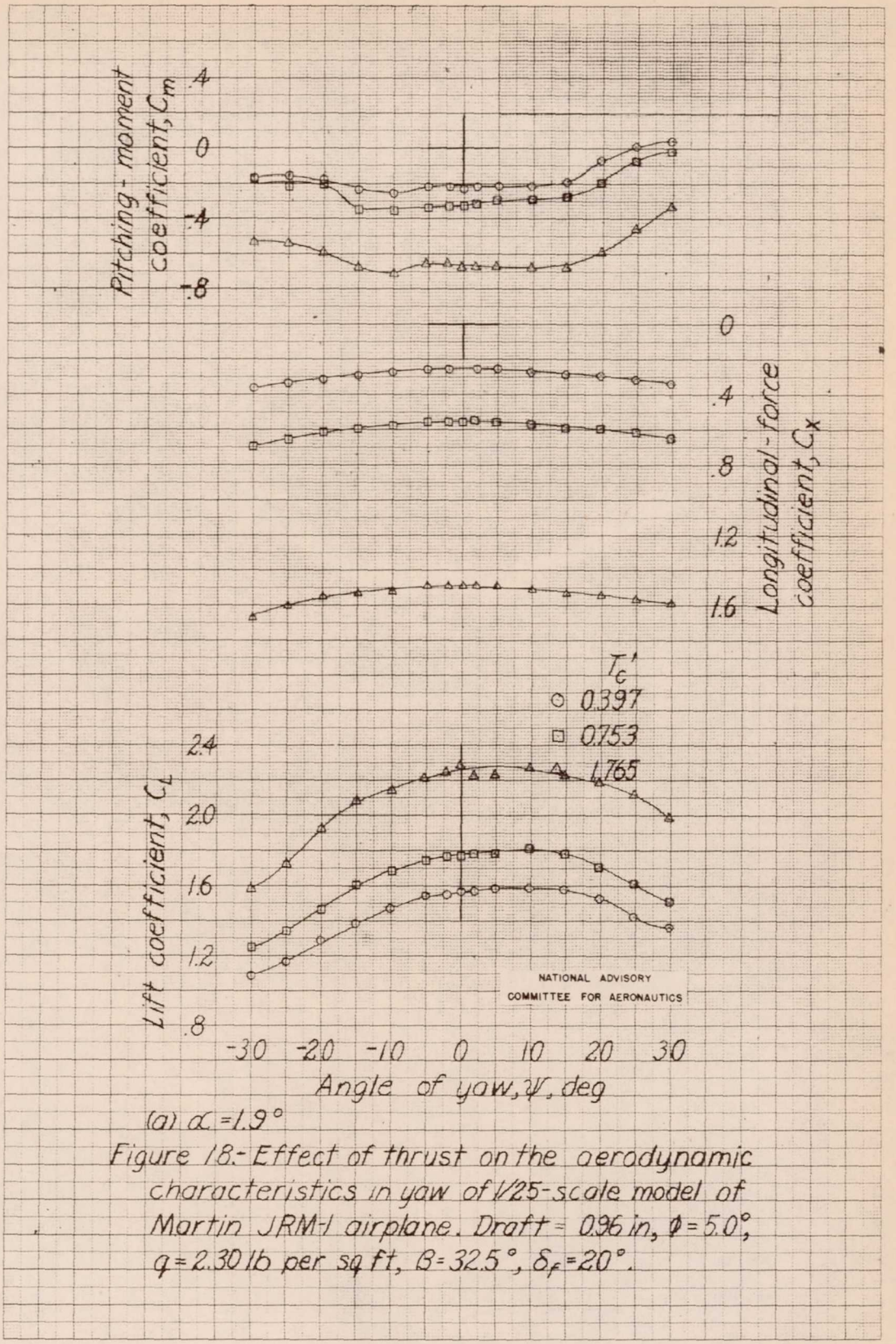

(a) $\alpha = 1.9°$

Figure 18.- Effect of thrust on the aerodynamic characteristics in yaw of 1/25-scale model of Martin JRM-1 airplane. Draft = 0.96 in., $\phi = 5.0°$, $q = 2.30$ lb per sq ft, $\beta = 32.5°$, $\delta_f = 20°$.

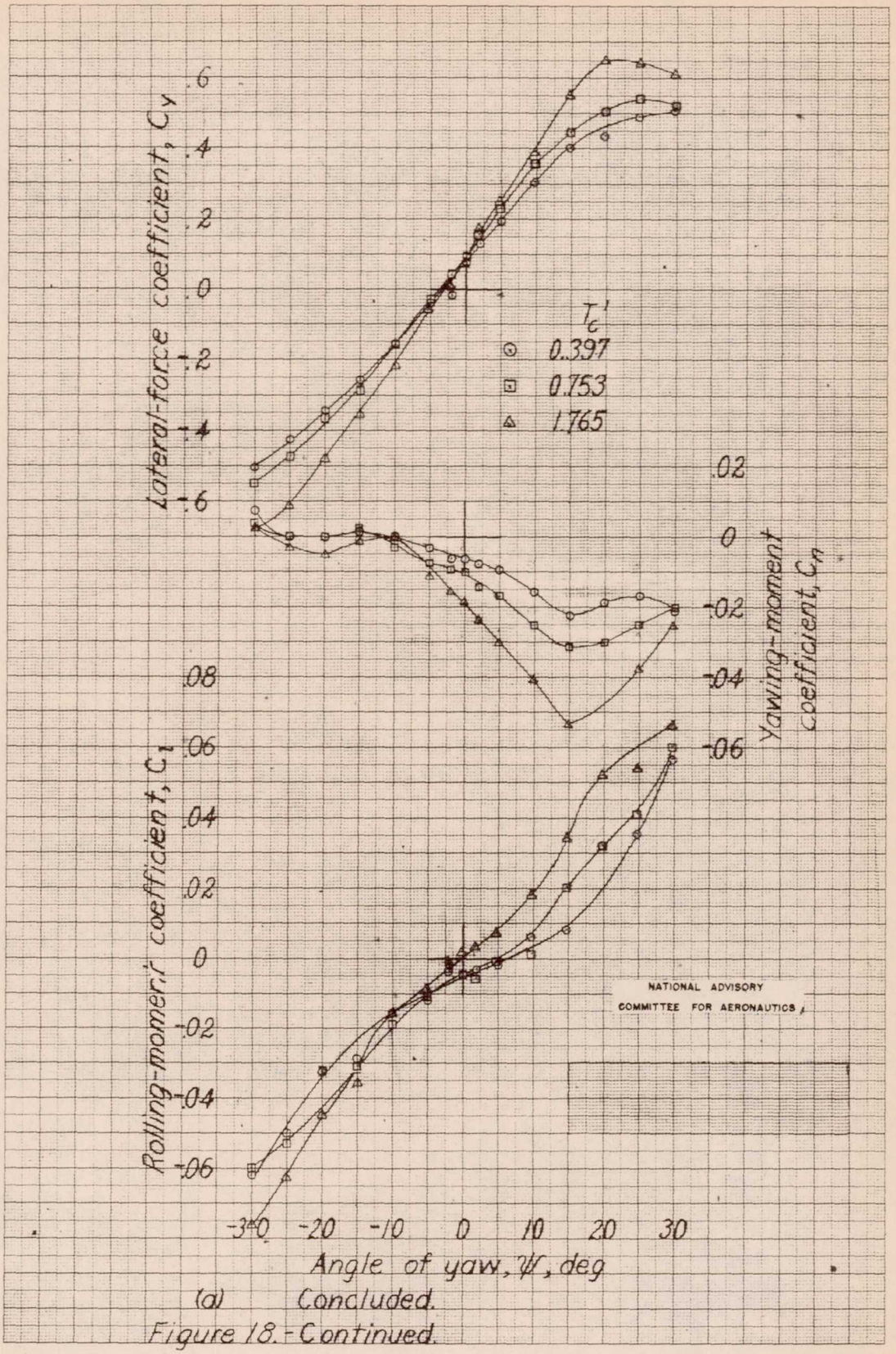

(a) Concluded.

Figure 18.- Continued.

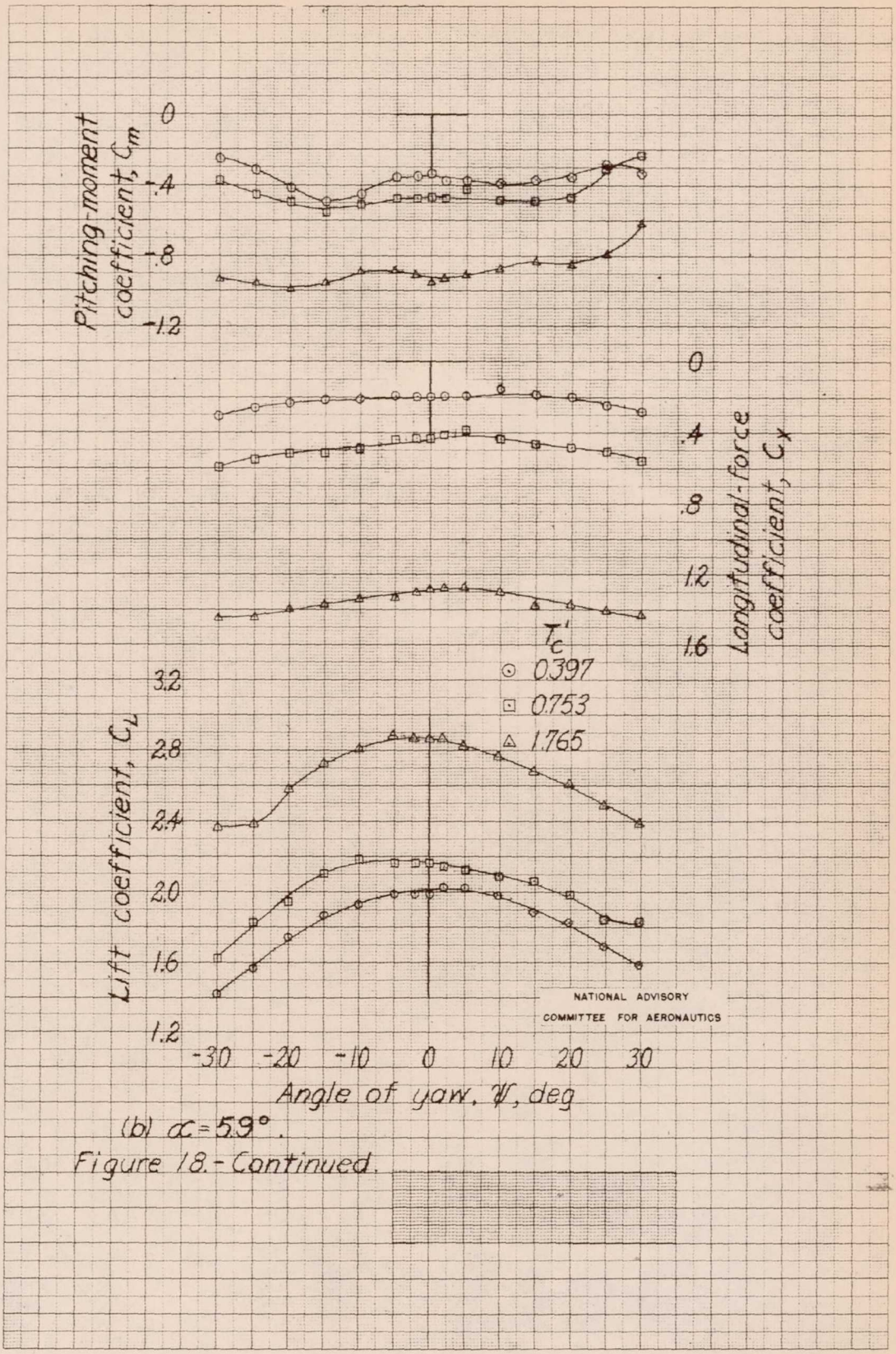

(b) $\alpha = 5.9°$.

Figure 18.- Continued.

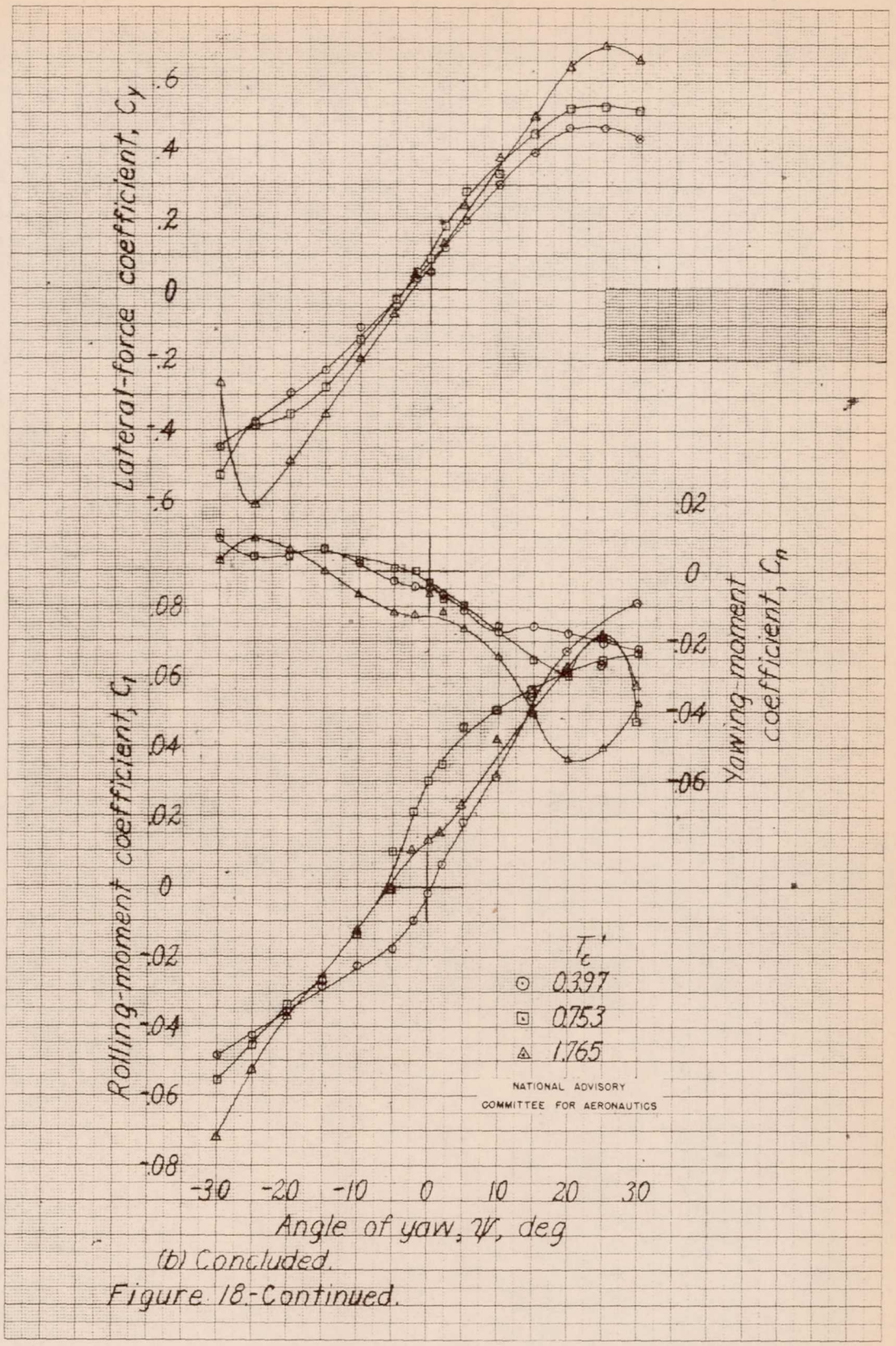

(b) Concluded.

Figure 18.-Continued.

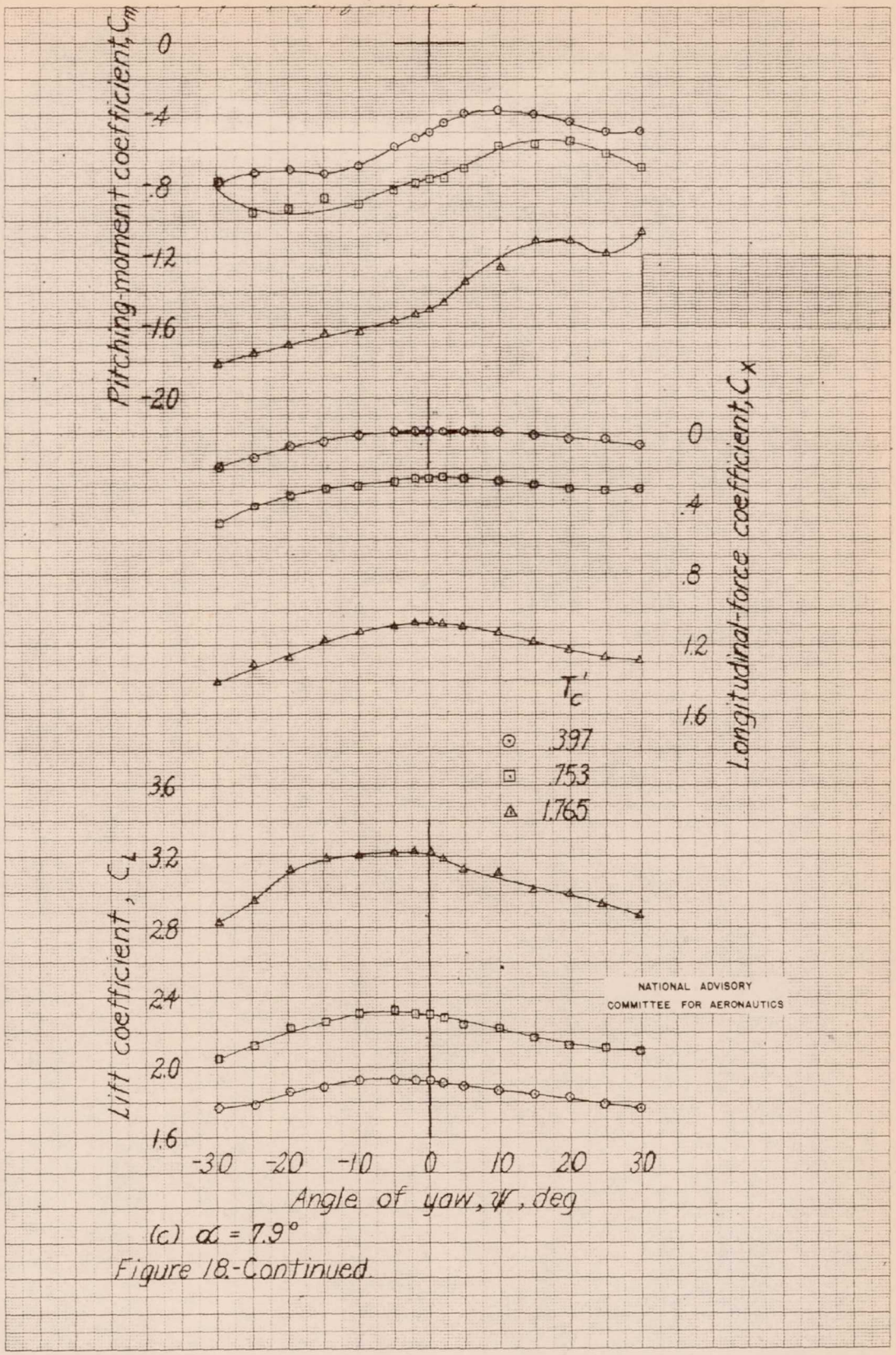

(c) $\alpha = 7.9°$

Figure 18.-Continued

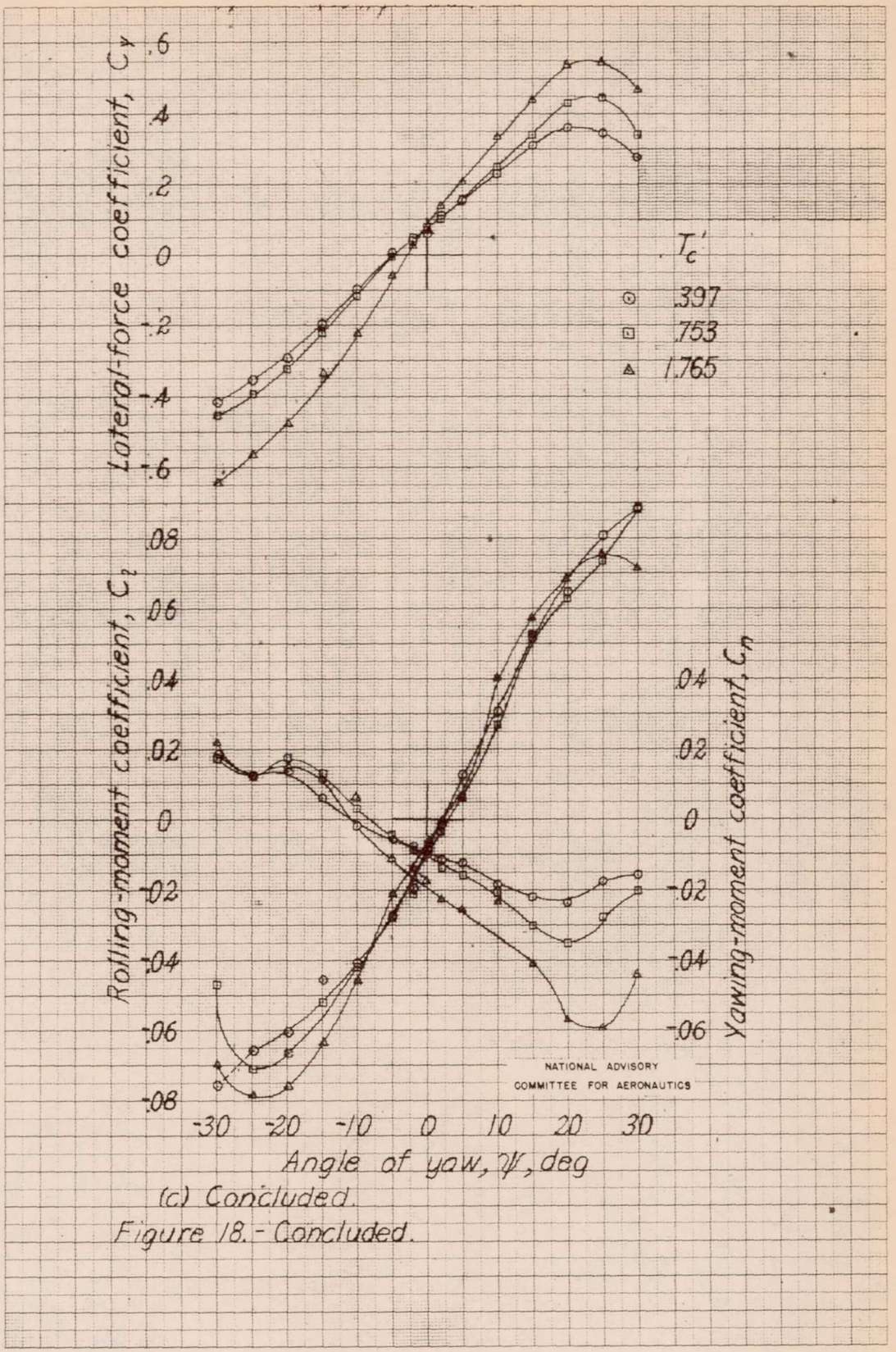

(c) Concluded.

Figure 18.- Concluded.

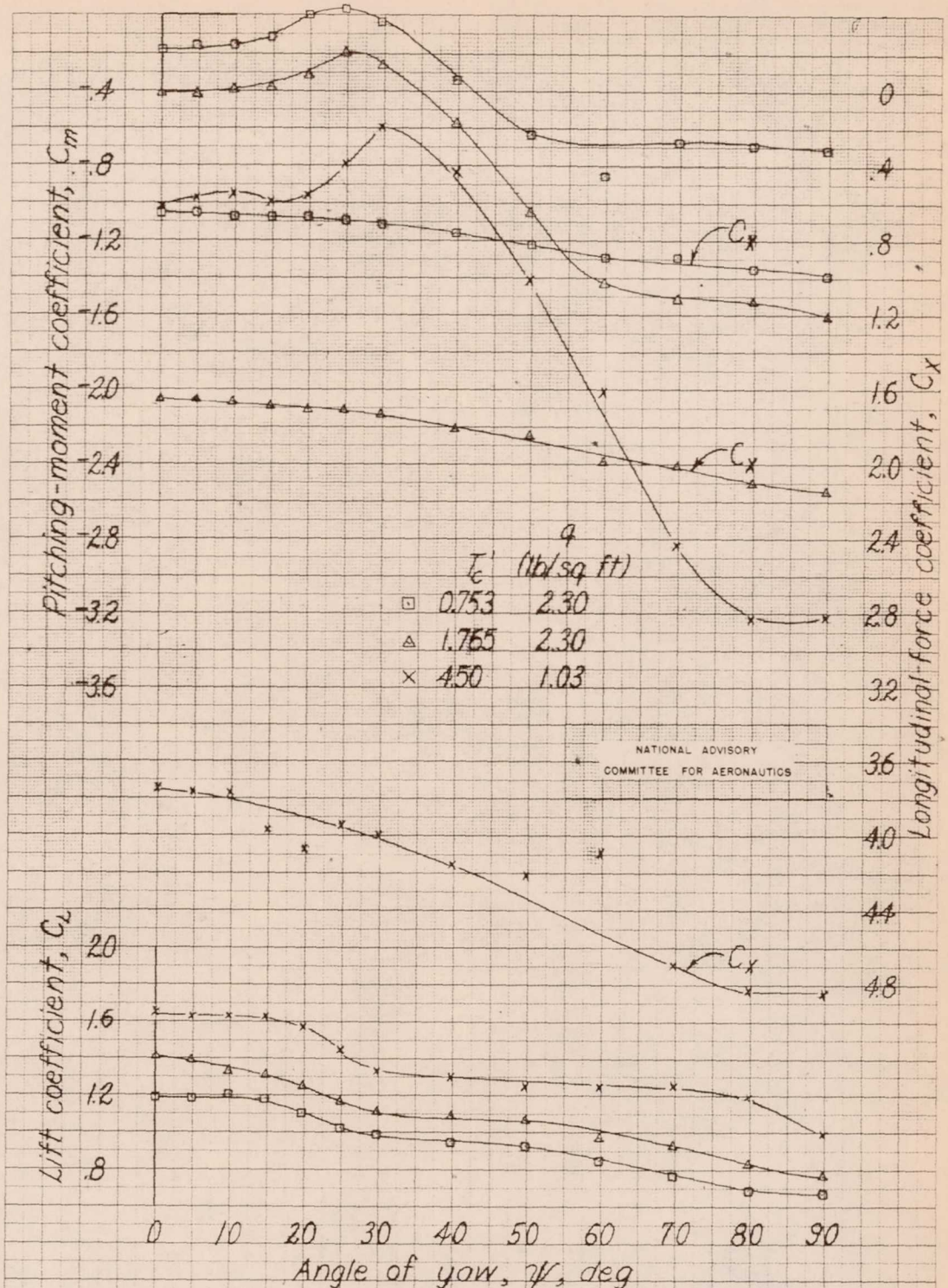

(a) $\alpha = 1.9°$.

Figure 19.- Effect of thrust on the aerodynamic characteristics in yaw of 1/25-scale model of Martin JRM-1 airplane. Draft = 1.8 in., $\phi = 3.0°$, $\beta = 32.5°$, $\delta_f = 0°$.

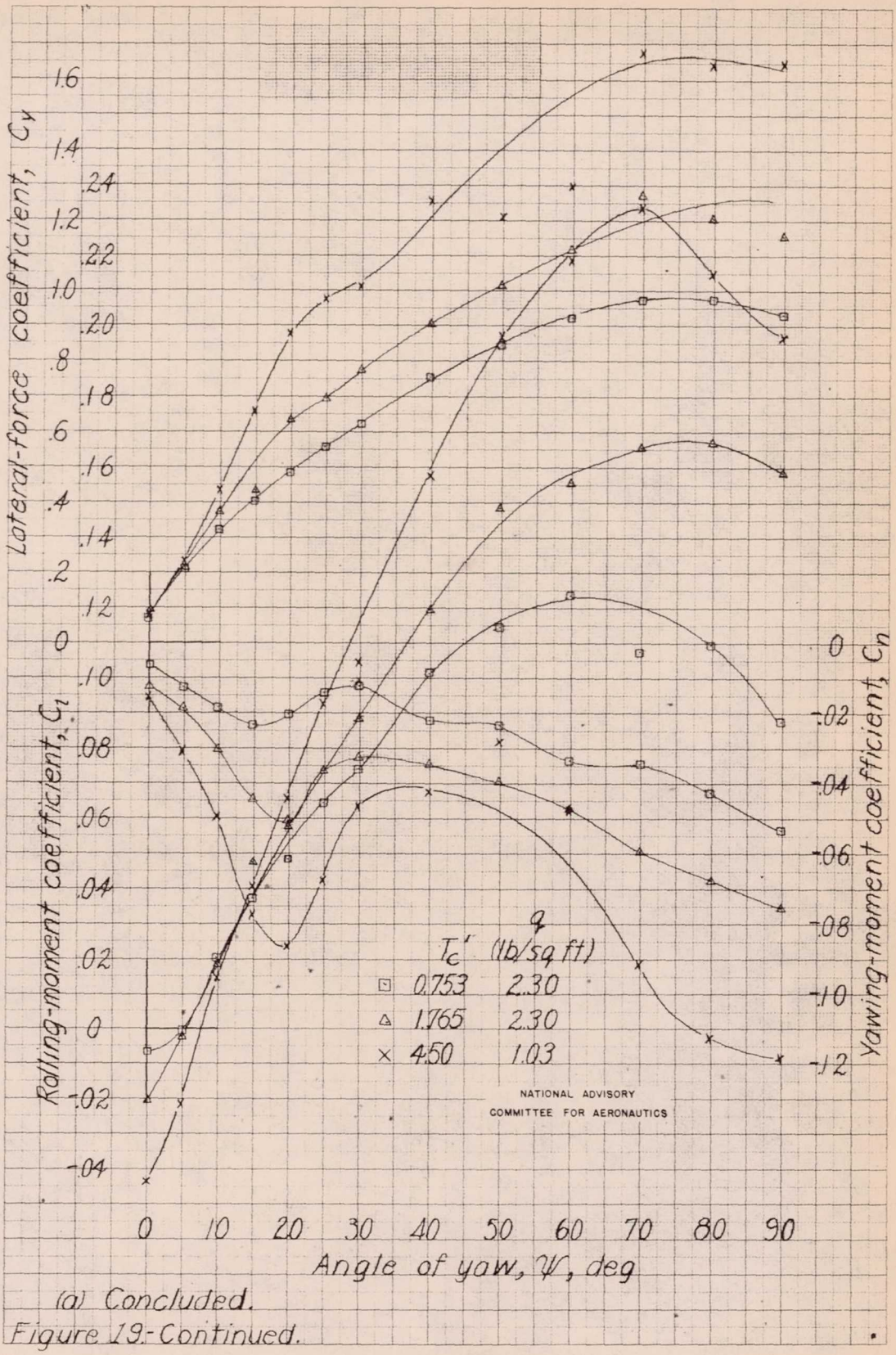

(a) Concluded.

Figure 19.- Continued.

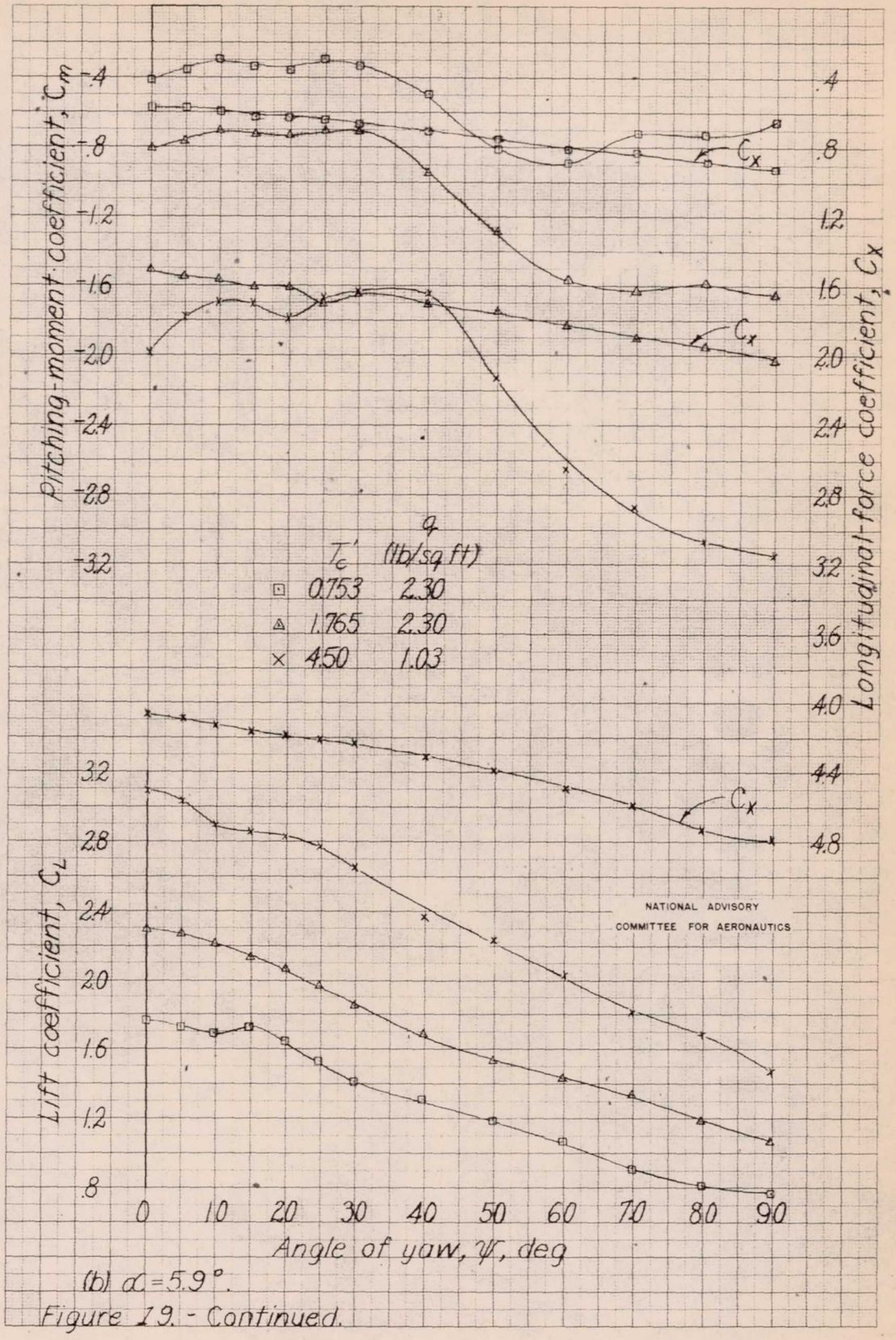

(b) $\alpha = 5.9°$.

Figure 19. - Continued.

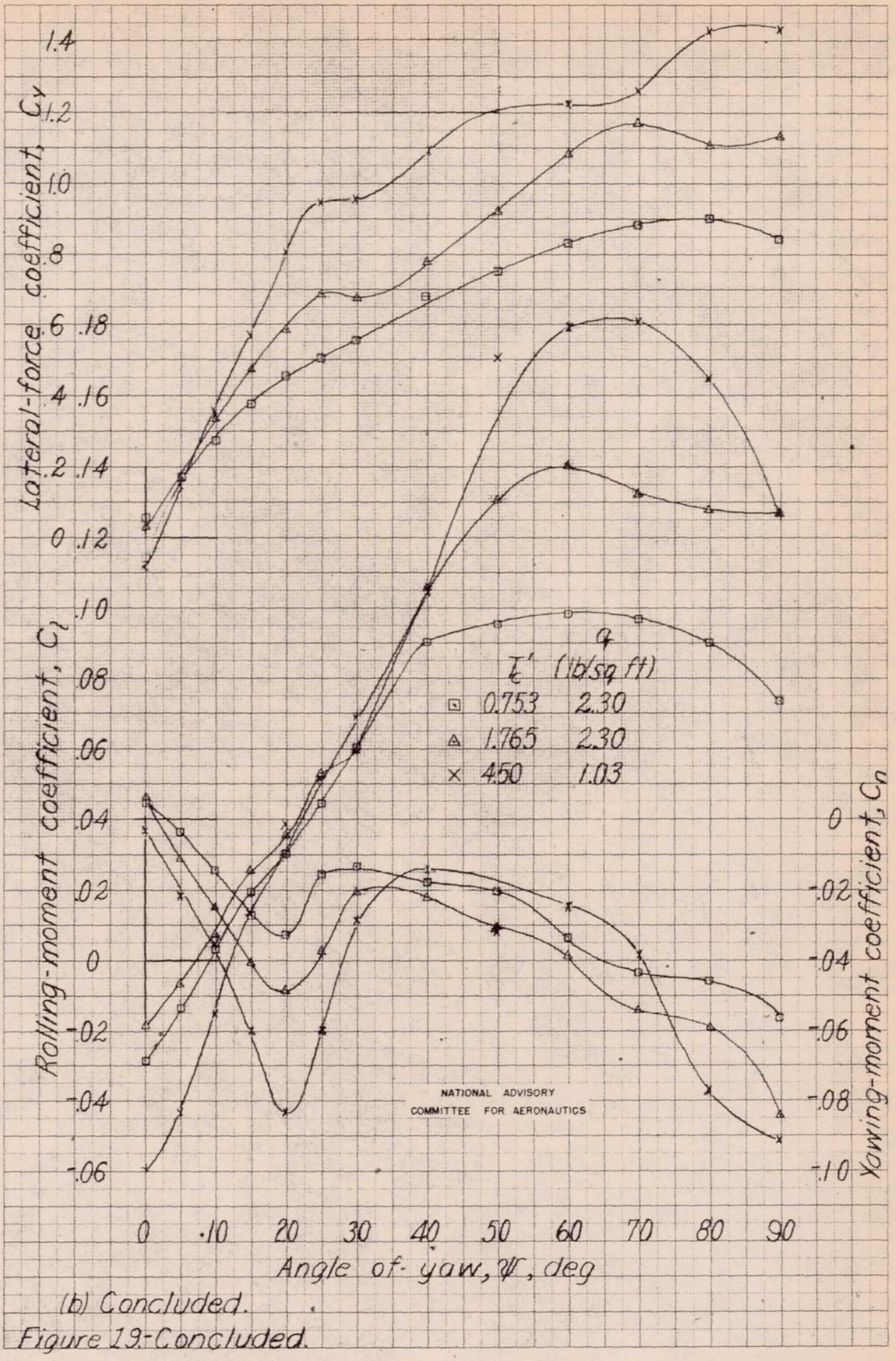

(b) Concluded.

Figure 19.- Concluded.

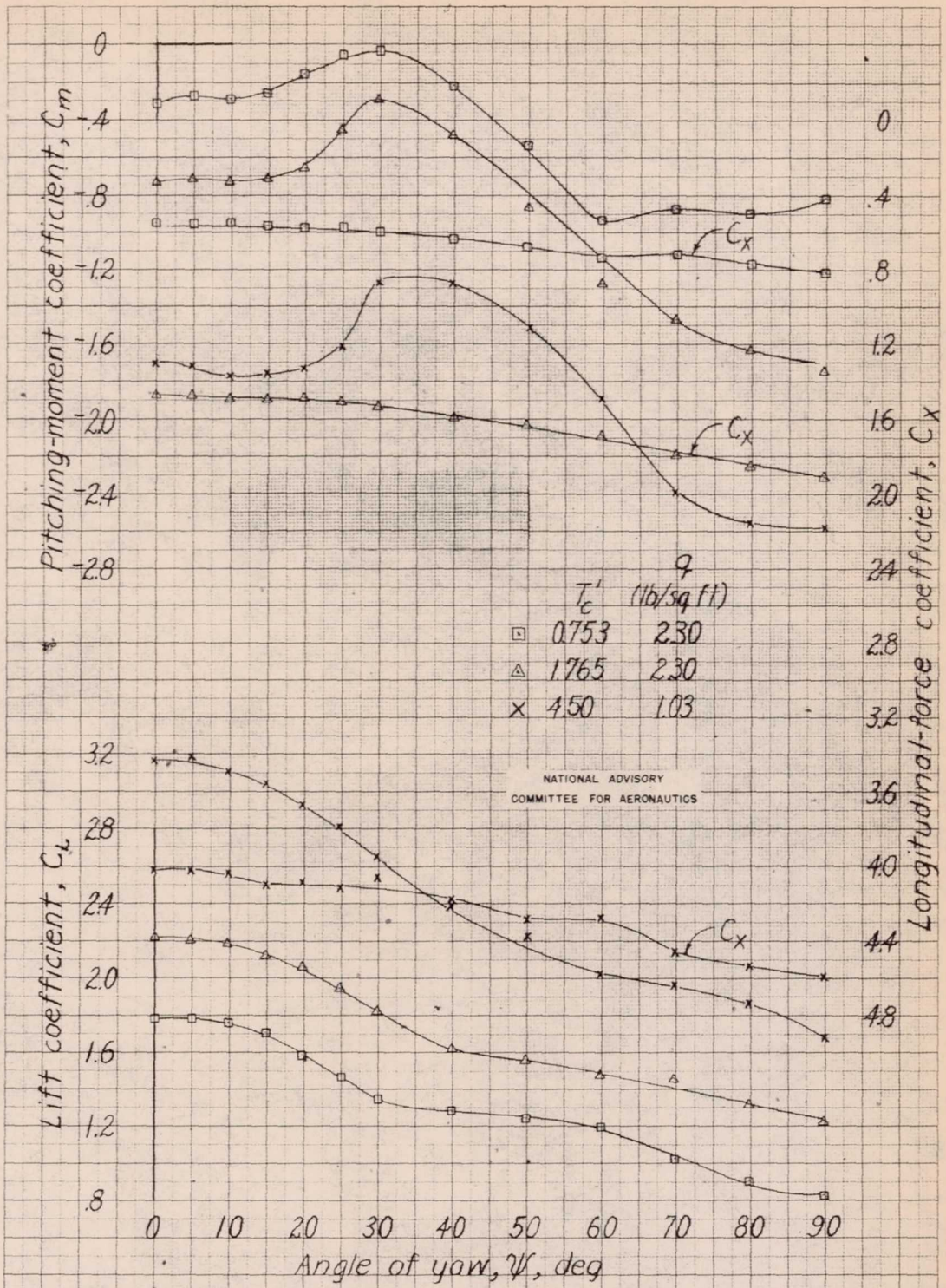

(a) $\alpha = 1.9°$.

Figure 20.- Effect of thrust on the aerodynamic characteristics in yaw of 1/25-scale model of Martin JRM-1 airplane. Draft = 1.8 in., $\Phi = 3.0°$, $B = 32.5°$, $\delta_f = 20°$.

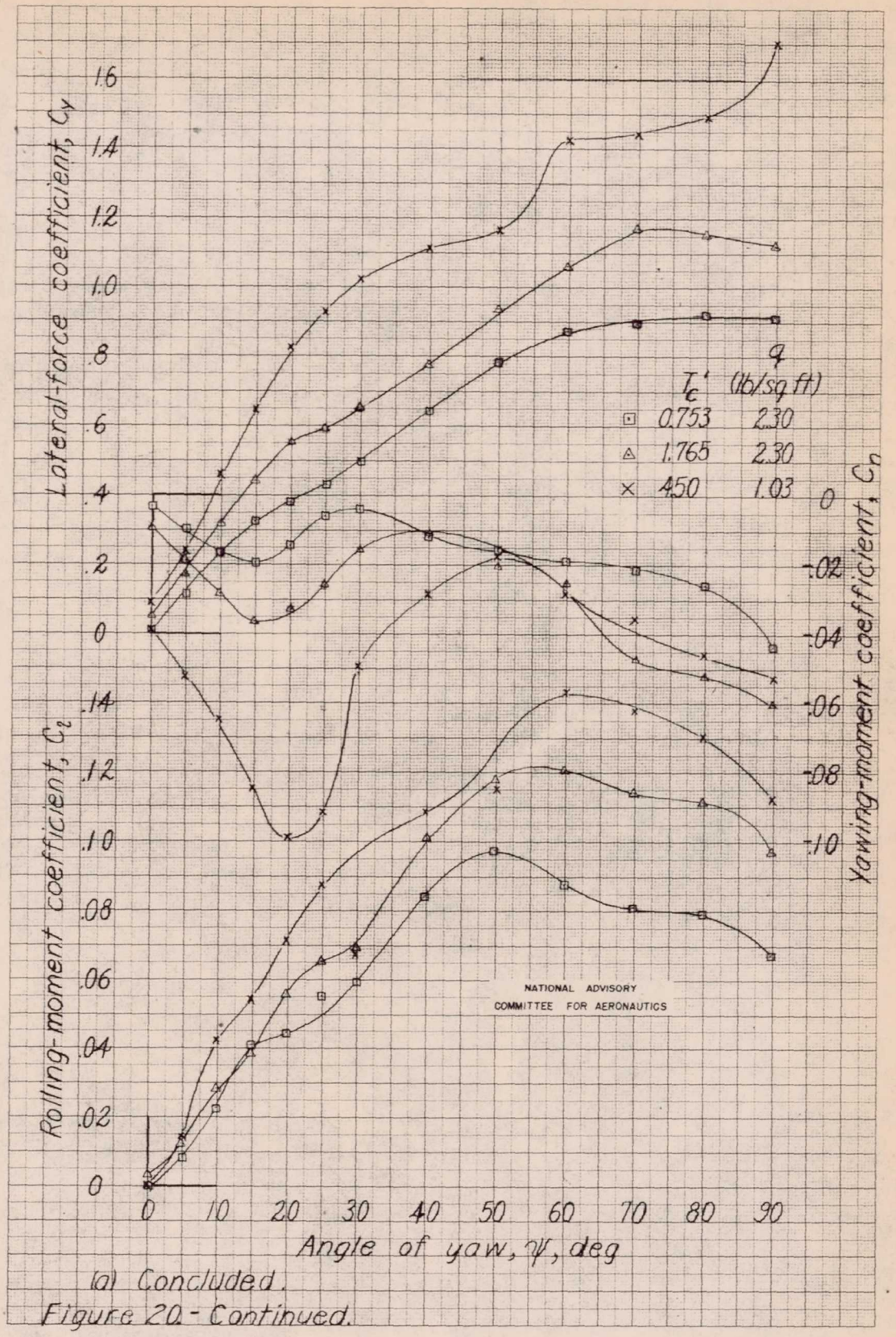

(a) Concluded.

Figure 20.- Continued.

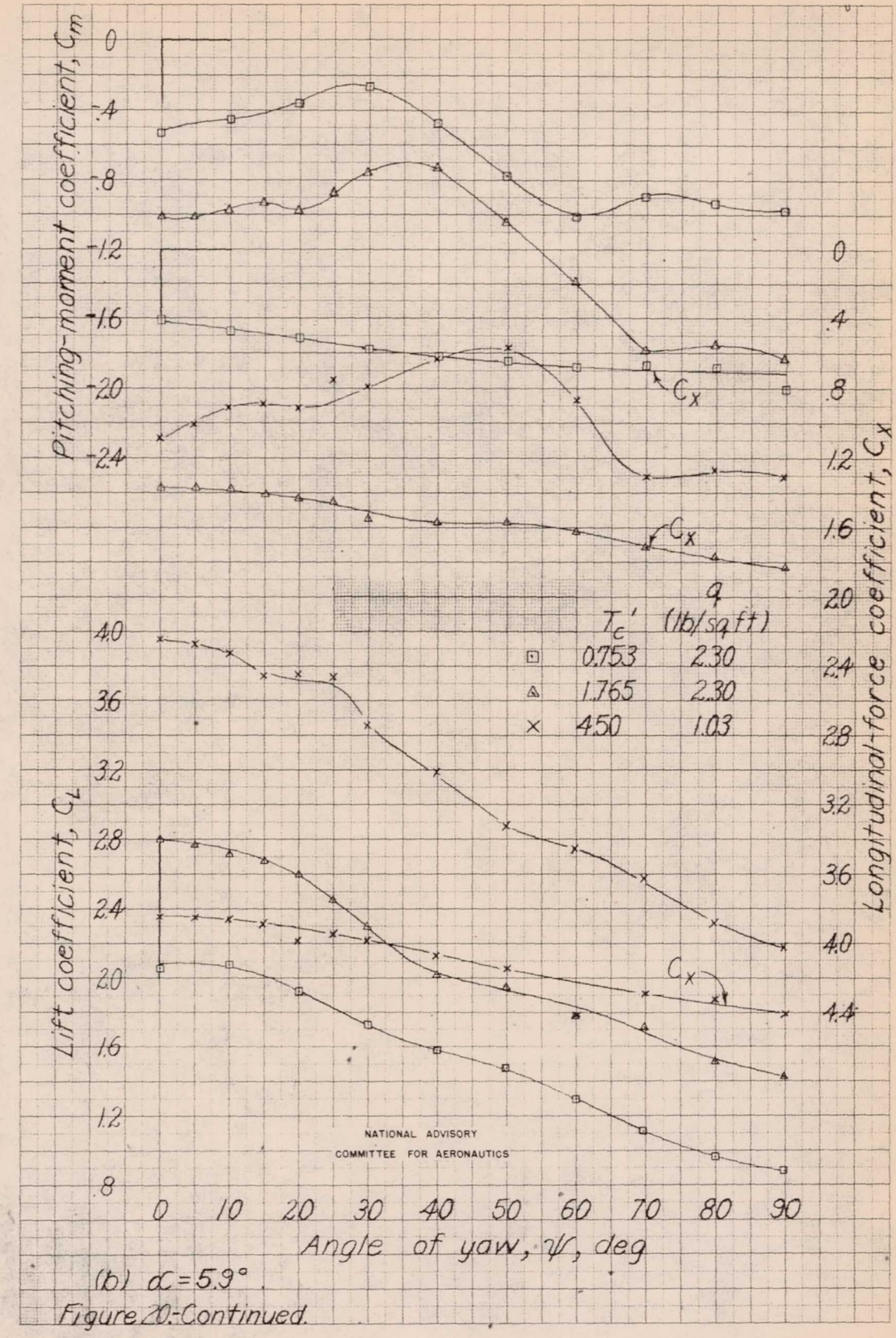

(b) $\alpha = 5.9°$.

Figure 20.-Continued.

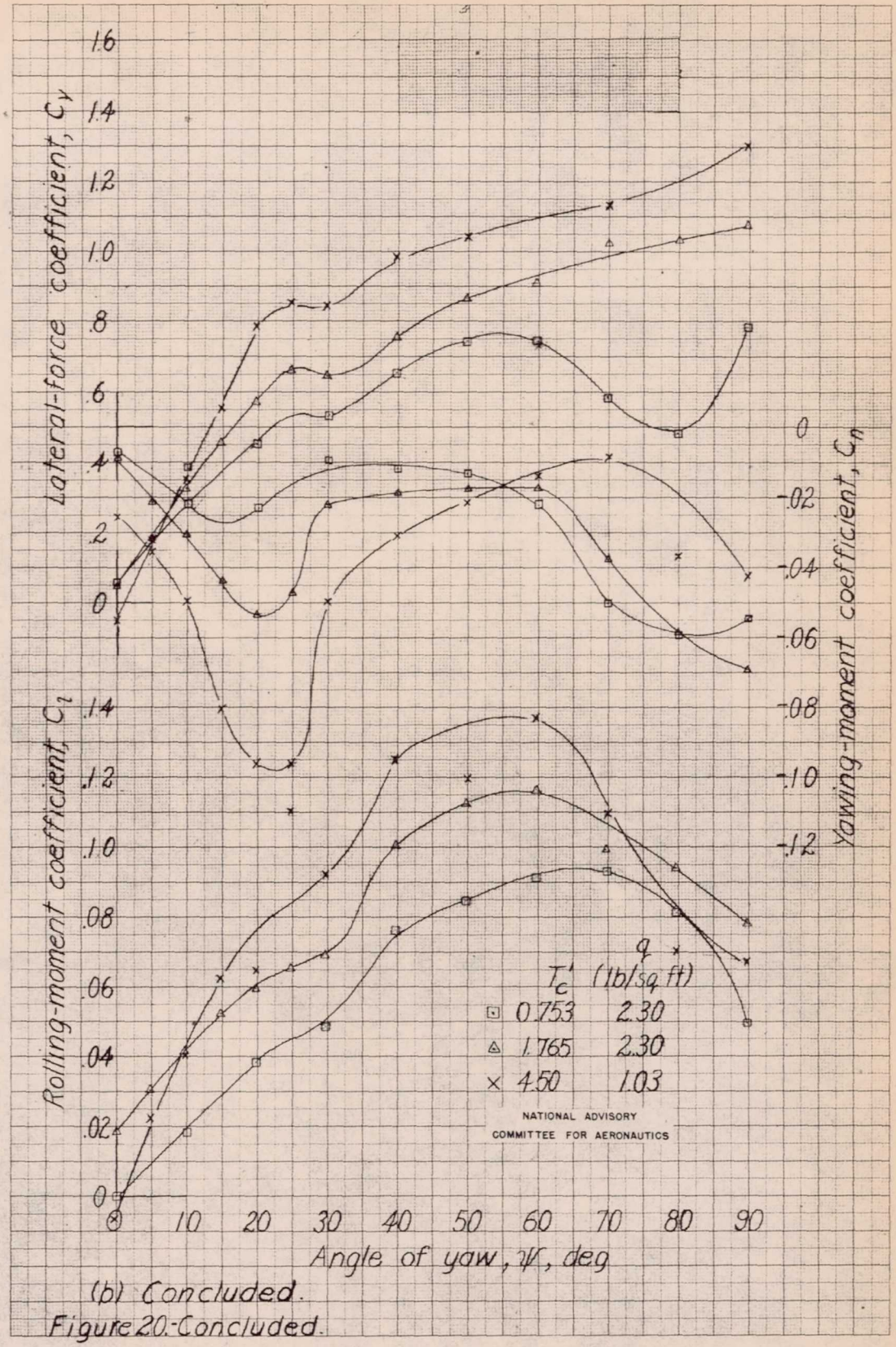

(b) Concluded.

Figure 20.-Concluded.

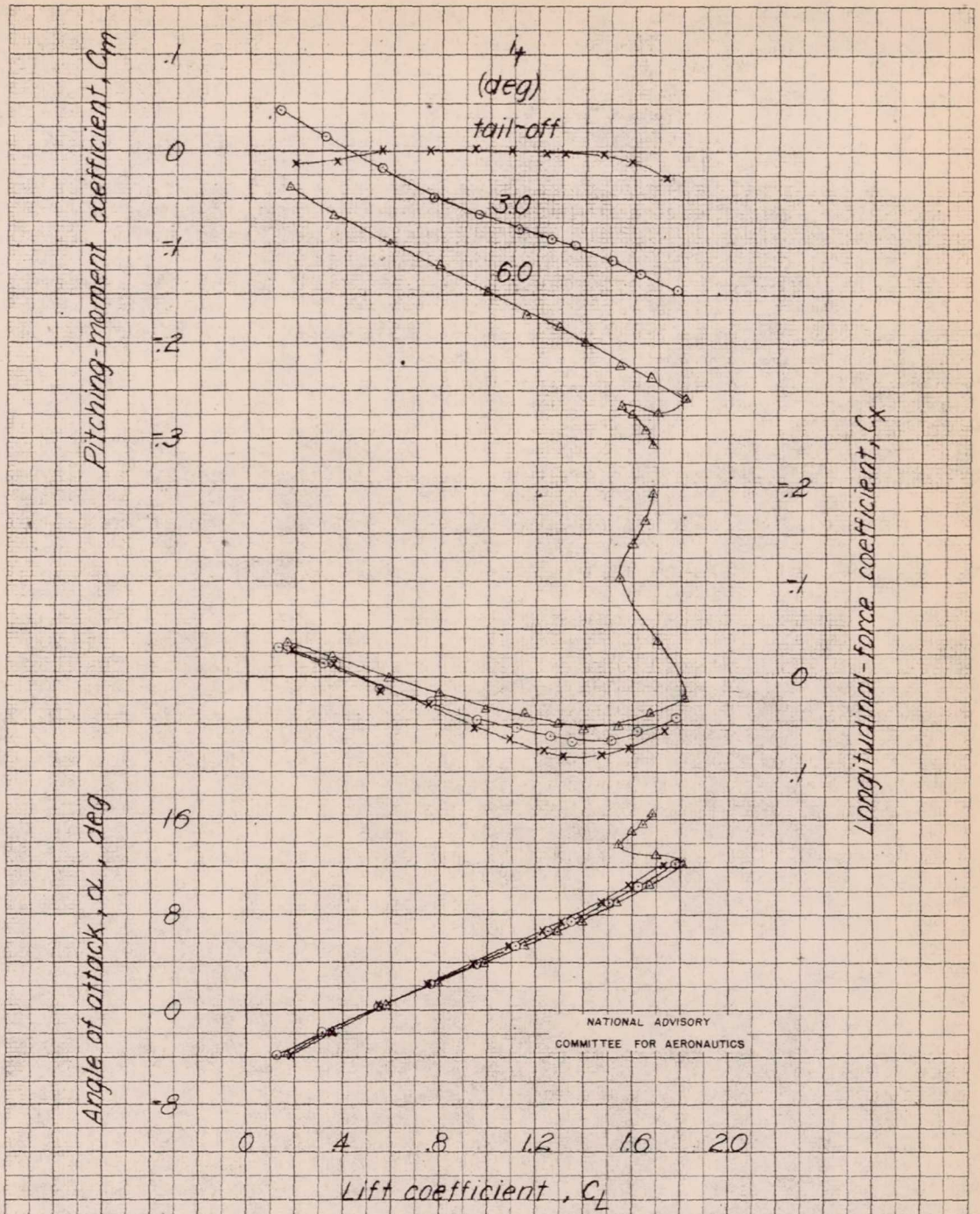

(a) Power A

Figure 21.- The effect of the stabilizer on the aerodynamic characteristics in pitch of the 1/25-scale model of the Martin JRM-1 airplane. Modified outer wing panels, $q = 4.09$ lb/sq ft, $\delta_f = 0°$

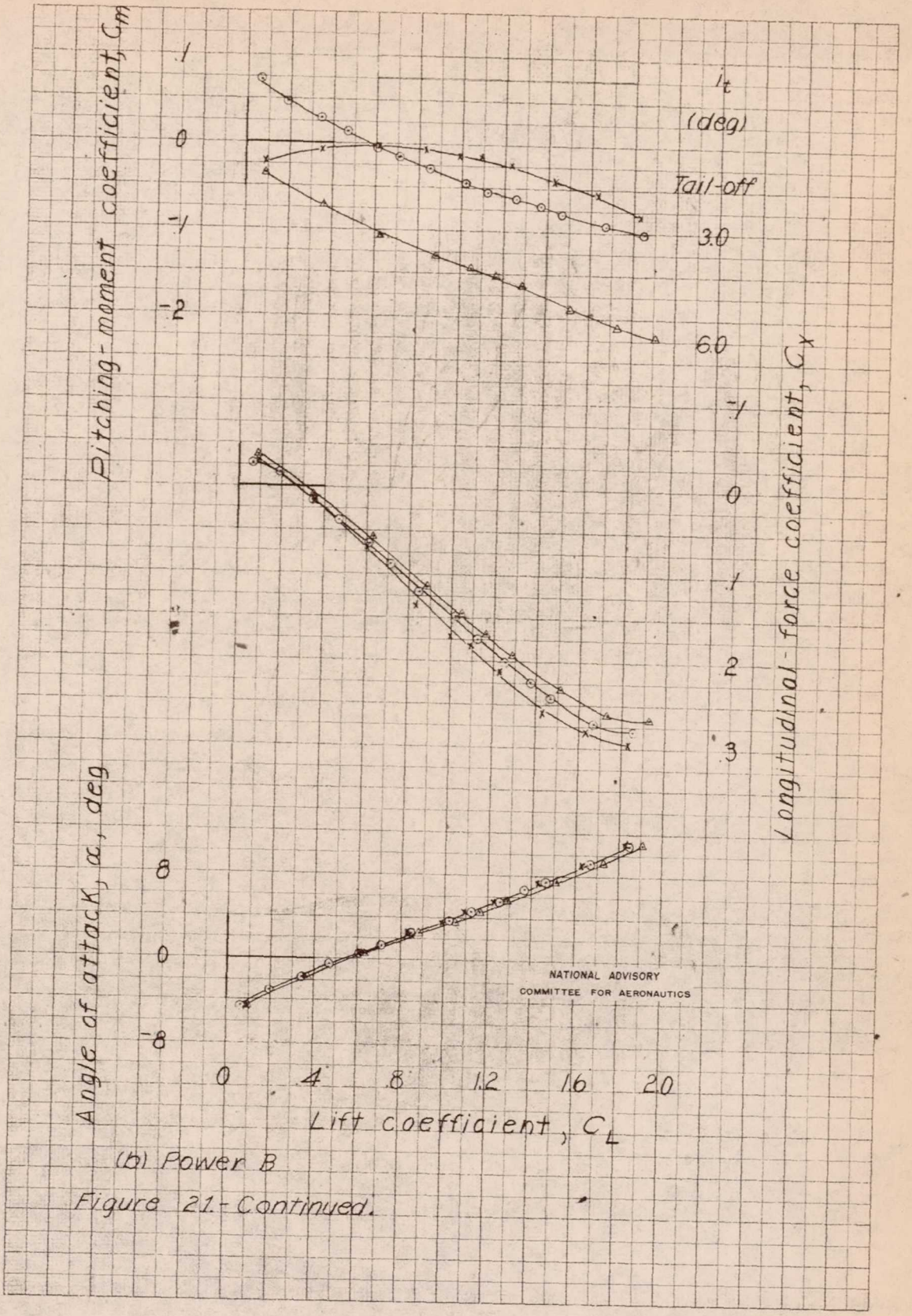

(b) Power B

Figure 21.- Continued.

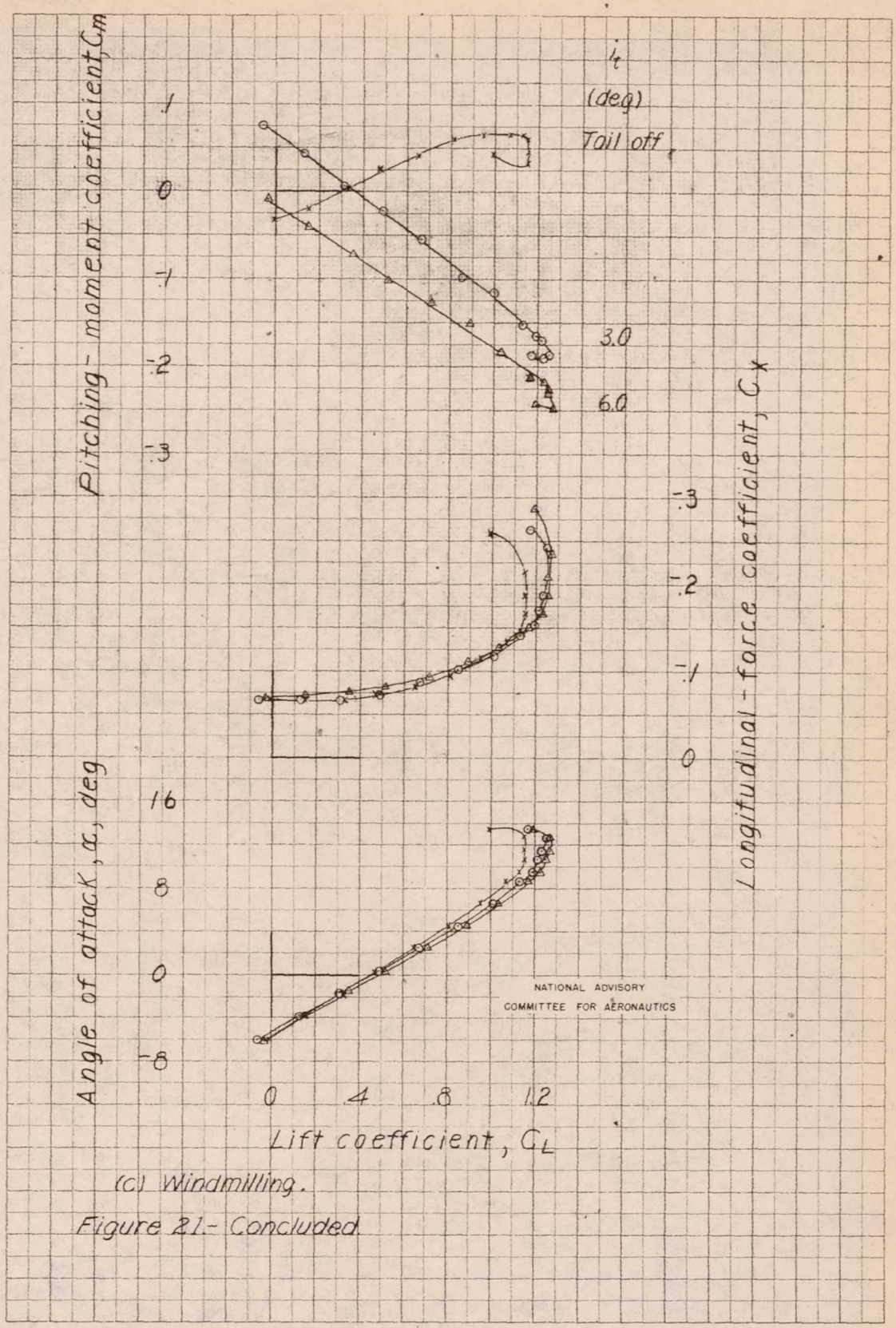

(c) Windmilling.

Figure 21.- Concluded.

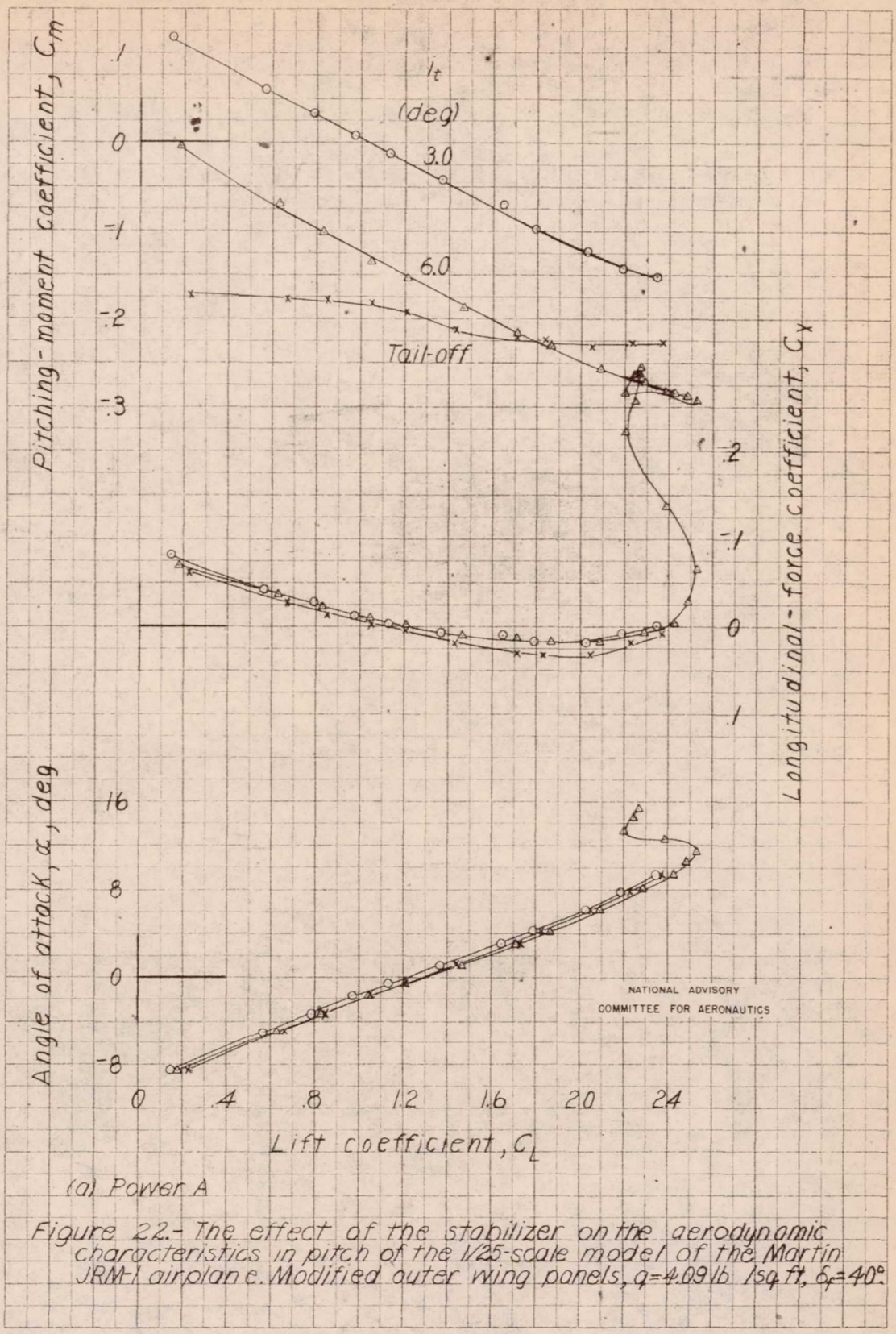

(a) Power A

Figure 22.- The effect of the stabilizer on the aerodynamic characteristics in pitch of the 1/25-scale model of the Martin JRM-1 airplane. Modified outer wing panels, q=4.09 lb/sq ft, δ_f=40°.

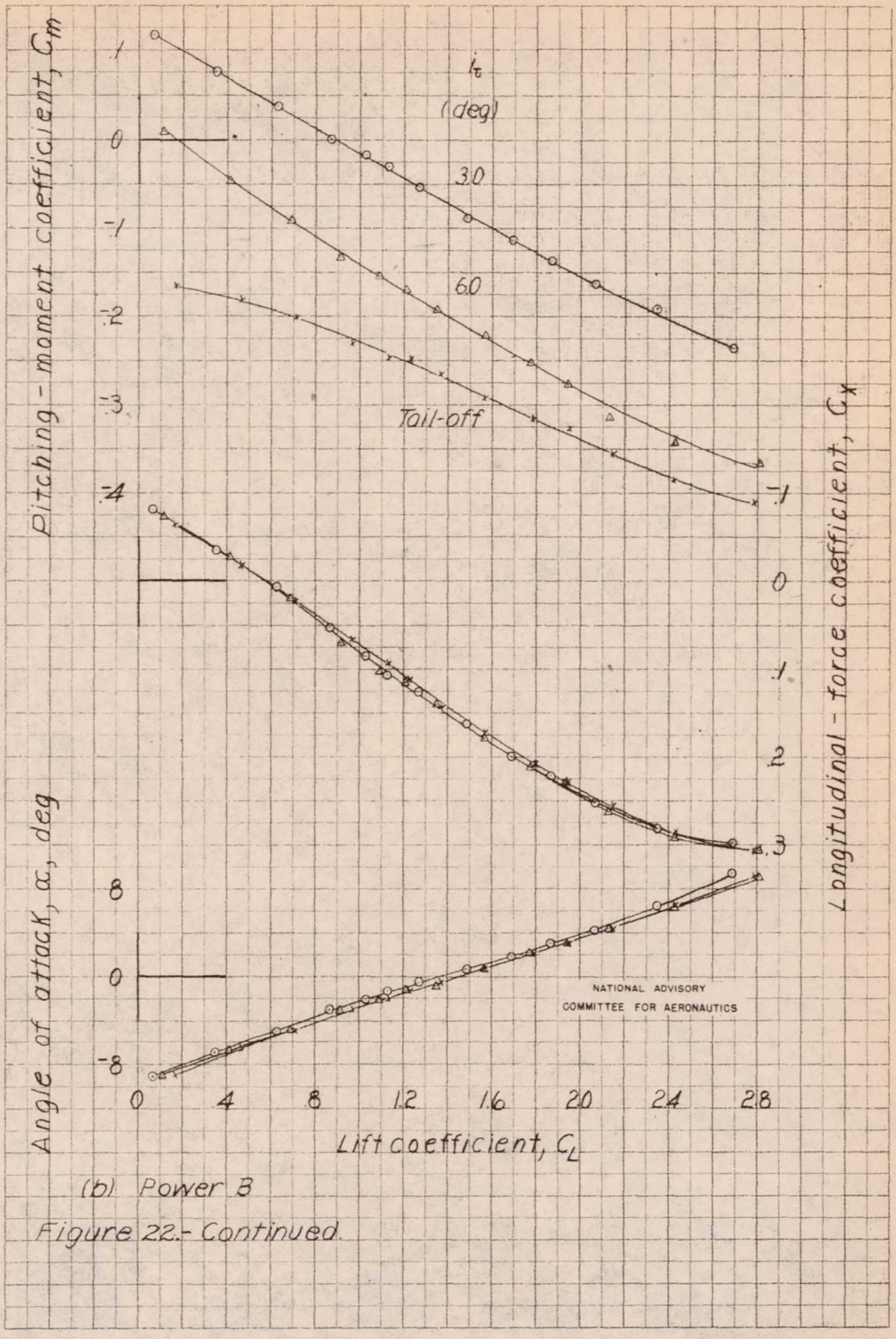

(b) Power B

Figure 22.- Continued.

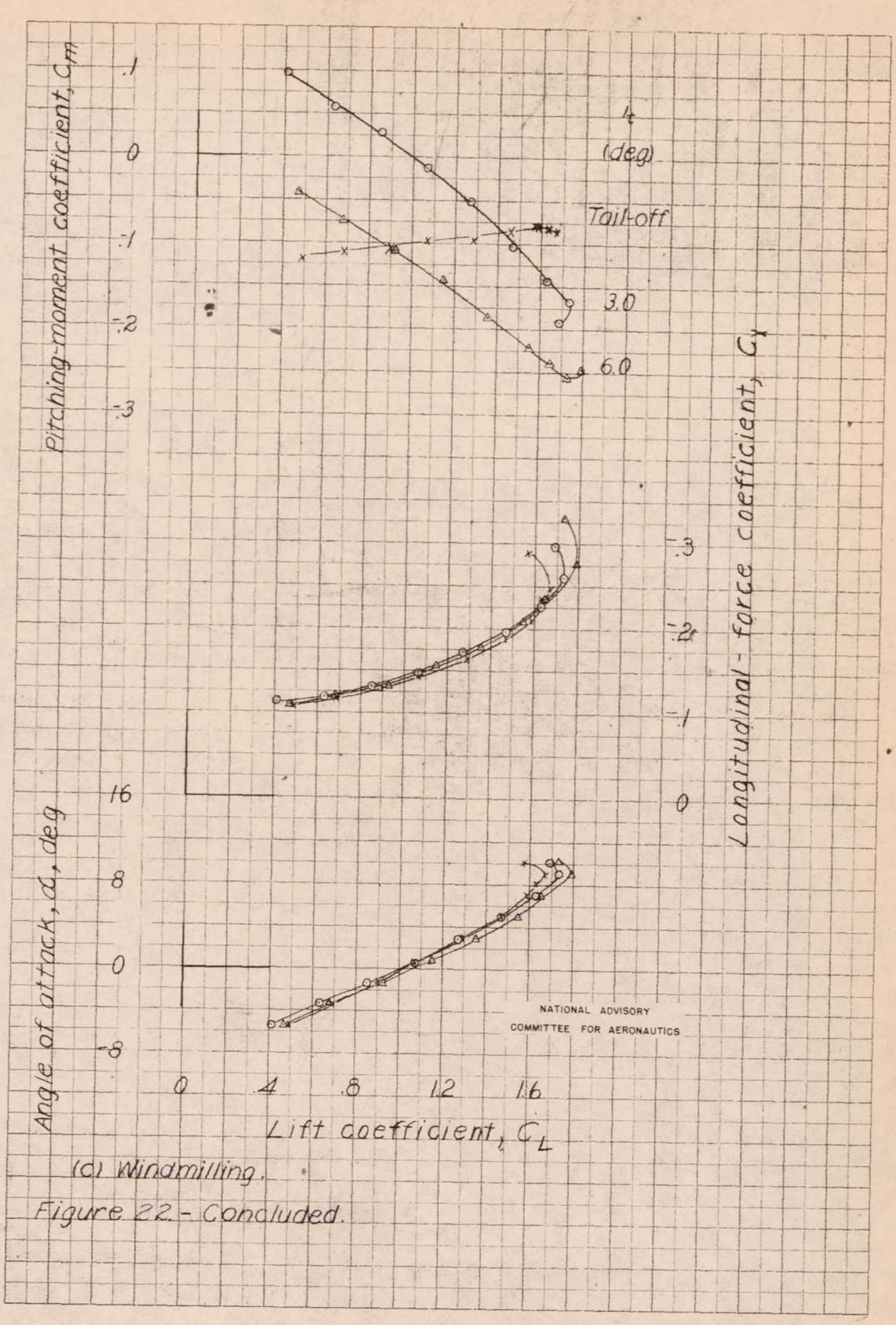

(c) Windmilling.

Figure 22.- Concluded.

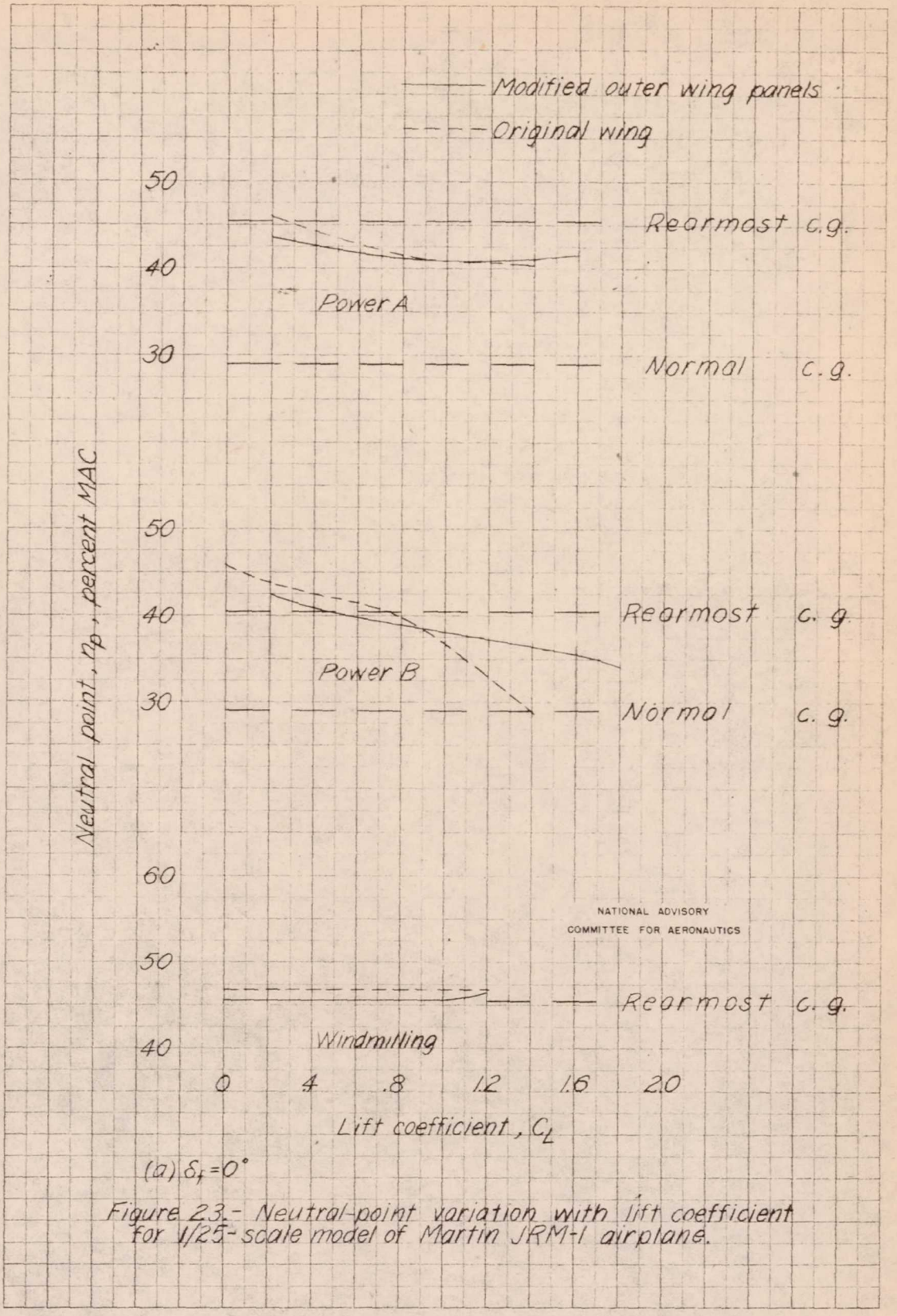

Figure 23.- Neutral-point variation with lift coefficient for 1/25-scale model of Martin JRM-1 airplane.

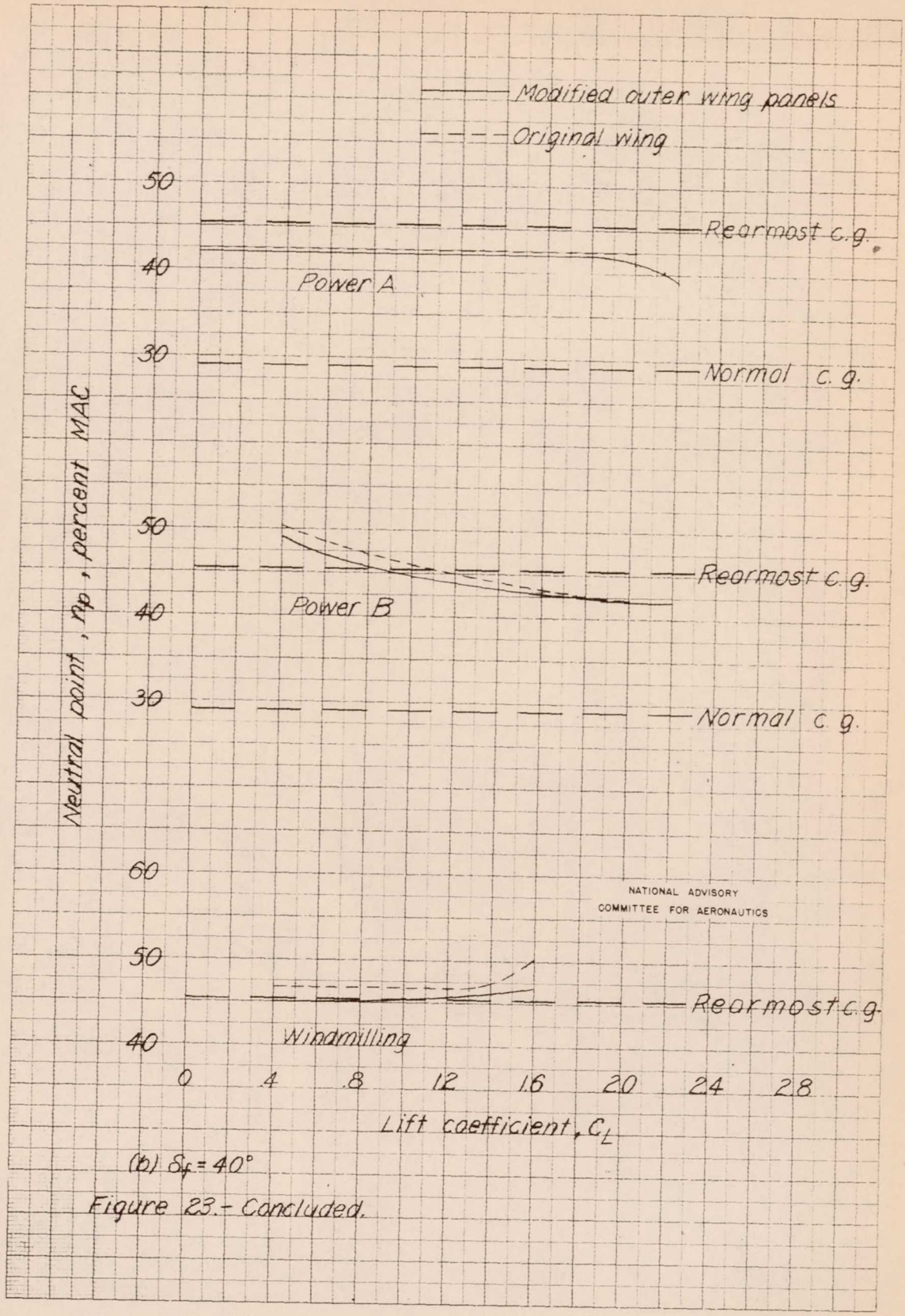

(b) $\delta_f = 40°$

Figure 23.- Concluded.

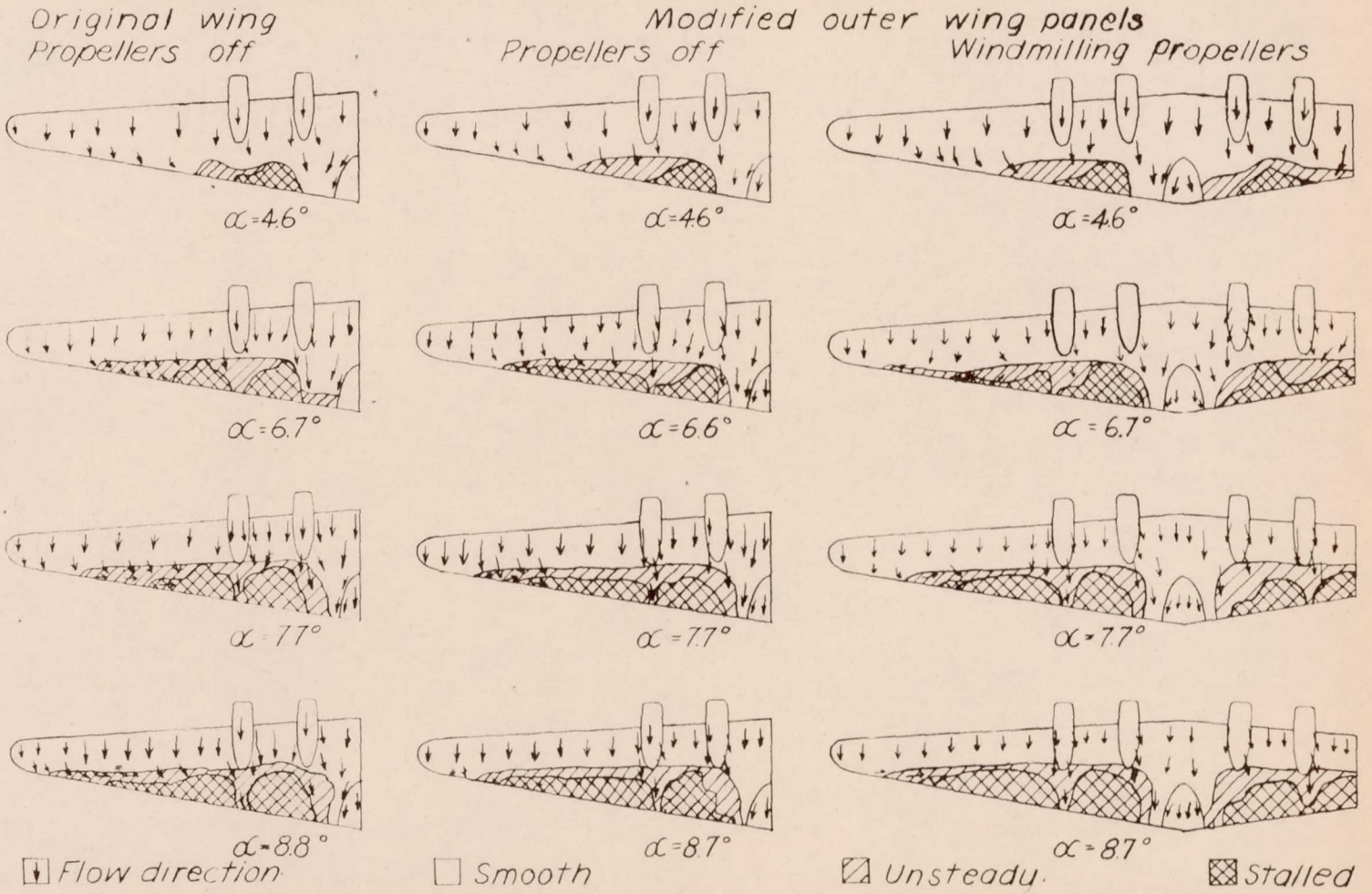

Figure 24.-Interpretation of air flow over wing of 1/25-scale model of Martin JRM-1 airplane from tuft photographs of the original wing (ref 1) and modified outer wing panel. $q = 16.37$ lb per sq ft, $\delta_f = 0°$.

NATIONAL ADVISORY
COMMITTEE FOR AERONAUTICS

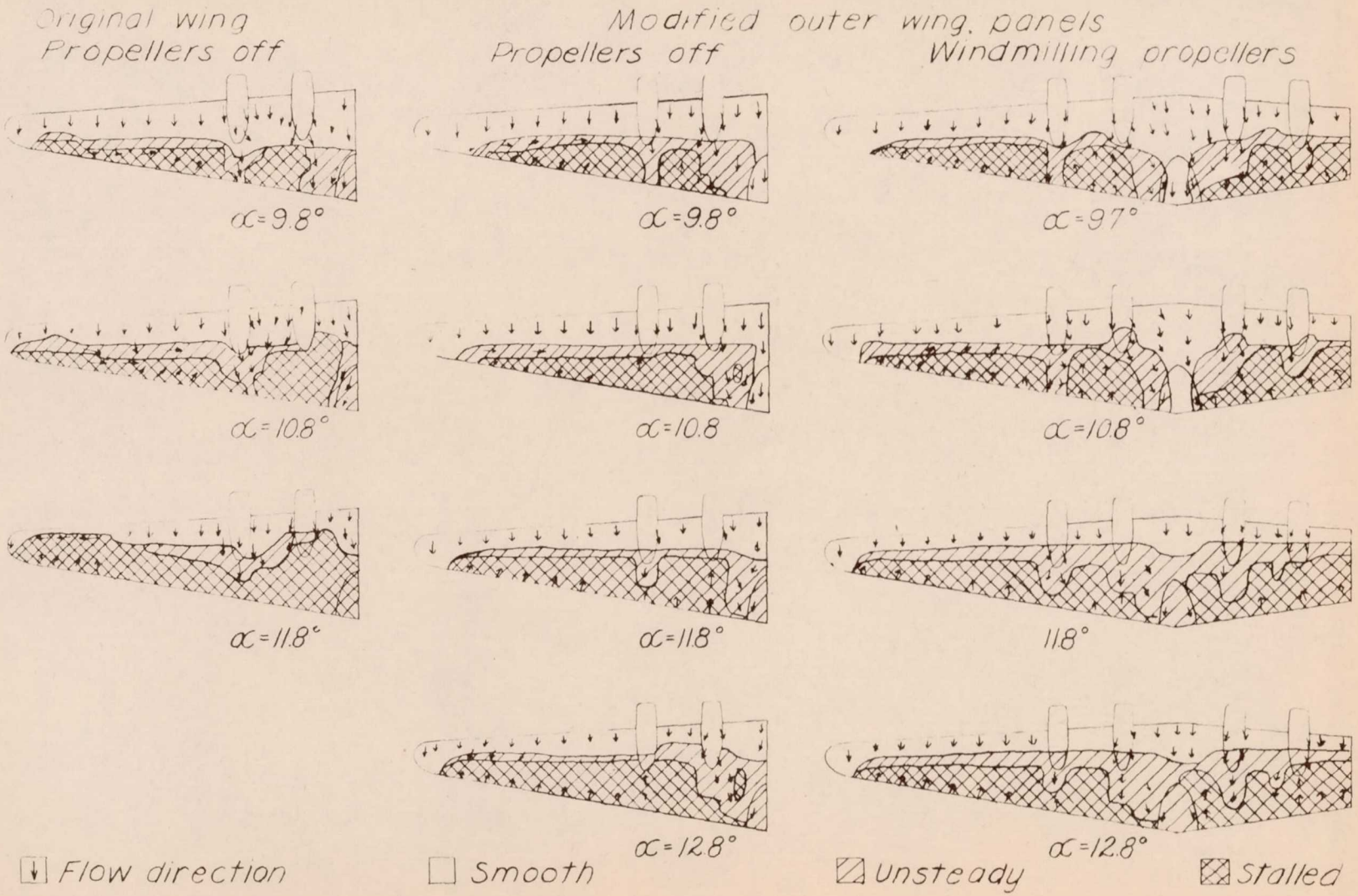

NATIONAL ADVISORY
COMMITTEE FOR AERONAUTICS

Figure 24-Continued.

Fig. 24 cont.

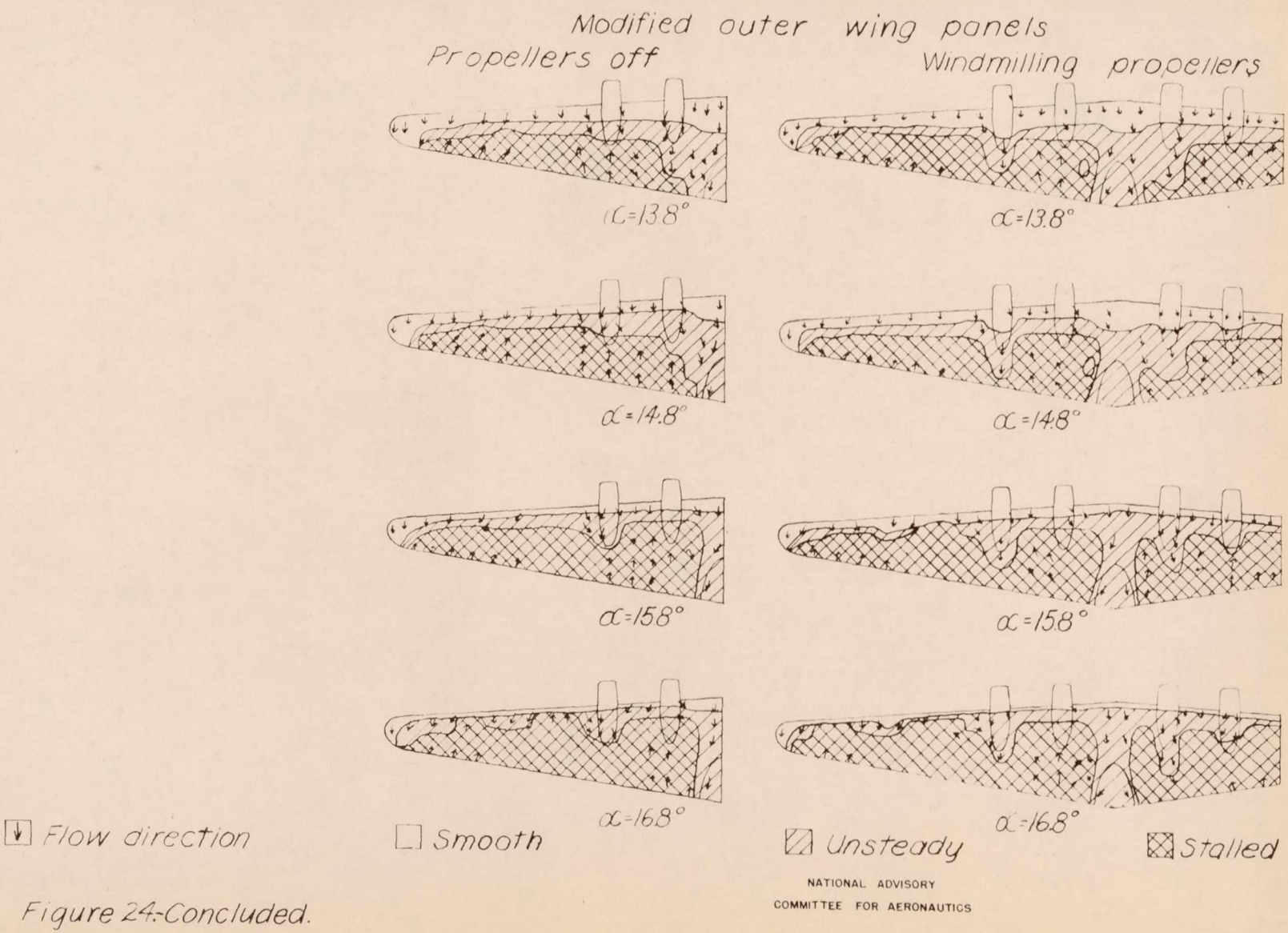

Figure 24.-Concluded.

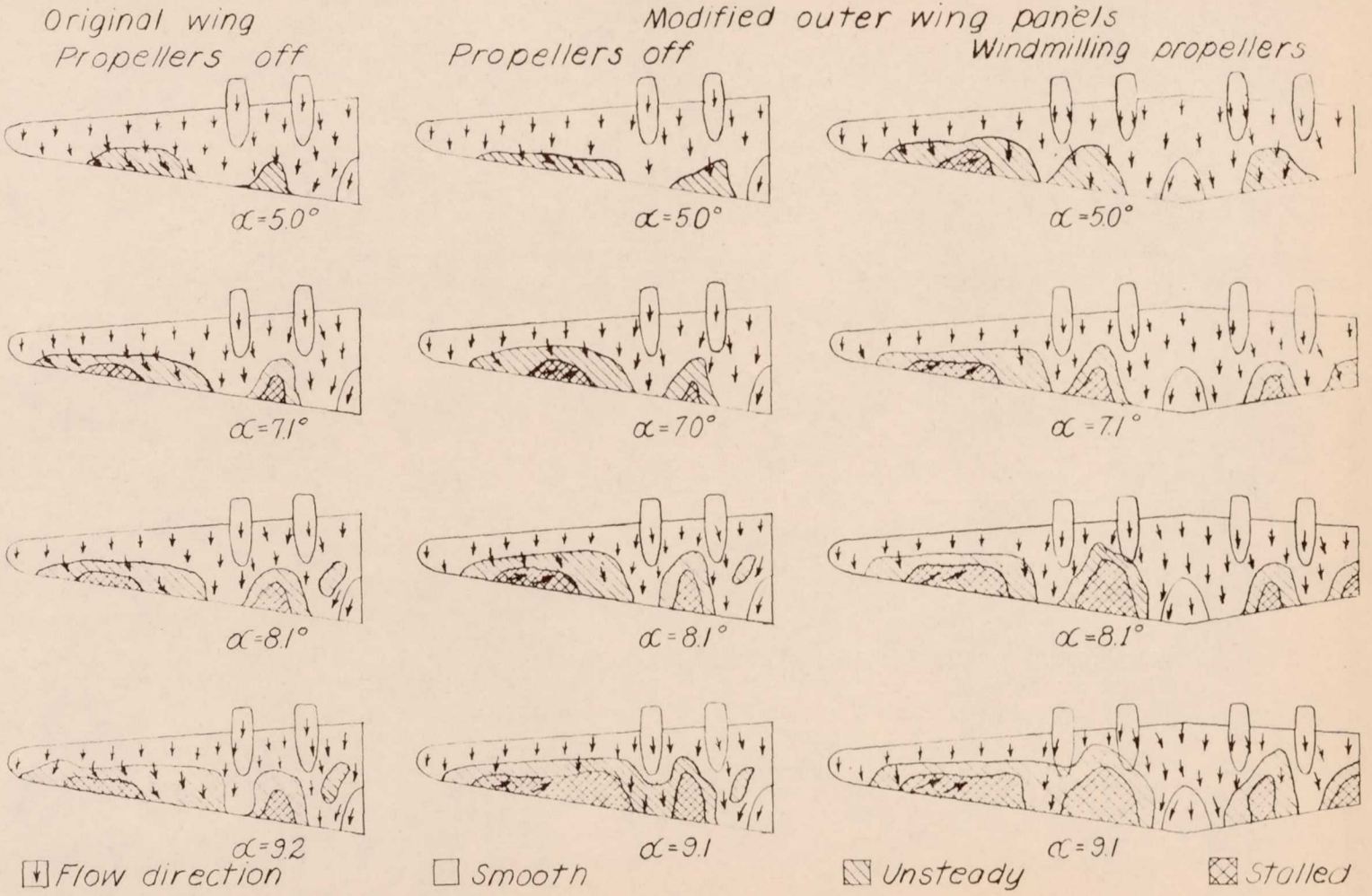

Figure 25.- Interpretation of airflow over wing of 1/25-scale model of Martin JRM-1 airplane from tuft photographs of the original wing (ref 1) and modified outer wing panel. $q = 16.37$ lbs per sq ft. $\delta_f = 40°$.

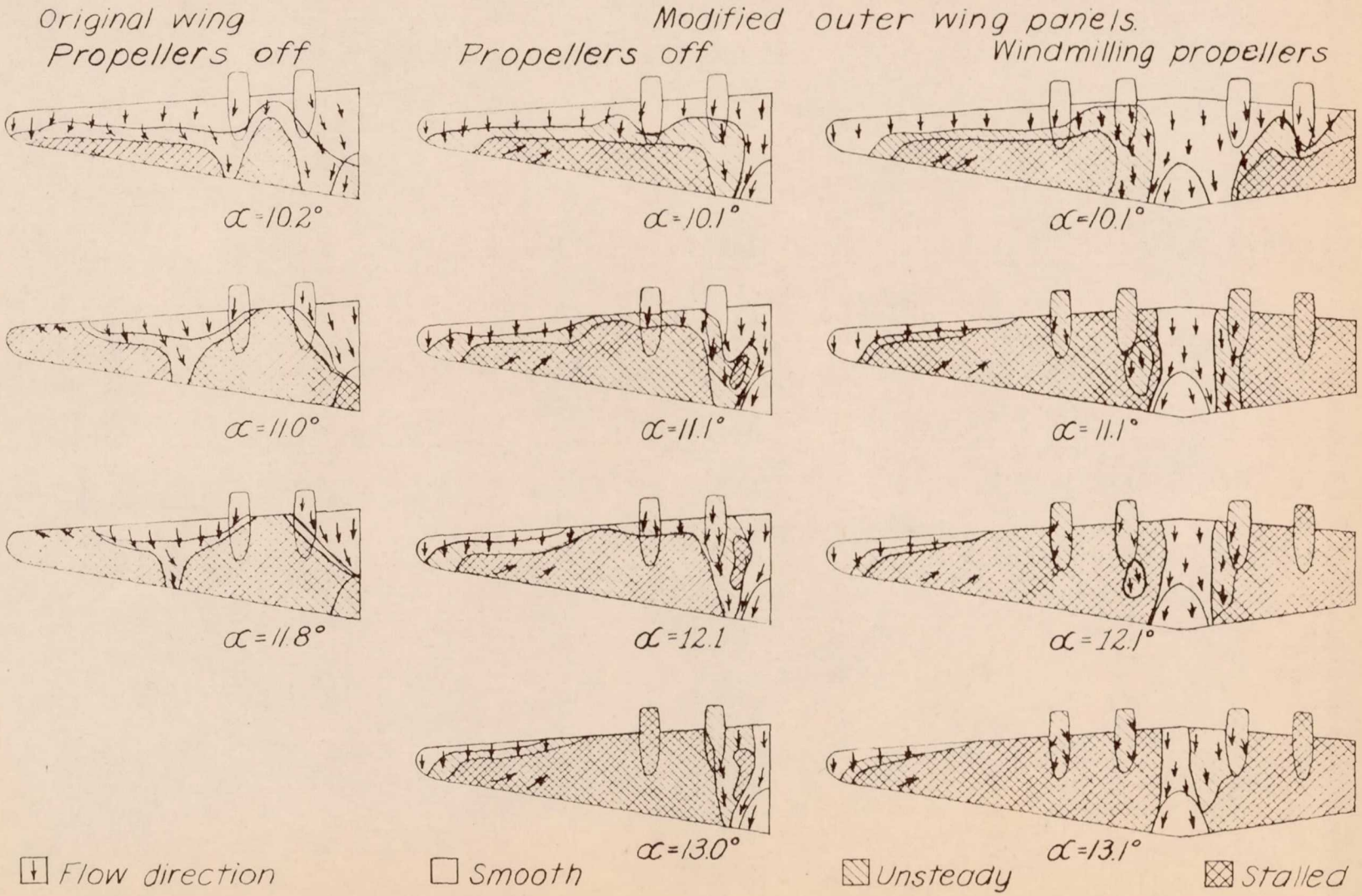

NATIONAL ADVISORY
COMMITTEE FOR AERONAUTICS

Figure 25.-Concluded.

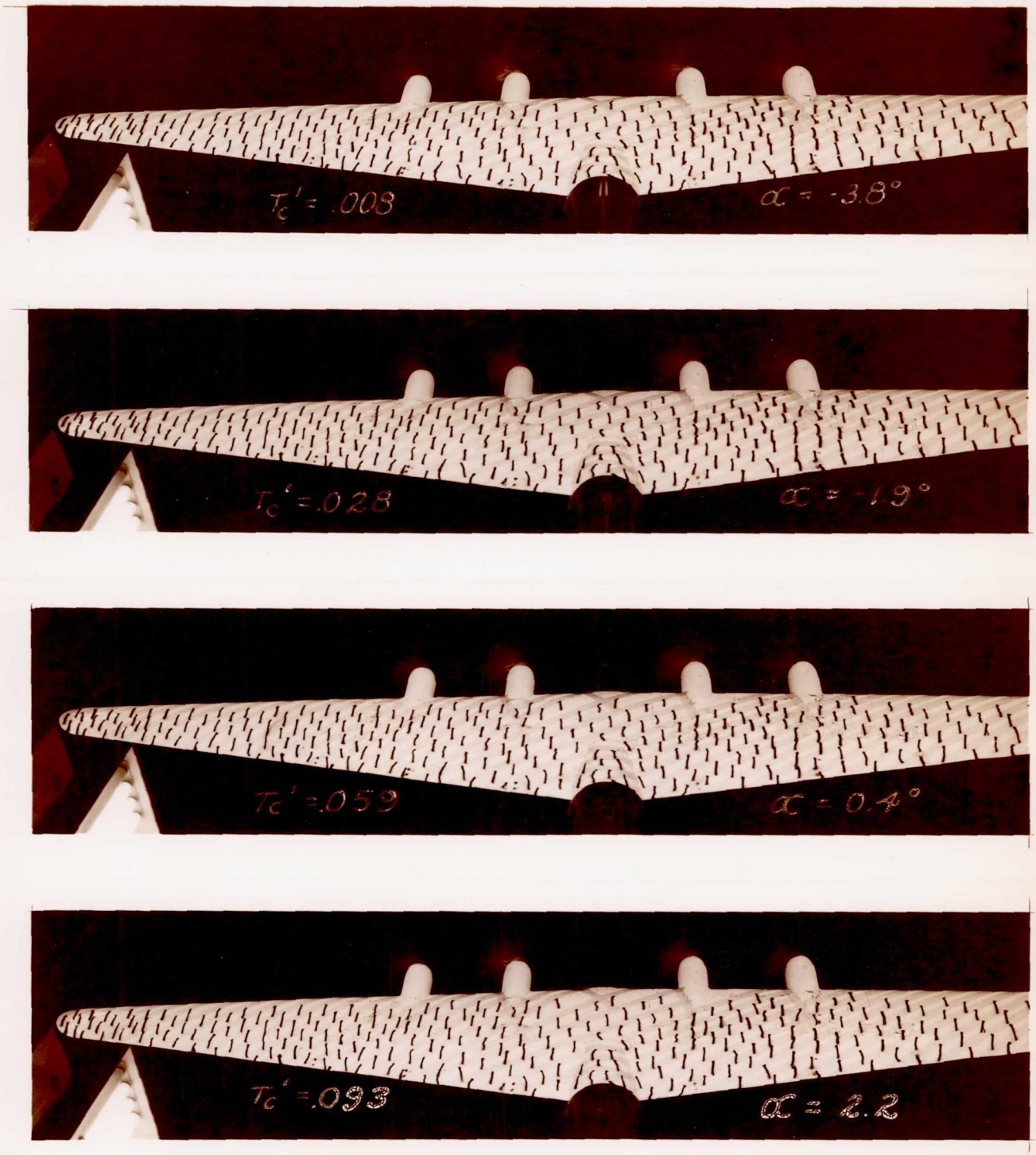

Figure 26.- Tuft studies of $\frac{1}{25}$-scale model of the Martin JRM-1 airplane with modified outer wing panels. Power A, $\delta_f = 0°$.

NATIONAL ADVISORY COMMITTEE FOR AERONAUTICS
LANGLEY MEMORIAL AERONAUTICAL LABORATORY - LANGLEY FIELD, VA.

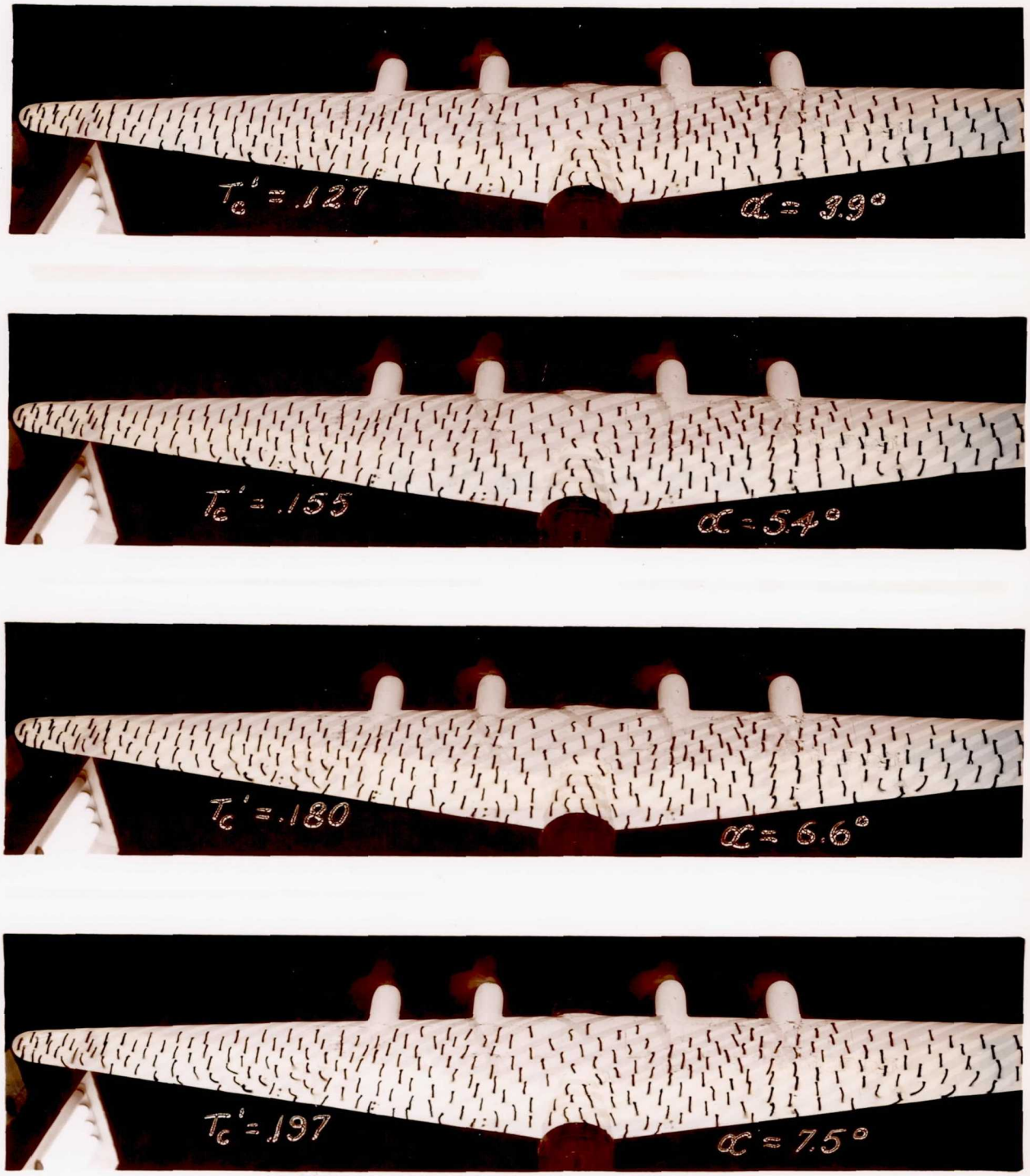

Figure 26.- Continued.

NATIONAL ADVISORY COMMITTEE FOR AERONAUTICS
LANGLEY MEMORIAL AERONAUTICAL LABORATORY – LANGLEY FIELD, VA

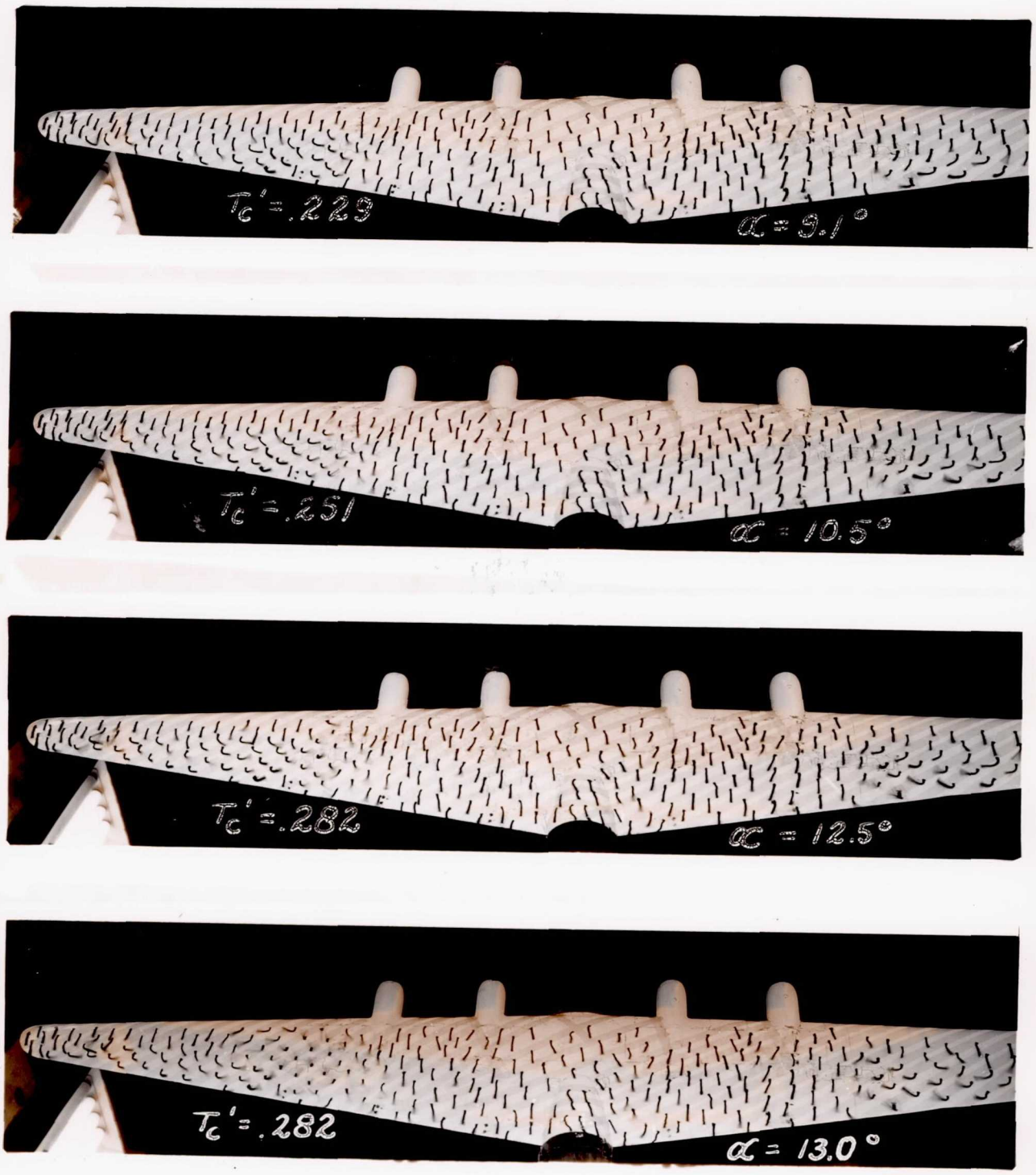

Figure 26.- Continued.

NATIONAL ADVISORY COMMITTEE FOR AERONAUTICS
LANGLEY MEMORIAL AERONAUTICAL LABORATORY – LANGLEY FIELD, VA.

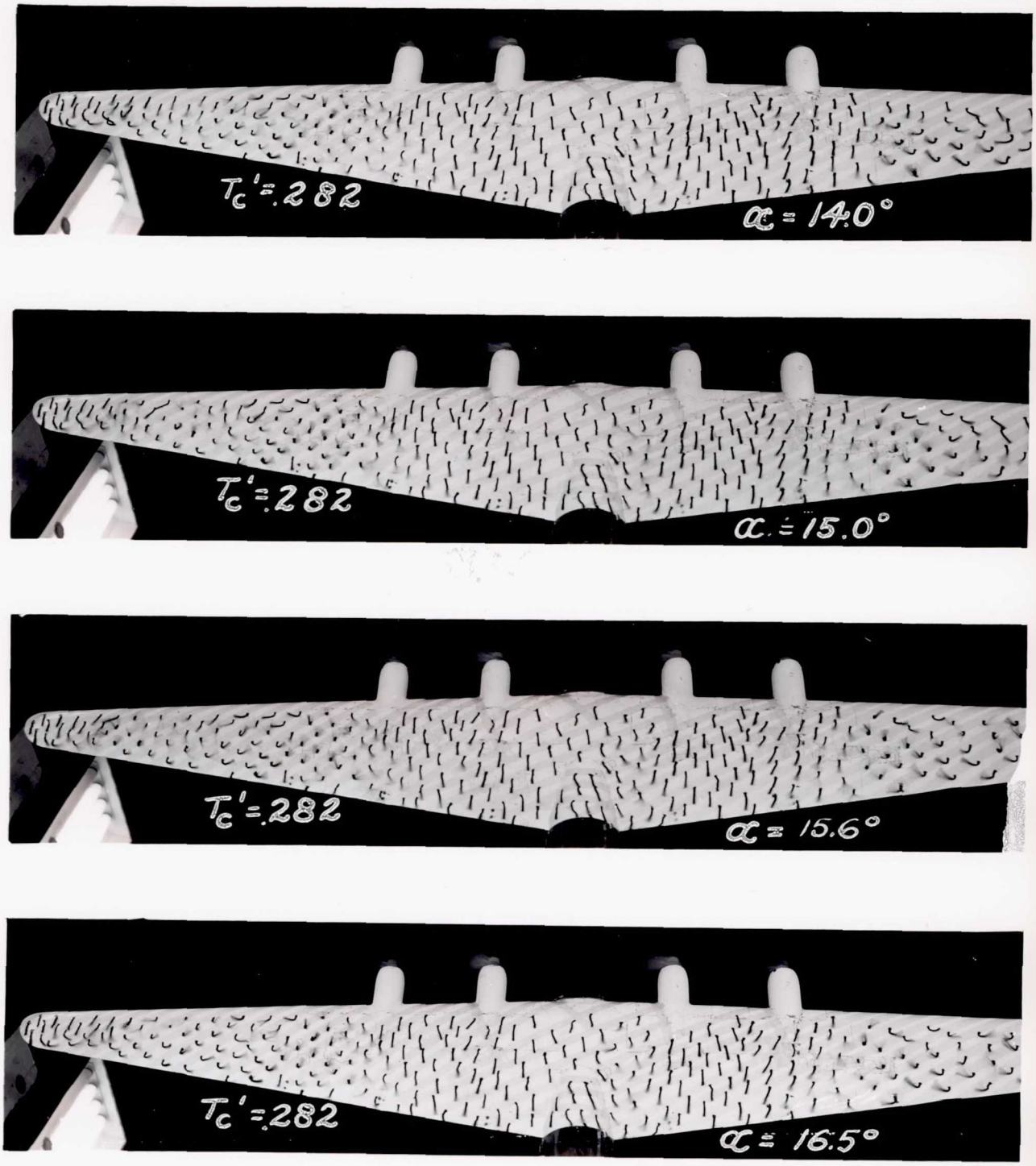

Figure 26.- Concluded.

NATIONAL ADVISORY COMMITTEE FOR AERONAUTICS
LANGLEY MEMORIAL AERONAUTICAL LABORATORY - LANGLEY FIELD, VA.

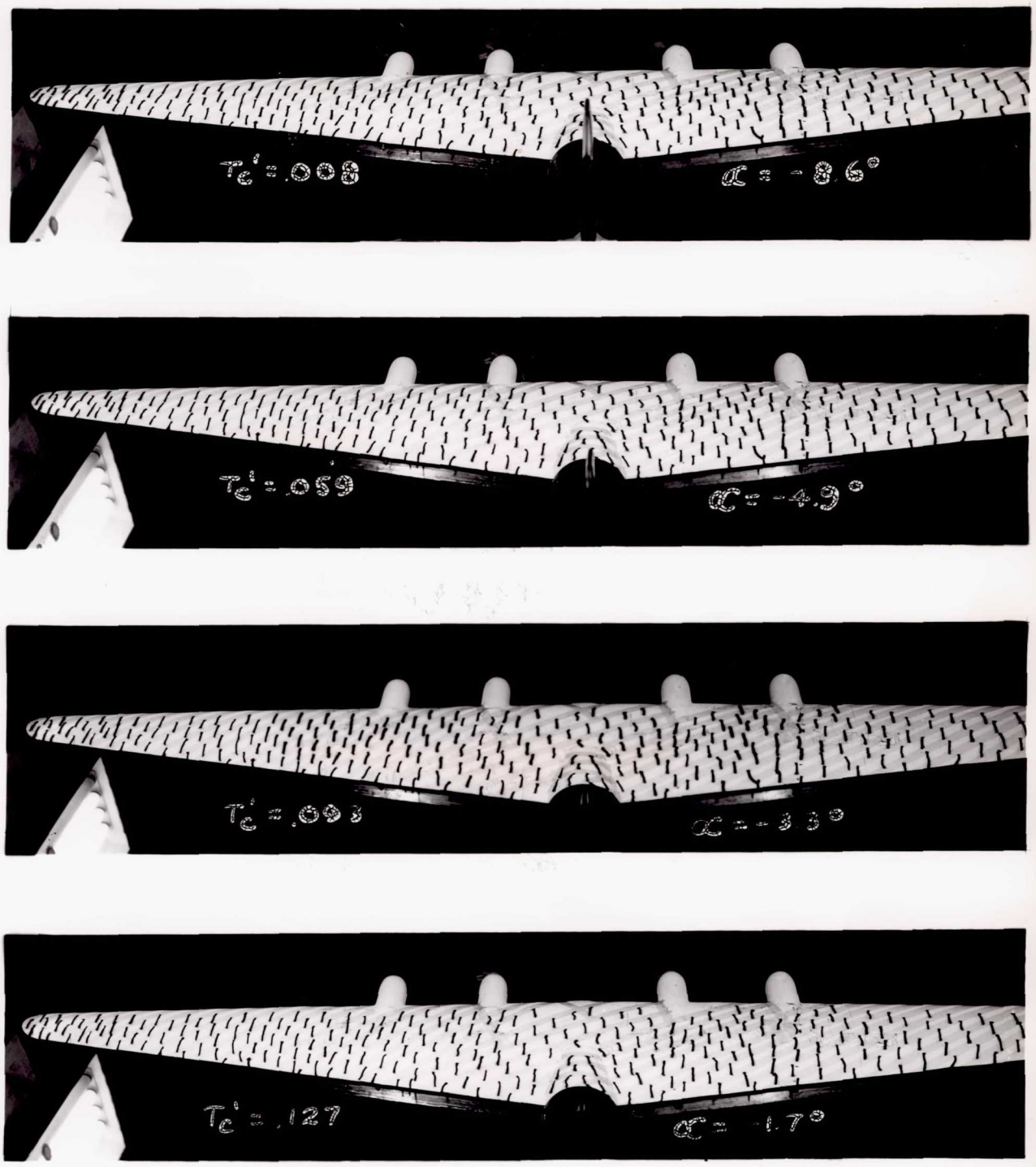

Figure 27.- Tuft studies of $\frac{1}{25}$-scale model of the Martin JRM-1 airplane with modified outer wing panels. Power A, $\delta_f = 40^o$.

NATIONAL ADVISORY COMMITTEE FOR AERONAUTICS
LANGLEY MEMORIAL AERONAUTICAL LABORATORY – LANGLEY FIELD, VA.

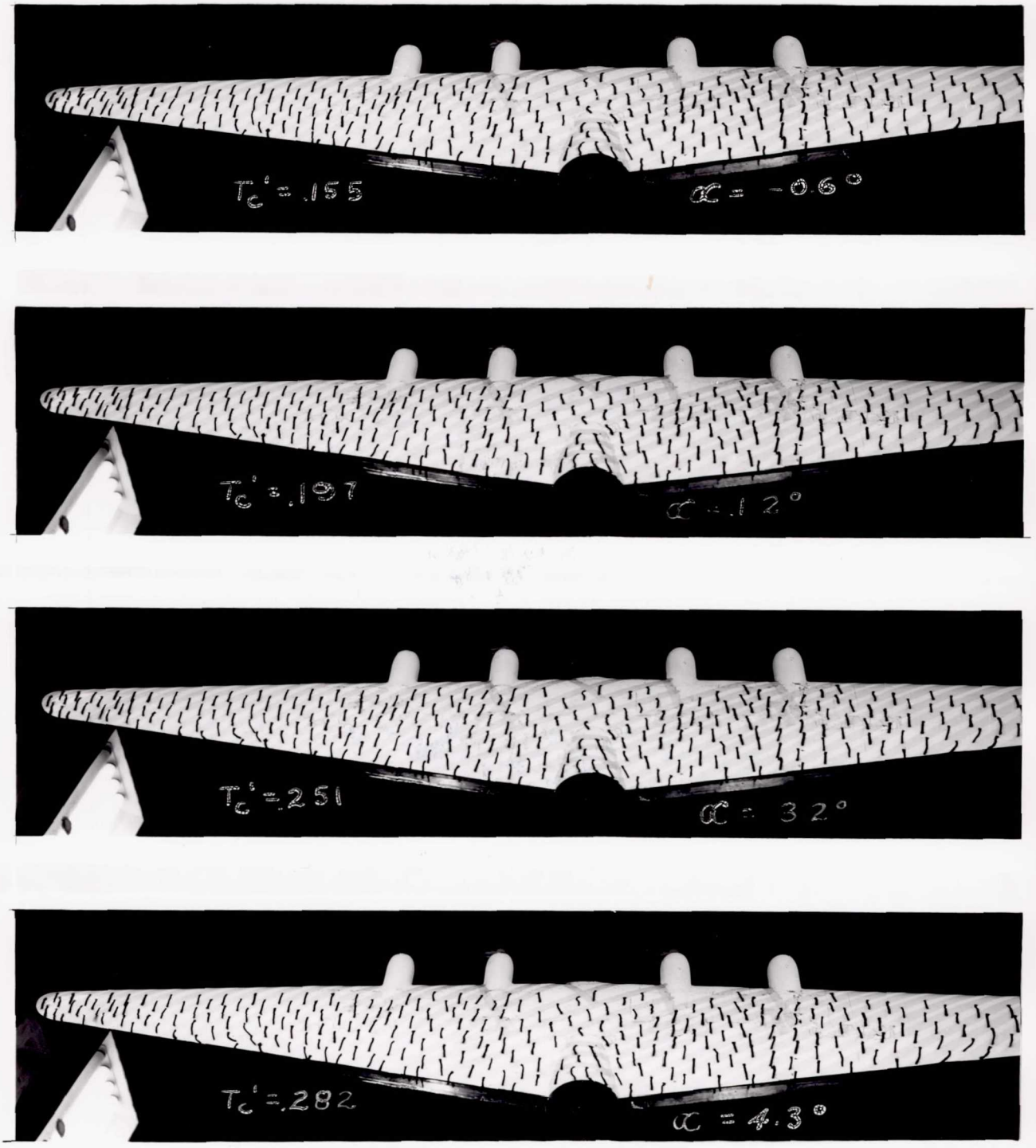

Figure 27.- Continued.

NATIONAL ADVISORY COMMITTEE FOR AERONAUTICS
LANGLEY MEMORIAL AERONAUTICAL LABORATORY - LANGLEY FIELD, VA.

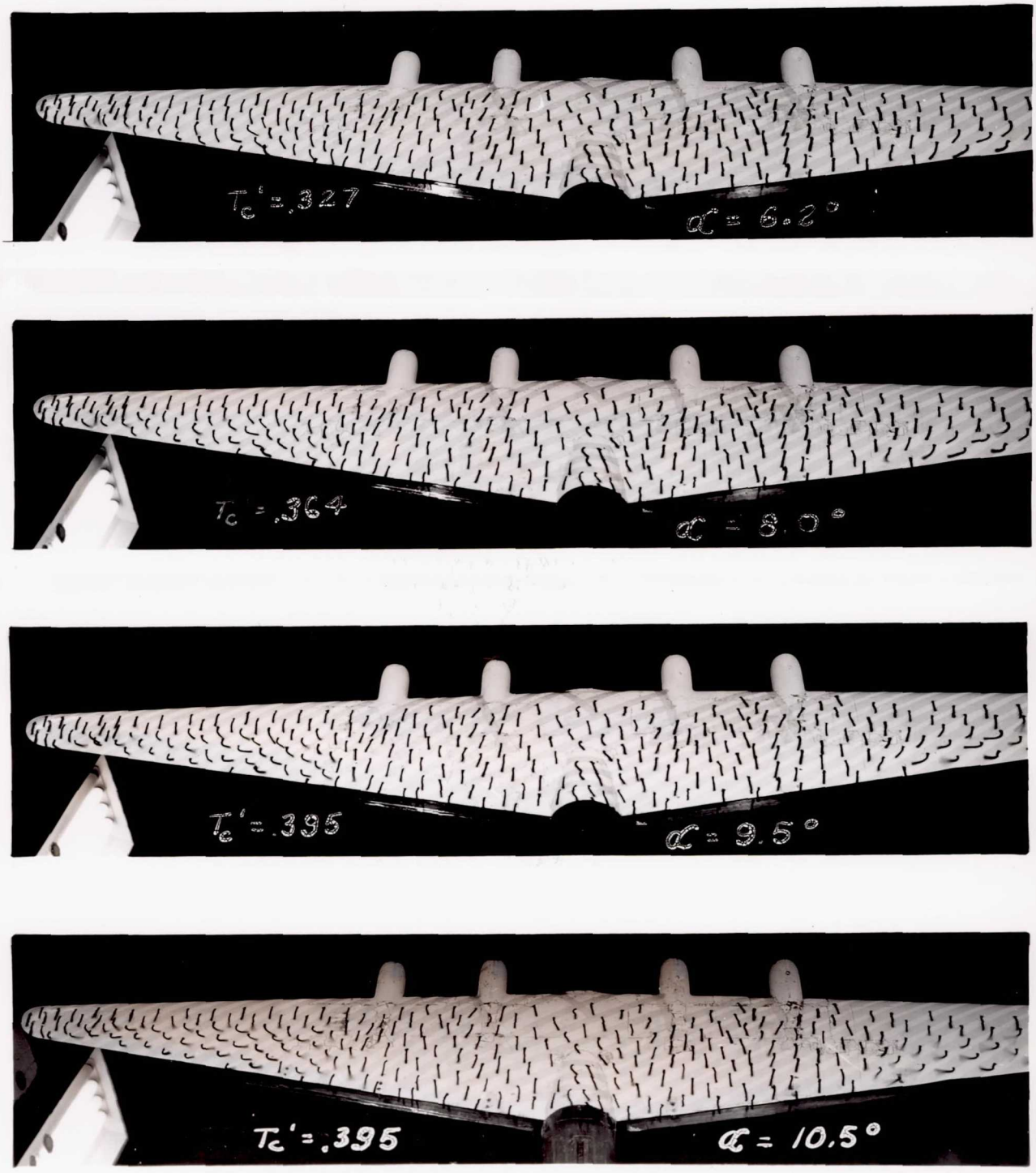

Figure 27.- Continued.

NATIONAL ADVISORY COMMITTEE FOR AERONAUTICS
LANGLEY MEMORIAL AERONAUTICAL LABORATORY - LANGLEY FIELD, VA.

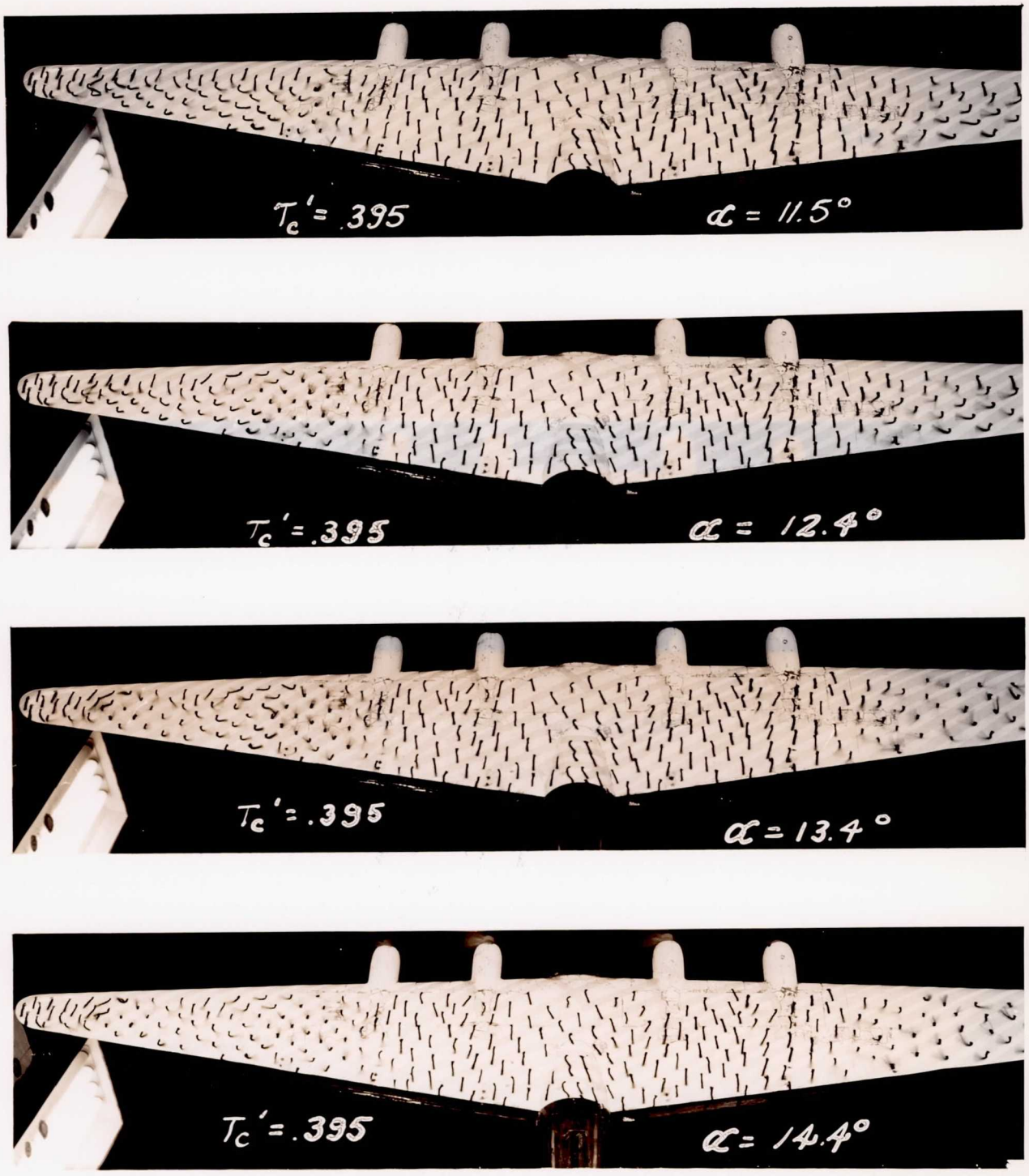

Figure 27.- Continued.

NATIONAL ADVISORY COMMITTEE FOR AERONAUTICS
LANGLEY MEMORIAL AERONAUTICAL LABORATORY – LANGLEY FIELD, VA

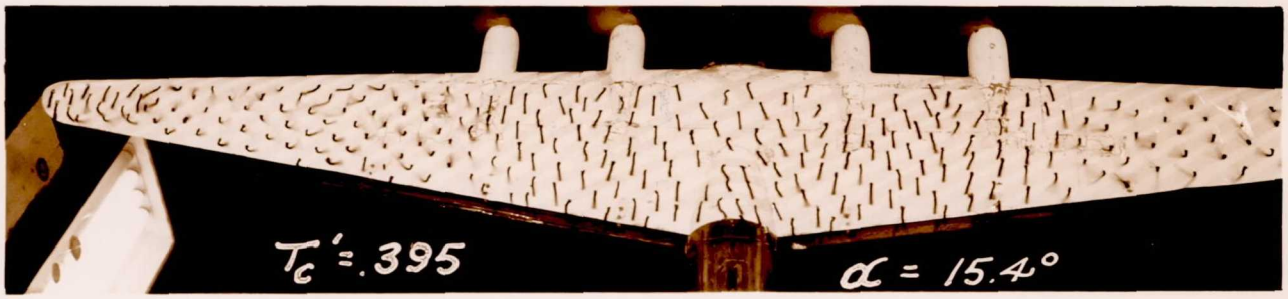

Figure 27.- Concluded.

NATIONAL ADVISORY COMMITTEE FOR AERONAUTICS
LANGLEY MEMORIAL AERONAUTICAL LABORATORY - LANGLEY FIELD, VA.

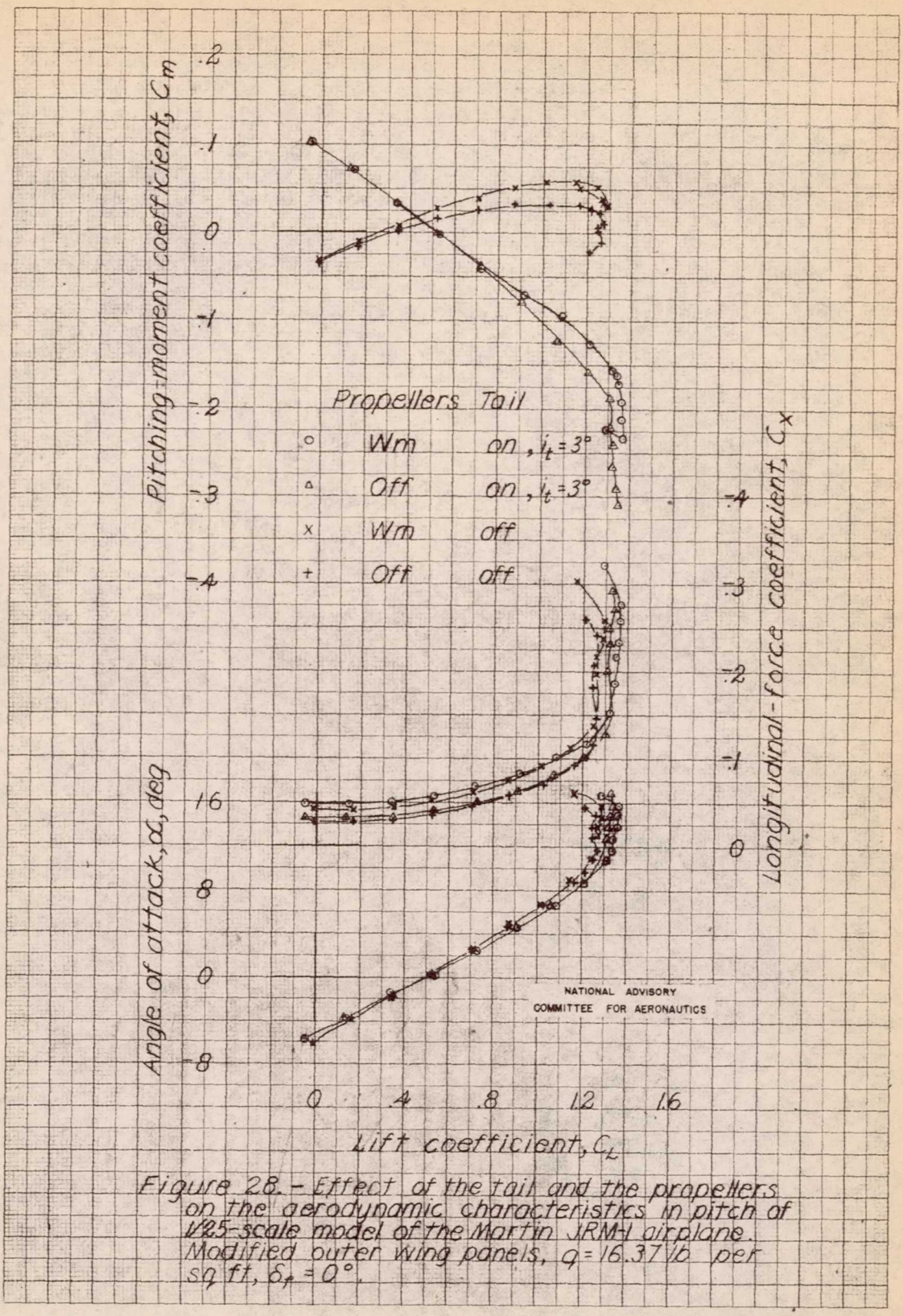

Figure 28.- Effect of the tail and the propellers on the aerodynamic characteristics in pitch of 1/25-scale model of the Martin JRM-1 airplane. Modified outer wing panels, $q = 16.37$ lb per sq ft, $\delta_f = 0°$.

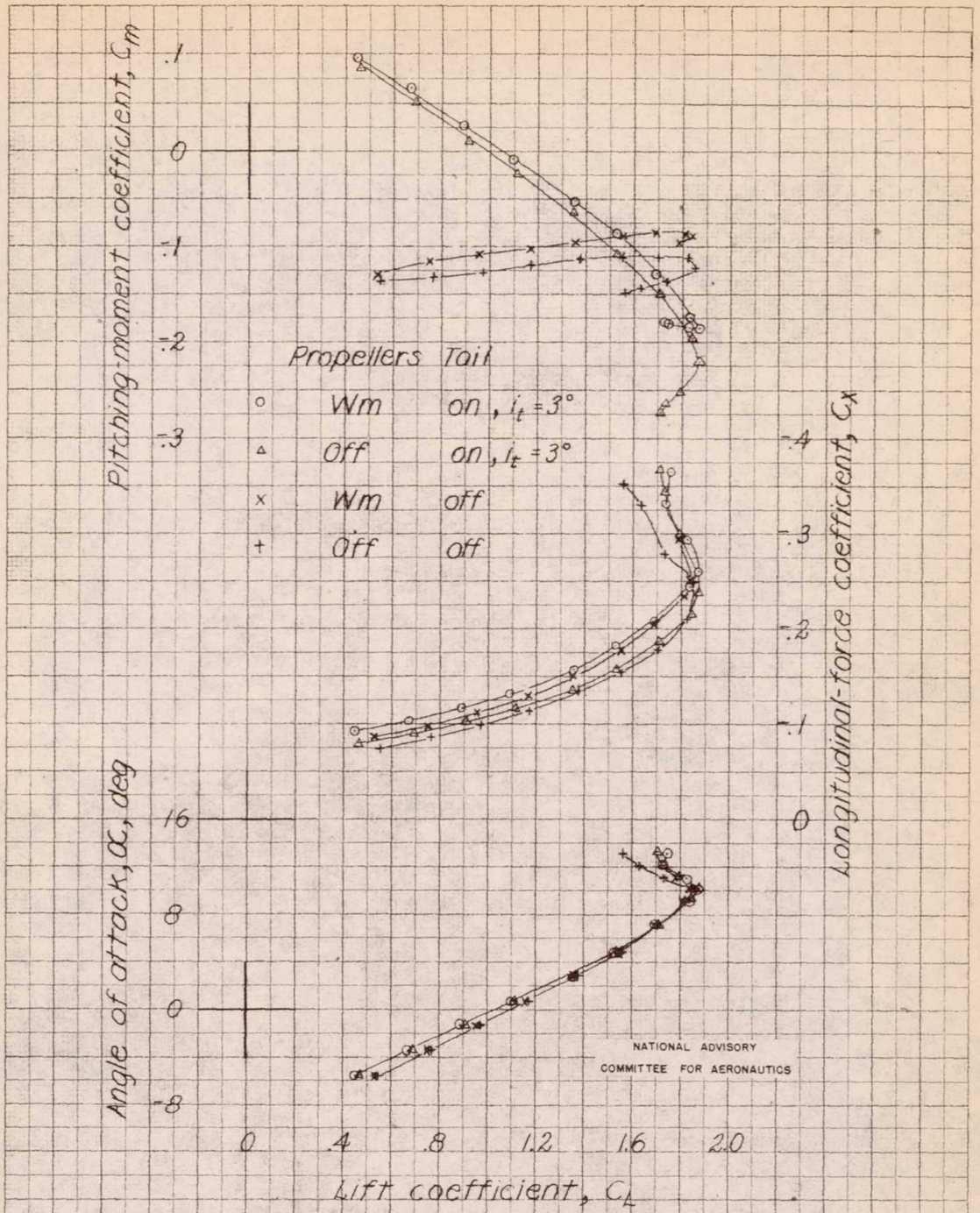

Figure 29.- Effect of the tail and the propellers on the aerodynamic characteristics in pitch of V25-scale model of the Martin JRM-1 airplane. Modified outer wing panels. q = 16.37 lb per sq ft, $\delta_f = 40°$.

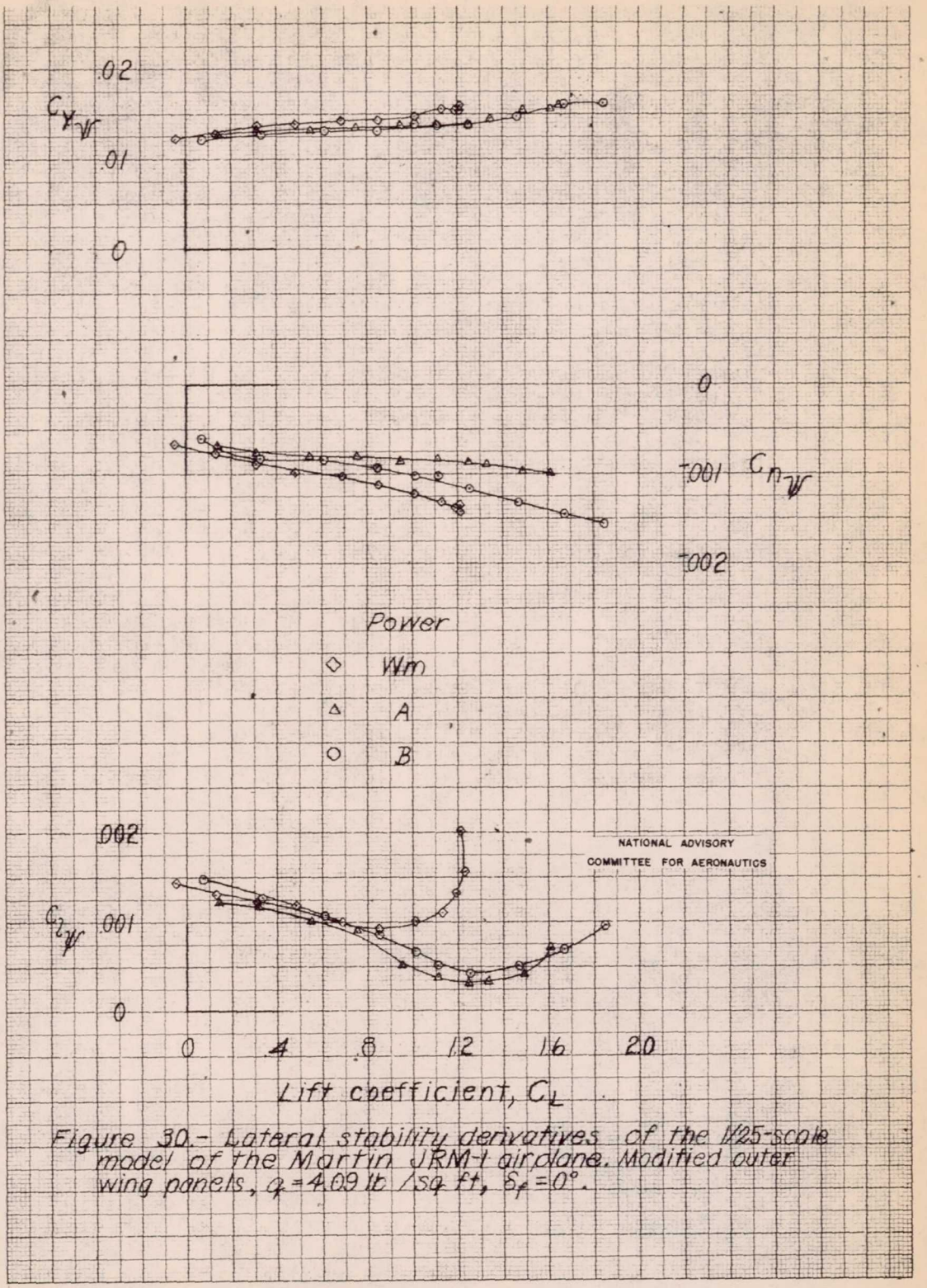

Figure 30.- Lateral stability derivatives of the 1/25-scale model of the Martin JRM-1 airplane. Modified outer wing panels, $q = 4.09$ lb/sq ft, $\delta_f = 0°$.

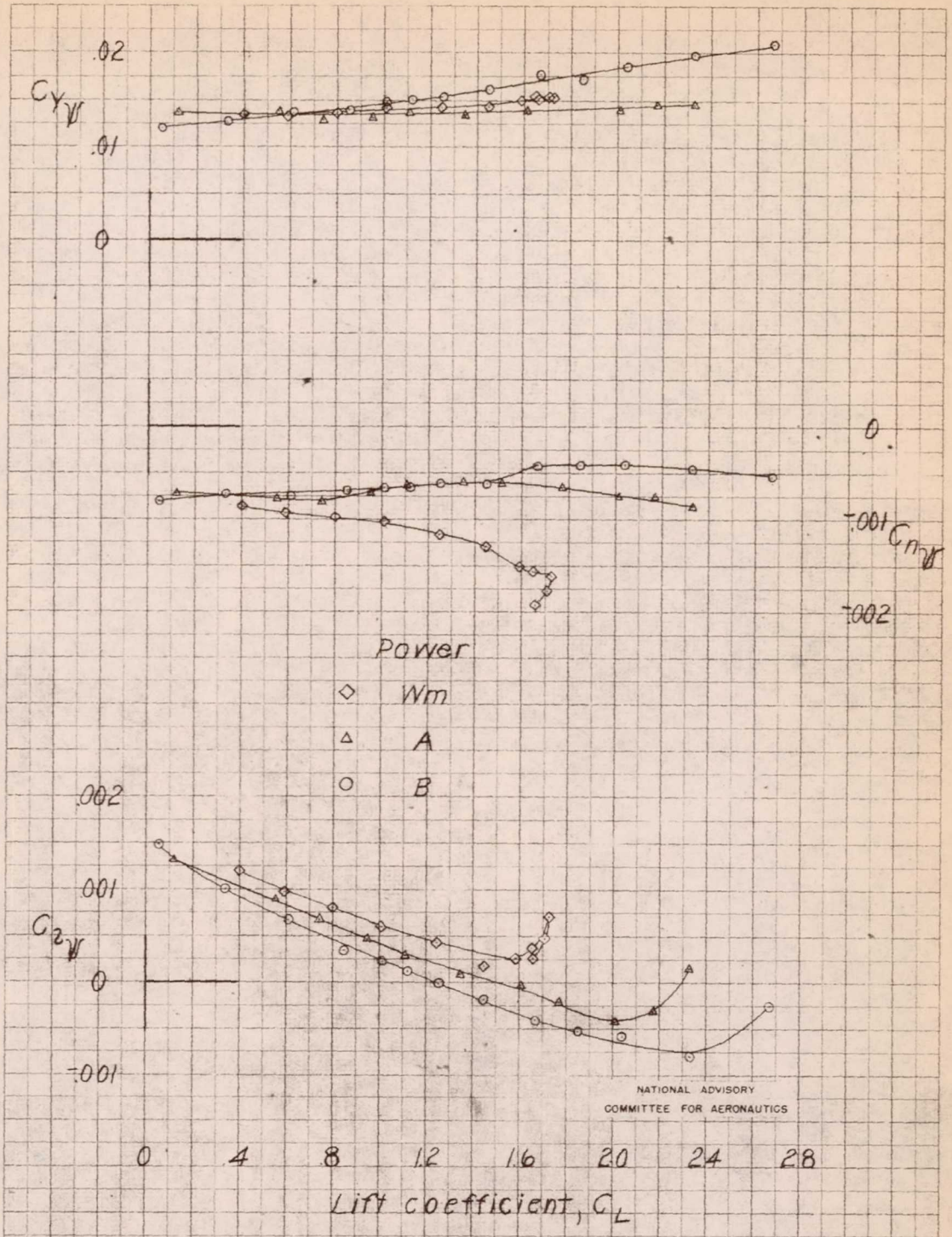

Figure 31.- Lateral-stability derivatives of the 1/25-scale model of the Martin JRM-1 airplane. Modified outer wing panels, $q = 4.09$ lb/sq ft, $\delta_f = 40°$.

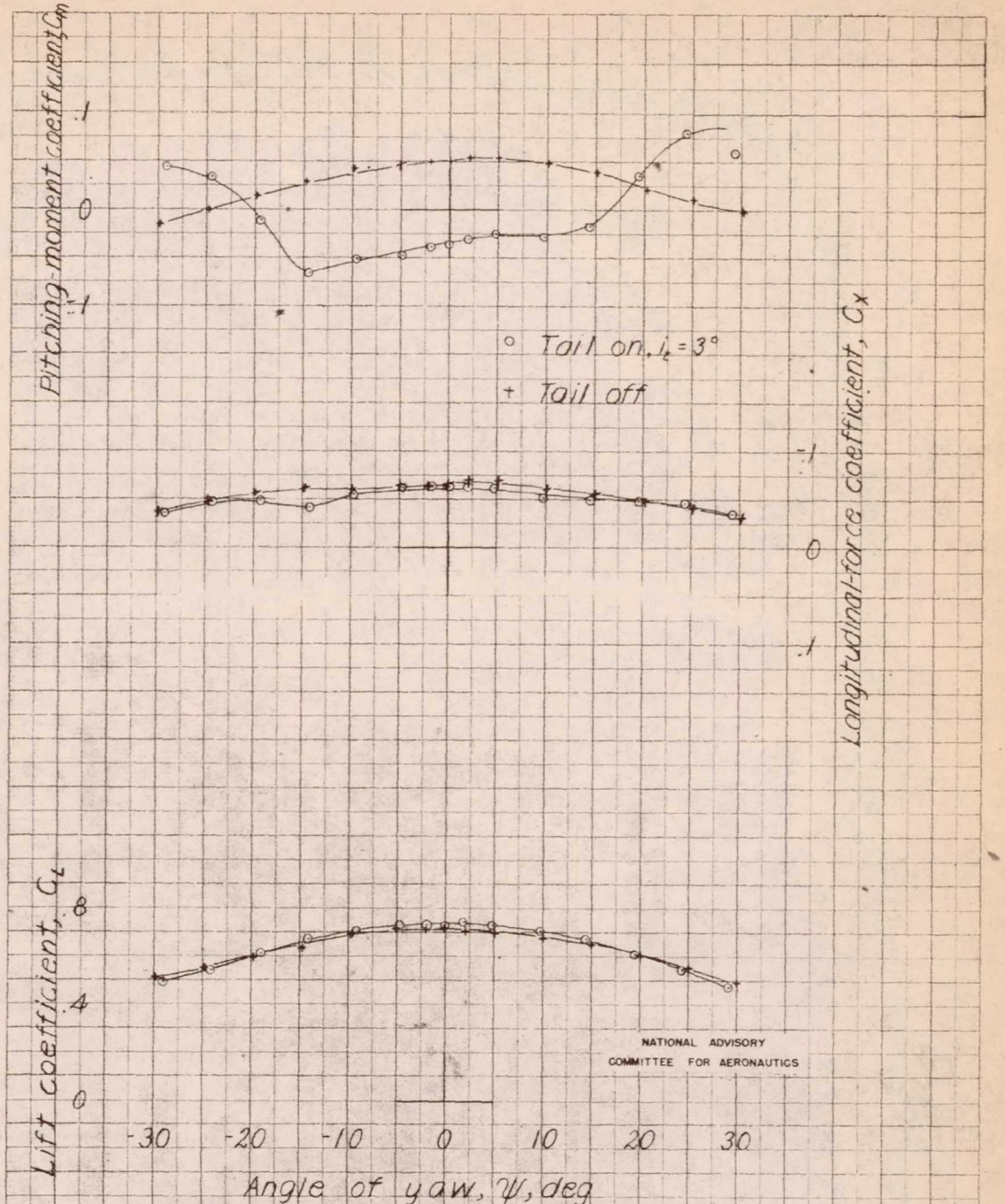

Figure 32.- Effect of the tail on the aerodynamic characteristics in yaw of 1/25-scale model of the Martin JRM-1 airplane. $\alpha = 2.5°$, $\delta_f = 0°$, Windmilling propellers, Modified outer wing panels. $q = 16.37$ lb per sq ft.

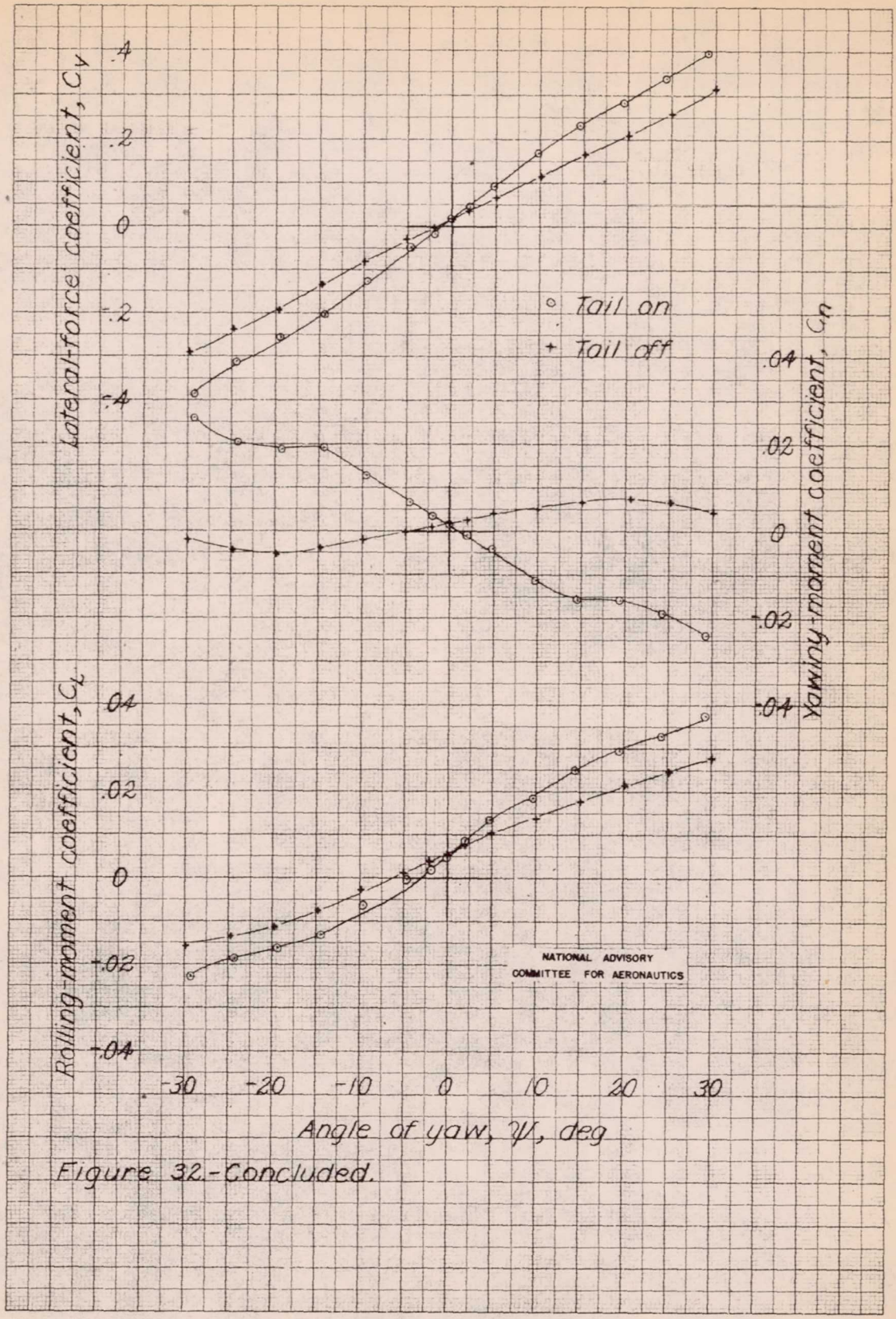

Figure 32.- Concluded.

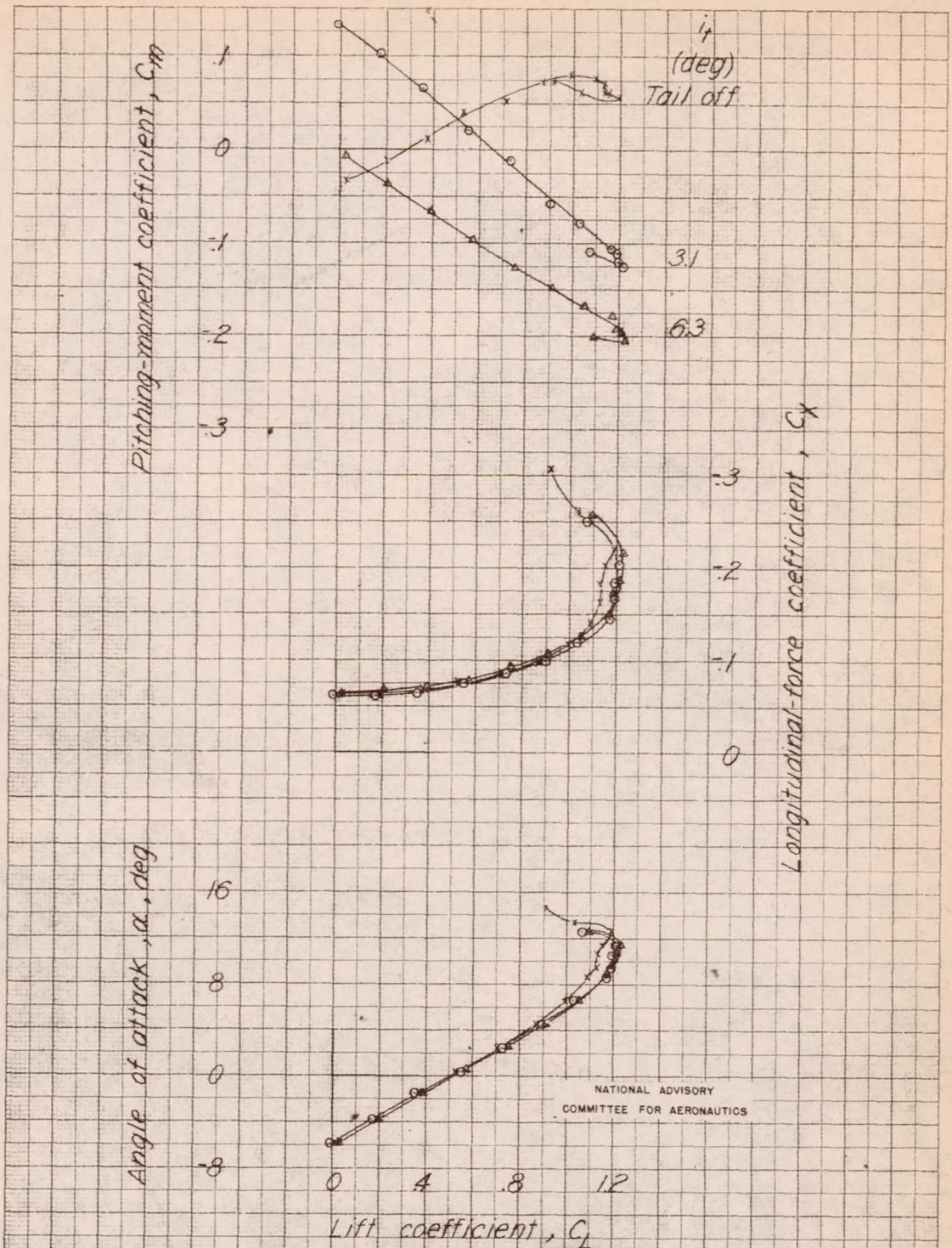

Figure 33.- The effect of the stabilizer on the aerodynamic characteristics in pitch of the 1/25-scale model of a long-range flying boat, JRM-1 tail and modified outer wing panels, Hull model 180. q = 4.09 lb/sq ft, windmilling propellers. $i_s = 0°$.

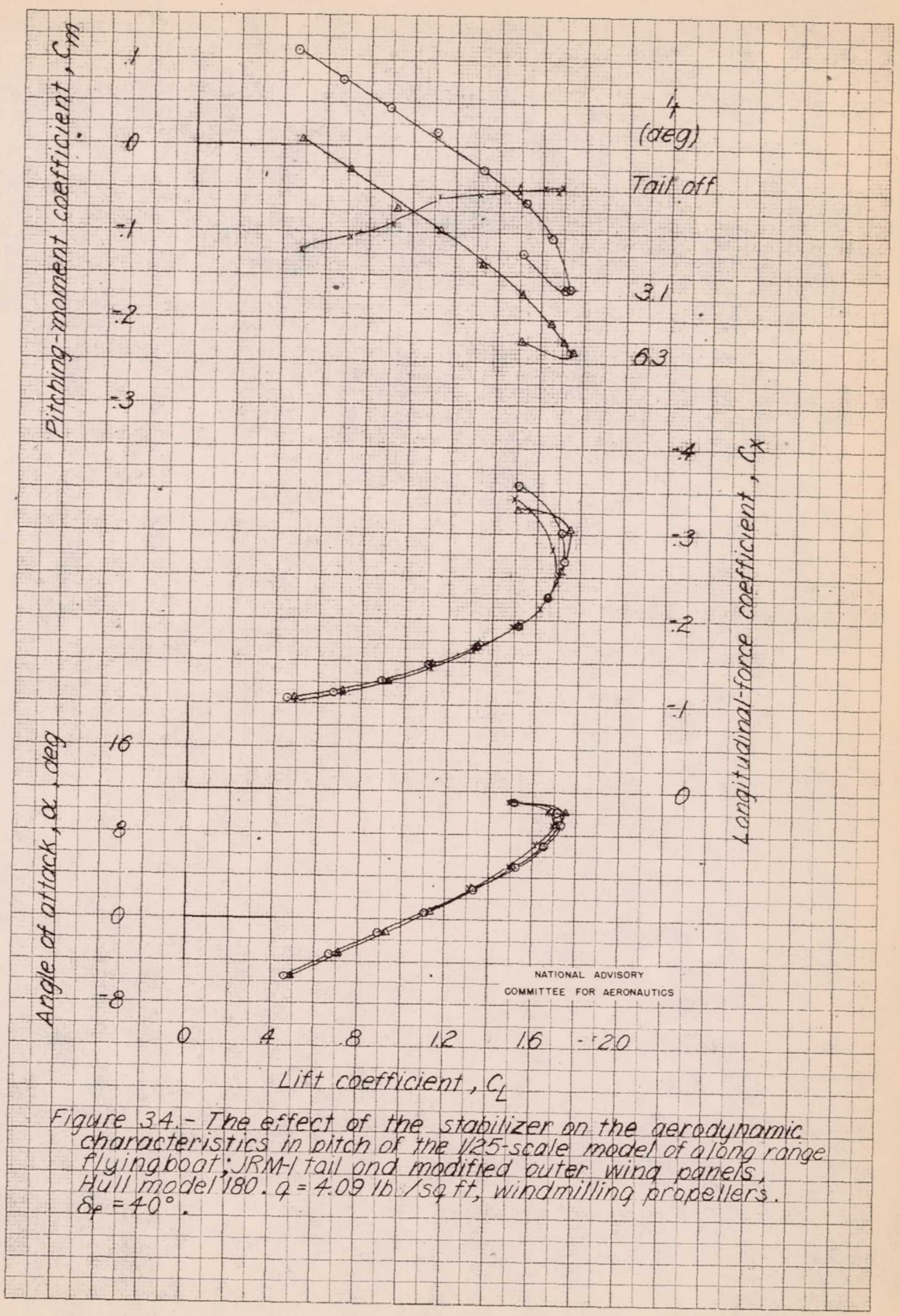

Figure 34.- The effect of the stabilizer on the aerodynamic characteristics in pitch of the 1/25-scale model of a long range flying boat; JRM-1 tail and modified outer wing panels. Hull model 180. q = 4.09 lb/sq ft, windmilling propellers. $\delta_f = 40°$.

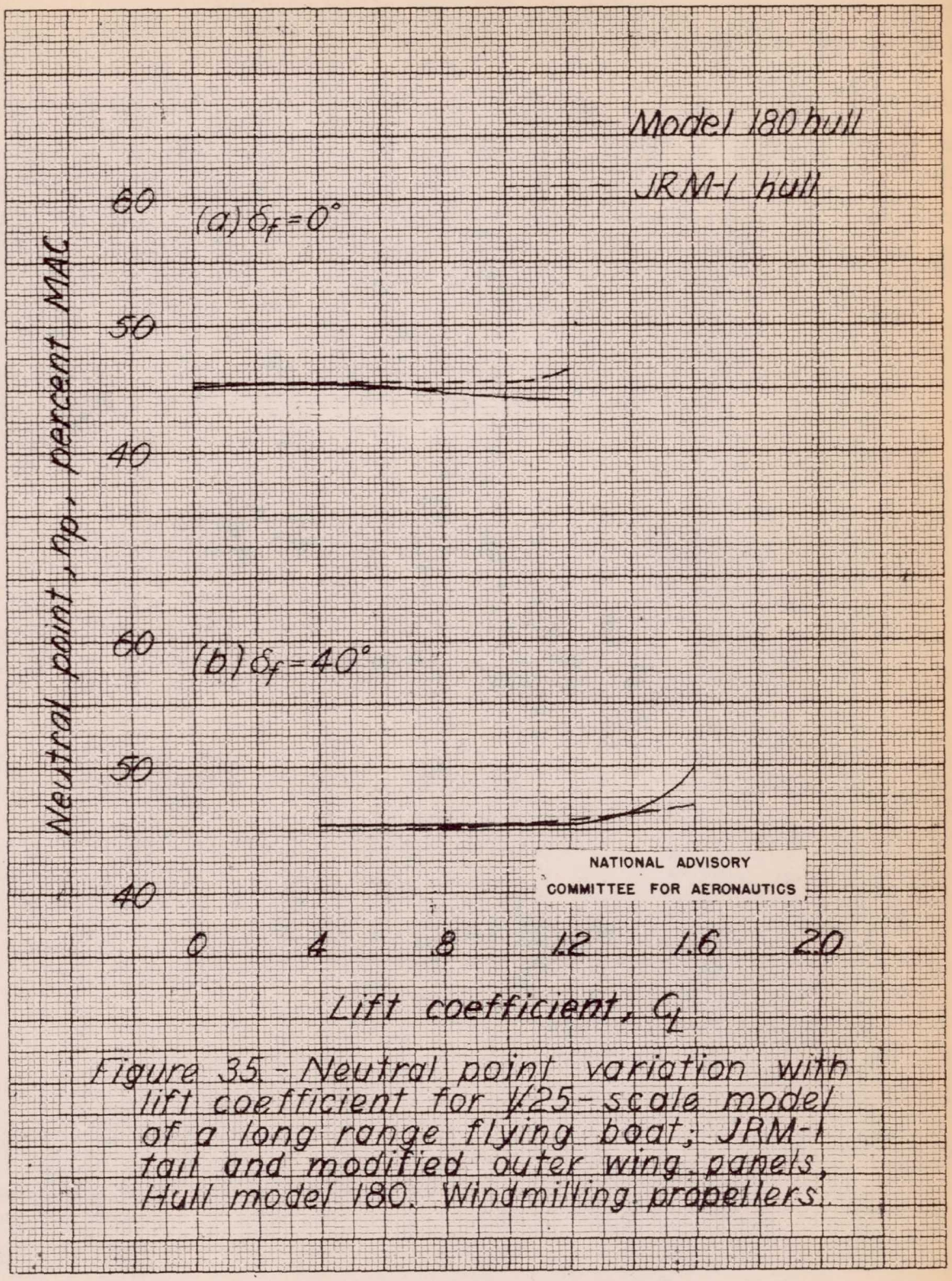

Figure 35.- Neutral point variation with lift coefficient for 1/25-scale model of a long range flying boat; JRM-1 tail and modified outer wing panels, Hull model 180. Windmilling propellers.

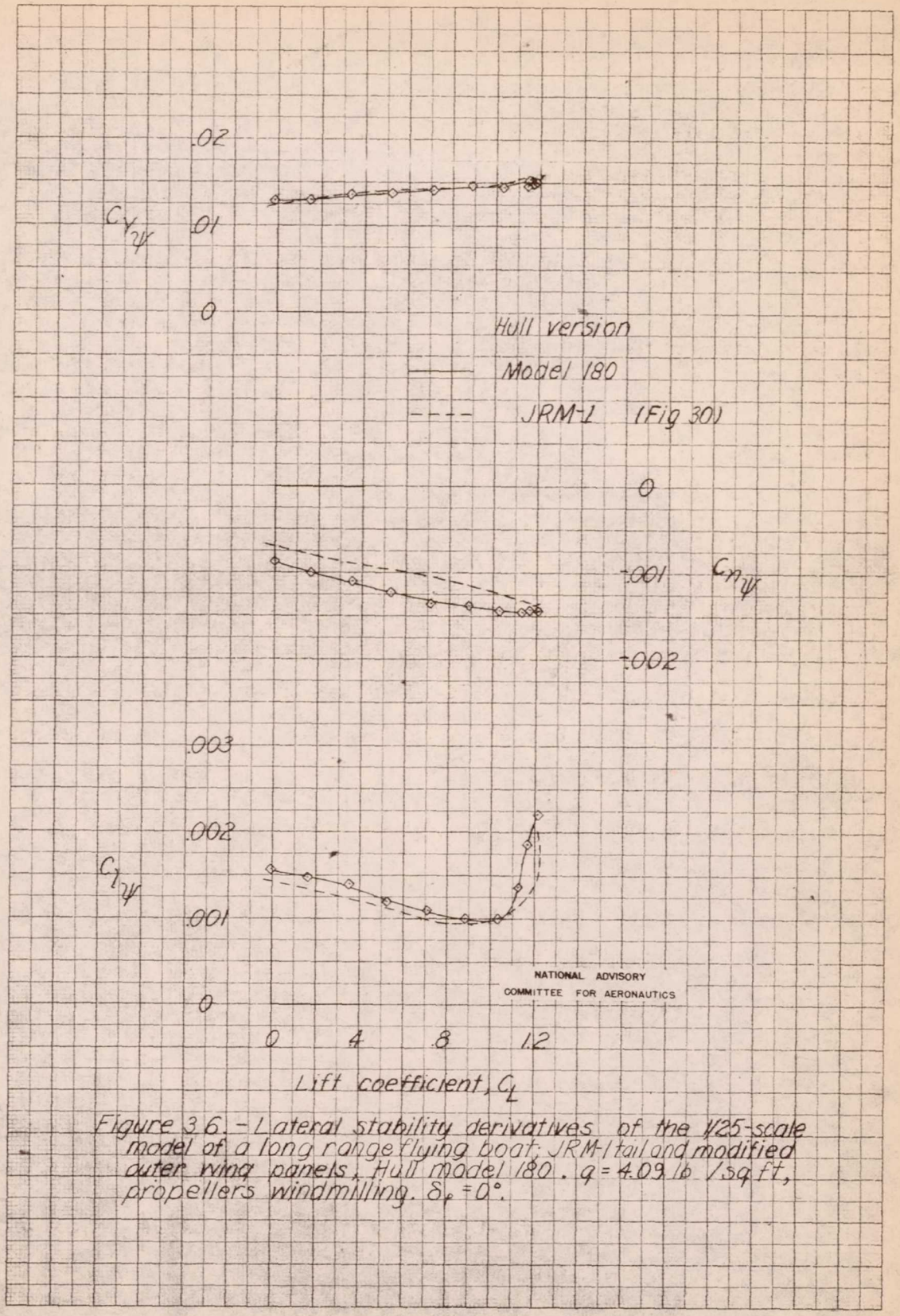

Figure 36. - Lateral stability derivatives of the 1/25-scale model of a long range flying boat; JRM-1 tail and modified outer wing panels, Hull model 180. $q = 4.09$ lb/sq ft, propellers windmilling. $\delta_f = 0°$.

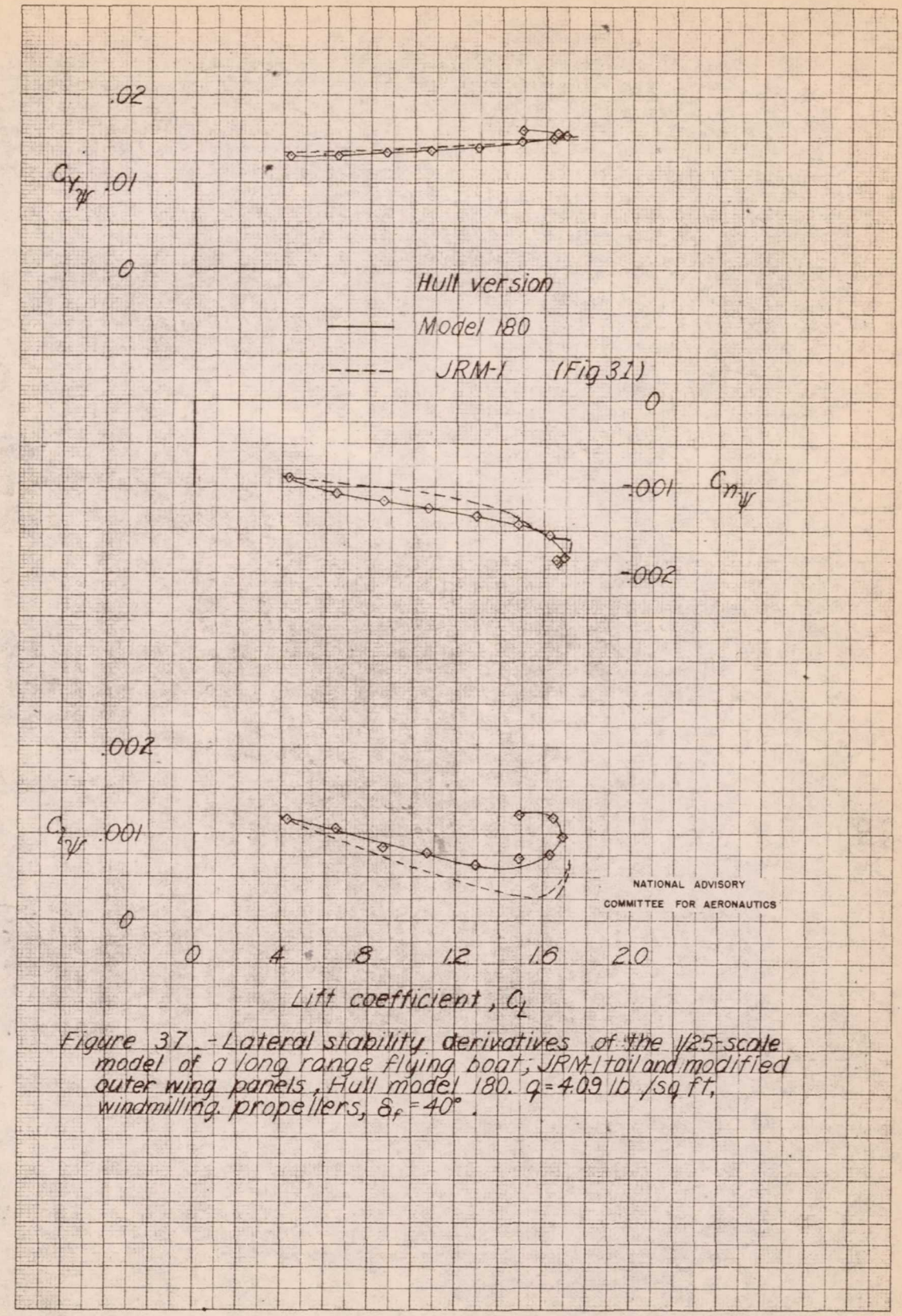

Figure 37.- Lateral stability derivatives of the 1/25-scale model of a long range flying boat; JRM-1 tail and modified outer wing panels, Hull model 180. $q = 4.09$ lb/sq ft, windmilling propellers, $\delta_f = 40°$.

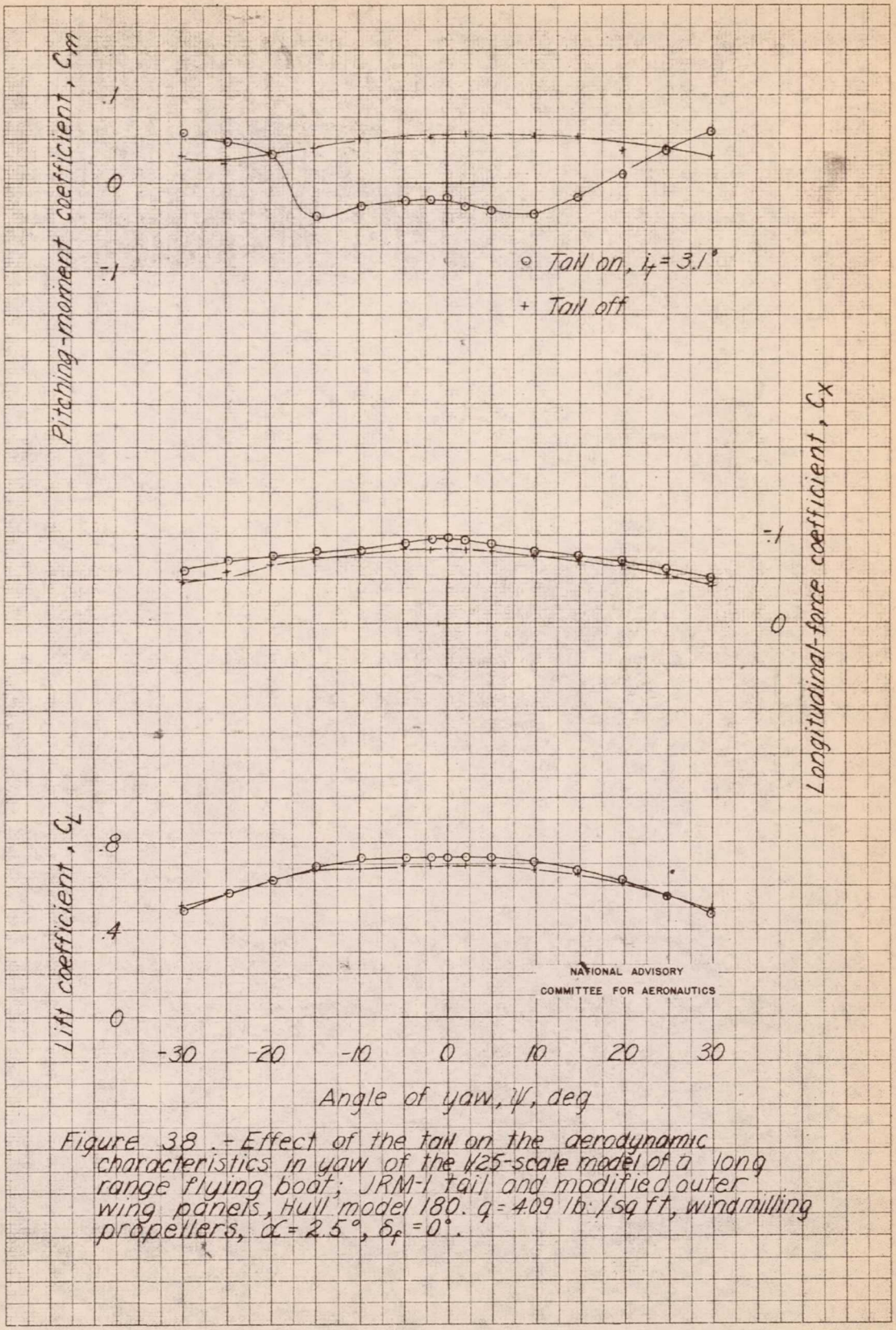

Figure 38.- Effect of the tail on the aerodynamic characteristics in yaw of the 1/25-scale model of a long range flying boat; JRM-1 tail and modified outer wing panels, Hull model 180. $q = 4.09$ lb/sq ft, windmilling propellers, $\alpha = 2.5°$, $\delta_f = 0°$.

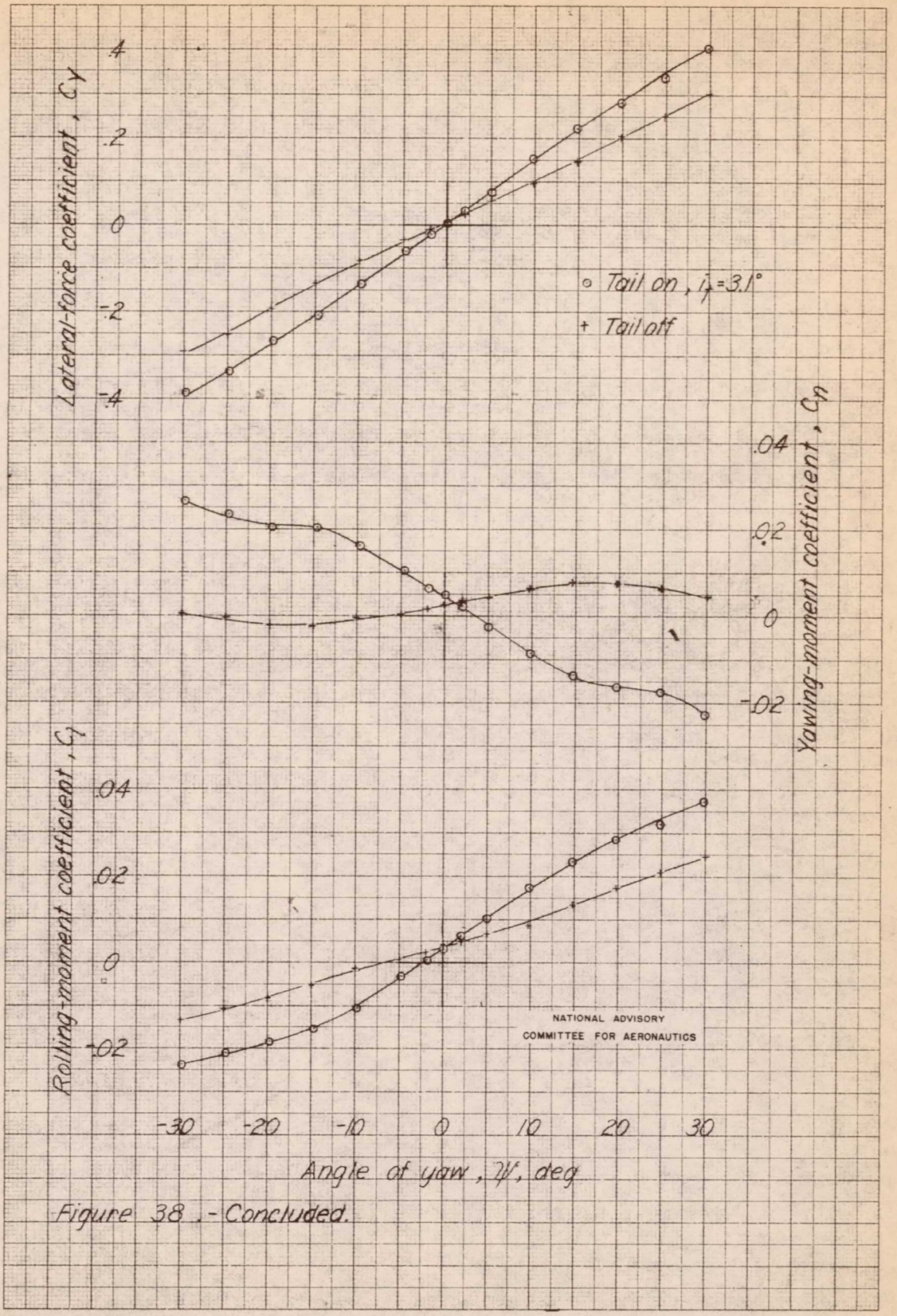

Figure 38.- Concluded.